AD_____

Award Number: DAMD17-00-1-0394

TITLE: Negative Regulation of Tumor Suppressor p53 Transcription in Breast Cancer Cells

PRINCIPAL INVESTIGATOR: Jingwen Liu, Ph.D.

CONTRACTING ORGANIZATION: Palo Alto Institute for Research and Education
Palo Alto, California 94304

REPORT DATE: July 2002

TYPE OF REPORT: Annual

PREPARED FOR: U.S. Army Medical Research and Materiel Command
Fort Detrick, Maryland 21702-5012

REPORT DOCUMENTATION PAGE

Form Approved
OMB No. 074-0188

1. AGENCY USE ONLY (Leave blank)	2. REPORT DATE	3. REPORT TYPE AND DATES COVERED
	July 2002	Annual (1 Jul 01 - 30 Jun 02)

4. TITLE AND SUBTITLE
Negative Regulation of Tumor Suppressor p53 Transcription in Breast Cancer Cells

5. FUNDING NUMBERS
DAMD17-00-1-0394

6. AUTHOR(S)
Jingwen Liu, Ph.D.

7. PERFORMING ORGANIZATION NAME(S) AND ADDRESS(ES)
Palo Alto Institute for Research and Education
Palo Alto, California 94304

Email: Jingwen.Liu@med.va.gov

8. PERFORMING ORGANIZATION REPORT NUMBER

9. SPONSORING / MONITORING AGENCY NAME(S) AND ADDRESS(ES)
U.S. Army Medical Research and Materiel Command
Fort Detrick, Maryland 21702-5012

10. SPONSORING / MONITORING AGENCY REPORT NUMBER

11. SUPPLEMENTARY NOTES

12a. DISTRIBUTION / AVAILABILITY STATEMENT
Approved for Public Release; Distribution Unlimited

12b. DISTRIBUTION CODE

13. Abstract *(Maximum 200 Words)* *(abstract should contain no proprietary or confidential information)*

Recently, there is emerging information to link STAT3 signaling pathway with tumor suppressor p53. Our previous studies have demonstrated that the transcription of the p53 gene in breast cancer cells was down regulated by cytokine oncostatin M (OM). The second goal of our proposal was to evaluate the critical role of STAT3 in OM-mediated regulation of p53 transcription. In this report, we show that blocking STAT3 transactivating activity by the expression of a dominant negative mutant of STAT3 (dnStat3) reversed the OM inhibitory effects on p53 promoter activity and p53 protein expression, demonstrating an involvement of STAT3 in OM-mediated negative regulation of the p53 transcription. In addition, to determine functional roles p53 in the process of proliferation and differentiation of breast cancer cells, we generated stable cell lines (MCF-7 ptsp53) that express $p53Val^{135}$ temperature-sensitive mutant. When cultured at 37°C, $p53Val^{135}$ transfectants expressed exogenous p53 in a mutant conformation that acted as a dominant negative mutant and inhibited the transactivation of endogenous p53. In contrast, at permissive temperature 32°C, the $p53Val^{135}$ mutant resumed normal conformation and behaved as the wild-type p53. We found that overexpression of functional p53 in MCF-7 cells leads to growth arrest at the G_2/M phase of the cell cycle without an induction of apoptosis.

14. SUBJECT TERMS	15. NUMBER OF PAGES
breast cancer, tumor suppressor p53, transcriptional regulation, cell signaling	66
	16. PRICE CODE

17. SECURITY CLASSIFICATION OF REPORT	18. SECURITY CLASSIFICATION OF THIS PAGE	19. SECURITY CLASSIFICATION OF ABSTRACT	20. LIMITATION OF ABSTRACT
Unclassified	Unclassified	Unclassified	Unlimited

Table of Contents

Cover.....

SF 298.....

Table of Contents.....1

Introduction..... 2

Body.....3-5

Key Research Accomplishments.....6

Reportable Outcomes.....6

Conclusions.....6

Figure Legends 7-8

References.....9

Figures.....10-18

Appendices.....

INTRODUCTION

Currently, little information is available to link p53 transcription with the signal transduction pathways that relay the extracellular signals to the nucleus to control the transcription of the p53 gene. We have found that the p53 protein expression was significantly decreased in differentiated breast cancer cells induced by cytokine oncostatin M (OM) (1). Analysis of p53 mRNA by northern blot and measuring the transcription rate of the p53 gene by nuclear run-on assays demonstrate that transcriptional suppression of the p53 gene by OM accounts for the decreased expression of p53 mRNA and protein. We further identified the cis-regulatory element (PE21) on the p53 promoter that mediates the inhibitory effect of OM on p53 transcription (2). OM activates the MEK/ERK pathway and the STAT pathway in breast cancer cells (3). Inhibition of ERK activation partially blocked the suppressive effect of OM on p53 expression (4), suggesting that additional signaling machinery is involved in the regulation of p53 transcription.

In order to delineate the molecular mechanisms by which OM regulates p53 transcription and to understand the relationship between p53 expression and proliferation and differentiation of breast cancer cells, the Task 2 of my Idea grant is to evaluate the critical roles of ERK and STAT3 in OM-mediated regulation of p53 transcription. Since we have already demonstrated the participation of the ERK pathway in OM-regulated p53 transcription by utilizing specific MEK inhibitors (4), in the past 12 months, we have focused our investigation on STAT signaling cascade to determine whether activation of STAT3 or STAT1 is a critical event in the OM-regulated p53 transcription (5). In addition, we have initiated the Task 3 of my proposal to investigate the relationship between p53 expression and the differentiation of breast cancer cells.

BODY

Blockade of OM-induced STAT3 and STAT1 transactivation by dominant negative STAT mutant proteins

OM activates both STAT3 and STAT1 in MCF-7 cells. To determine whether STAT3 or STAT1 activation is a key event in the OM-induced growth inhibition of MCF-7 cells, we established stable MCF-7 clones that express a dominant negative STAT3 mutant (dnStat3, Y705F) or a dominant negative STAT1 mutant (dnStat1, Y701F). MCF-7 clones (neo) transfected with the empty vector (pEFneo) were also generated and were used in this study as negative controls to access possible side effects associated with antibiotic selection.

To determine the effect of mutant STAT proteins on OM-induced STAT DNA binding activity, gel shift and supershift assays using a ^{32}P-labeled oligonucleotide probe (c-FosSIE), containing the high affinity STAT3 binding site of c-fos gene promoter, were performed with nuclear extracts prepared from MCF-7 stable clones that were untreated or treated with OM for 15 min. As shown in Figure 1A, in MCF-7-neo cells, OM induced the formation of 3 specific DNA-protein complexes (lane 2). Supershift assays with antibodies specific to STAT1 or to STAT3 showed that the complex C3 was completely supershifted by anti-STAT1 antibody (lane 3), suggesting that C3 is the homodimer of STAT1. The C2 complex was supershifted by both anti-STAT1 and anti-STAT3 (lane 5), thereby demonstrating that C2 is the heterodimer of STAT1 and STAT3. The low intensity band C1 was completely supershifted by anti-STAT 3 antibody (lane 4), demonstrating its identity as the STAT3 homodimer. The OM-induced STAT binding activity was markedly reduced in clones of dnStat3 (lanes 8-11) and dnStat1 (lanes 12-15) as compared to the neo clone (lanes 1-7) and untransfected MCF-7 cells (data not shown).

To further demonstrate a blockade of STAT3 transactivating activity by the mutant dnStat3 a STAT3 luciferase reporter (pTKlucS3) was transiently transfected into MCF-7-neo and dnStat3 clones. Forty h after transfection, cells were treated with OM for 4 h and luciferase activities were measured. As shown in Figure 1B, OM induced 8-fold increase in the promoter activity of pTKlucS3 in the neo clone, but this induction was completely abolished in the clone of dnStat3.

We next examined the effect of OM on ERK activation in MCF-7 and stable clones. Western blot analysis detected comparable levels of activated ERK in parental MCF-7 cells and stable clones (Figure 2). These results clearly demonstrate that expression of the DN STATs specifically abolished STAT DNA binding and transactivating activity without subverting the OM-induced MEK/ERK signaling pathway.

Expression of dnStat3 but not dnStat1 abolished the antiproliferative activity of OM

The impact of dnStat3 or dnStat1 expression on OM-induced growth suppression was first evaluated by cell proliferation assays that measured the binding of a fluorescent dye to cellular nucleic acids which produces fluorescent signals in proportion to the cell number. Figure 3A shows that the cellular proliferation of MCF-7, the neo clones, and the clones expressing dnStat1 was inhibited by 60-75% as compared to control after incubation with OM for 5 days, whereas the growth rate of dnStat3 clones were

unaffected by OM. To further verify the blocking effect of DN STAT3 on OM growth inhibitory activity, a time course of cell growth rate in the absence or the presence of OM was conducted by direct accounting of the viable cell numbers of MCF-7 cells and the dnStat3 clone. Figure 3B shows that OM exerted a time-dependent inhibitory effect on MCF-7 cells. By 7 days of the OM treatment, the number of viable cells was decreased by more than 50% as compared to control. Consistent with the results of Fig. 3A, the growth of dnStat3 cells was not inhibited by OM through the entire duration of the experiment. These results demonstrate that expression of the dominant negative mutant of STAT3 but not STAT1 blocked the OM-mediated growth arrest in MCF-7 cells.

STAT3 participates in OM-mediated downregulation of p53

OM downregulates p53 expression in MCF-7 cells by inhibiting the gene transcription (1,4). Since blocking the MEK/ERK pathway only partially reversed the OM inhibitory effect on p53 protein expression, it is possible that other signaling pathways could also be involved. To evaluate the role of STAT3 in p53 transcription, a p53 promoter luciferase reporter construct pGL3-p53 was cotransfected with pEF-dnStat3 or with a control vector (pEFneo) into MCF-7 cells along with pRL-SV40 for normalization of variations in transfection efficiency. Cells were treated with OM or OM dilution buffer for 40 h and duel luciferase activities were measured in total cell lysates. The p53 promoter activity was decreased by 50% in OM treated cells in the absence of pEF-dnStat3. Expression of dnStat3 reversed the OM inhibitory effect on p53 promoter activity (Figure 4A). We further examined p53 protein levels in MCF-7 neo and dnStat3 clones untreated or treated with OM. Western blot analysis shows that while OM treatment lowered p53 protein level to 35% of control in the neo clone, the level of p53 protein in the dnStat3 clone was not decreased by OM treatment (Figure 4B). Taken together, these results demonstrate that activation of STAT3 signaling pathway is a necessary step in the OM-mediated regulation of p53 transcription.

Overexpression of the wildtype p53 leads to the growth arrest of breast cancer cells at the G2/M phase of the cell cycle

Previously, we have shown that treatment of breast cancer cells with OM induces growth arrest and downregulates the expression of the tumor suppressor gene p53 concurrently. Currently, it remains elusive whether p53 is directly involved in OM-induced growth inhibition. The Task III of my Idea grant proposal is to investigate the relationship between p53 expression and the differentiation of breast cancer cells, and to determine whether p53 plays a negative role in the OM-induced differentiation process of breast cancer cells. Therefore, very recently, we have initiated the Task III by generation of stable cell lines (MCF7-ptsp53) that express $p53Val^{135}$ temperature-sensitive mutant (Figure 5). When cultured at 37°C, $p53Val^{135}$ transfectants expressed exogenous p53 in a mutant conformation that acted as a dominant negative mutant and inhibited the transactivation of endogenous p53. In contrast, at permissive temperature 32°C the $p53Val^{135}$ mutant resumed normal conformation and behaved as the wild-type p53 that activate gene transcription determined by a p53 reporter assay (Figure 6). The growth rate of $p53Val^{135}$ cells at 37°C was similar to the untransfected and mock transfected MCF-7 cells (Figure 7 upper panel) and these cells were morphologically indistinguishable. However, $p53Val^{135}$ cells became growth arrested within 2 days after

switching the temperature from 37° C to permissive temperature (Figure 7 lower panel). Furthermore, the size of these cells was significantly larger than untransfected cells (Figure 8). Cell cycle analysis demonstrated that p53 overexpression arrested cells at the G_2/M phase without a significant effect on G_0/G_1 phase (Figure 9). Furthermore, overexpression of the wildtype p53 did not lead to increases of apoptotic cell populations under normal culture conditions or under stress condition in MCF-7 cells.

In the final 12 months of this award period, we will carry on experiments to investigate the relationship between p53 expression and the growth inhibitory activity of OM by using $p53Val^{135}$ cells. Additionally, we will take the advantage of these cells that express either mutant p53 or the wildtype p53 by temperature switching to conduct microarray studies to identify p53 regulated genes that are responsible for the growth arrest at the G2/M phase of the cell cycle.

KEY RESEARCH ACCOMPLISHMENTS

- Providing the first evidence that Stat3 plays a functional role in p53 transcription.
- Establishment of a stable cell line (MCF-7 ptsp53) that can turn on or turn off the wild-type p53 expression by temperature switch. This cell line will be a valuable key tool in our future investigation to further study the function roles of p53 in the process of breast cancer cell growth and differentiation.

REPORTABLE OUTCOMES

- Two manuscripts have been published in the first 18 months of the award period that identified a novel regulatory element PE21 on p53 promoter (*Oncogene* 20:8193-8202, 2001) and characterized the OM-activated signaling cascade in breast cancer cells (*Breast Cancer Res Treat.* 66:111-121, 2001).
- One manuscript entitled "Delineating an oncostatin M-activated STAT3 signaling pathway that modulates gene expression and cellular responses in MCF-7 cells" was submitted to the journal Oncogene on June 18, 2002.

CONCLUSIONS

Transcriptional regulation of the p53 gene contributes to the change in expression of wildtype p53 during the cell cycle and to the elevated expression of mutated p53 in tumor cells. However, currently, little is known regarding the regulation of p53 transcription in tumor cells and inadequate information is available to link p53 transcription with the signal transduction pathways that relay the extracellular signals to the nucleus to control the transcription of the p53 gene. We have successfully accomplished our Task I and II by identification of a novel cis-regulatory element on p53 promoter that mediates the inhibitory effect of OM on p53 transcription and by further characterizion of the signaling pathways that transduce the cytokine signal to modulate p53 transcription. These new findings add significantly to the current literature for the understanding of the role of p53 in normal and malignant cellular processes. We are currently working towards our Task III to determine whether p53 plays a negative role in the OM-induced differentiation process of breast cancer cells.

Figure Legends

Figure 1. Blocking STAT DNA binding and transactivation by STAT mutant proteins.
(A) EMSA analyses of nuclear proteins interacting with the STAT binding site. Nuclear extracts were prepared from MCF-7-neo clone, pEFneo-dnStat1 clone, and pEF-dnStat3 clone that were untreated (lanes 1), or treated with OM (15 min) (lanes 2-15). A double-stranded oligonucleotide, designated as c-FosSIE, was radiolabeled and incubated with 10 μg of nuclear extract per reaction for 10 min at 22°C in the absence (lanes 1,2,8,12) or the presence of 100-fold molar amounts of unlabeled competitor DNA (lanes 6,7). For supershift, antibodies were incubated with nuclear extracts at 22°C for 30 min prior the addition of the probe (lanes 3-5, 9-11, 13-15). The reaction mixtures were loaded onto a 6% polyacrylamide gel and run in TGE buffer at 30 mA for 3 h at 4°C.
(B) Analysis of STAT3 reporter luciferase activity. The STAT3 reporter pLucTKS3 was cotransfected with pRL-SV40 into neo or dnStat3 clones. Forty h after transfection, cells were treated either with OM (50 ng/ml) or with OM dilution buffer for 4 h prior to harvesting cell lysates. Luciferase activities in total cell lysates were measured using the Promega Dual Luciferase Assay System. Absolute firefly luciferase activity was normalized against renilla luciferase activity to correct for transfection efficiency. The normalized luciferase activity is expressed as the fold of luciferase activity in untreated control cells. The data presented are derived from 3 separate transfections in which triplicate wells were used in each condition.

Figure 2. Activation of MAP kinases ERK1 and ERK2 by OM in MCF-7 and stable clones. MCF-7, neo, dnStat1 and dnStat3 clones cultured in medium containing 0.5% FBS were stimulated with 50 ng/ml OM. At the indicated times, cells were scraped into lysis buffer and cell extracts were prepared. Soluble proteins (30 μg/lane) were applied to SDS-PAGE. Detection of phosphorylated ERK1 and ERK2 and the nonphosphorylated ERK2 was performed by immunoblotting.

Figure 3. Abrogation of OM antiproliferative activity by expression of DN STAT3 in MCF-7 cells.
(A) Untransfected parental MCF-7, 2 independently isolated neo clones, dnStat1 clones, and dnStat3 clones were cultured in 96-well plates at a density of 2000 cells/well in 0.1 ml RPMI containing 2% FBS with or without 50 ng/ml OM for 5 days. The medium was removed and cells were washed with PBS. Two hundred microliters of Cyquant GR dye mixed with cell lysis buffer were added to each well. The fluorescent signals were then measured using a fluorescence microplate reader
(B) Cells of MCF-7 and dnStat3 clone were cultured in 24-well culture plates at a density of $7x10^3$ cells/well in 0.5 ml RPMI containing 2% FBS with or without 50 ng/ml of OM for different days. At the indicated time, cells were trypsinized and viable cells (trypan blue excluding cells) were counted. Values are mean of triplicate wells. The figure shown is representative of 4 to 5 separate experiments.

Figure 4. Evaluation of the role of STAT3 in OM-mediated downregulation of p53 promoter activity and protein expression.

(A) The p53 promoter reporter pGL3-p53 was cotransfected with pEF-dnStat3 or with pEFneo into cells along with the normalizing vector pRL-SV40. Transfected cells were treated either with OM (50 ng/ml) or with OM dilution buffer for 40 h prior to harvesting cell lysates. The normalized luciferase activity is expressed as the percentage of luciferase activity in untreated control cells.

(B) Cells were cultured in the presence or absence of OM for 5 days and harvested. Western blot analysis of p53 protein expression was conducted using total cell lysates.

Figure 5. Characterization of MCF7-p53Val^{135} stable clones. Western blot analysis of the murine p53Val^{135} protein expression was performed by using anti-mouse p53 mAB (pAb240, Santa Cruze). Cell lysates were harvested from untransfected MCF-7, vector-transfected (pcDNA3.1), and the cells that were cotransfected with pcDNA3.1 and the plasmid ptsp53 that encodes murine p53 with a single AA mutation at codon 135 from glycine to valine.

Figure 6. Luciferase reporter assays to determine p53 transactivating activity in stable clones. Cells were cultured at either 37° C or the permissive temperature (32° C) overnight and then were transfected with a p53 luciferase reporter p53-Luc and a normalizing β-galactosidase vector RSV-βgal. Luciferase activity and the β-galactosidase activity were measured after 40 h. The normalized luciferase activity is expressed as the fold of luciferase activity in mock transfected cells.

Figure 7. Examination of the effect of p53 Val^{135} on the growth rate of MCF-7 cells at non-permissive and the permissive temperature.

(A) Cell number account: Cells of MCF-7 and stable clones were cultured in 24-well culture plates at either 37° C or at 32° C for different days. At the indicated time, cells were trypsinized and viable cells (trypan blue excluding cells) were counted. Values are mean of triplicate wells.

(B) DNA content: Cells were cultured in 96-well plates at a density of 2000 cells/well in 0.1 ml RPMI containing 10% FBS for different lengths of time. The medium then was removed and cells were washed with PBS. Two hundred microliters of Cyquant GR dye mixed with cell lysis buffer were added to each well. The fluorescent signals were then measured using a fluorescence microplate reader.

Figure 8. Over expression of p53 induces morphological changes in MCF-7 cells. MCF-7, pcDNA3.1 clone, and ptsp-53 clone were cultured at 37° C or at 32° C for 3 days and photographs were taken by using the Penguin 600CL digital camera at a magnification of 200.

Figure 9. Cell cycle analysis. MCF-7, pcDNA3.1 clone, and pts-p53 clone were set up at 37° C for 1 day then were cultured at 32° C for 2 days.

REFERENCES

1. Liu J, Li C, Ahlborn TE, Spence MJ, Meng L, and Boxer LM. The expression of 53 tumor suppressor gene in breast cancer cells is down-regulated by cytokine oncostatin M. *Cell Growth.&Differ., 5*: 15-18, 1999.

2. Li C, Ahlborn TE, Tokita K, Boxer LM, Noda A, and Liu J: The Critical Role of the PE21Element in Oncostatin M-Mediated Transcriptional Repression of the p53 Tumor suppressor Gene in Breast Cancer Cells. *Oncogene* 20:8193-8202, 2001.

3. Li C, Kraemer FB, Ahlborn TE, and **Liu J:** Oncostatin M–induced growth inhibition and morphological changes of MDA-MB231 breast cancer cells are mediated through the MEK/ERK signaling pathway. *Breast Cancer Res Treat.* 66:111-121, 2001

4. **Liu J**, Li C, Ahlborn TE, Spence MJ, Meng L, Boxer LM: The expression of p53 tumor suppressor gene in breast cancer cells is down regulated by cytokine oncostatin M. *Cell Growth & Differentiation*, 10:677-683, 1999

5. Zhang F, Li C, Halfter H, and **Liu J:** Delineating an oncostatin M-activated STAT3 signaling pathway that modulates gene expression and cellular responses in MCF-7 cells. Submitted to *Oncogene*

Figure 1

A

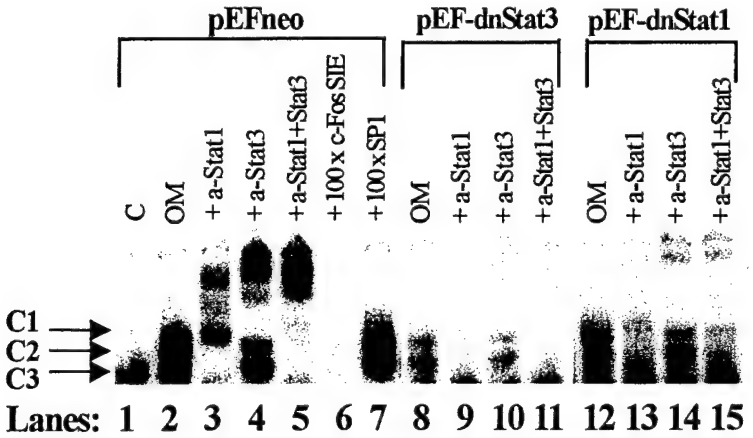
pEFneo
pEF-dnStat3
pEF-dnStat1
C
OM
+ a-Stat1
+ a-Stat3
+ a-Stat1+Stat3
+ 100 x c-Fos SIE
+ 100 x SP1
OM
+ a-Stat1
+ a-Stat3
+ a-Stat1+Stat3
OM
+ a-Stat1
+ a-Stat3
+ a-Stat1+Stat3
C1
C2
C3
Lanes: 1 2 3 4 5 6 7 8 9 10 11 12 13 14 15

B

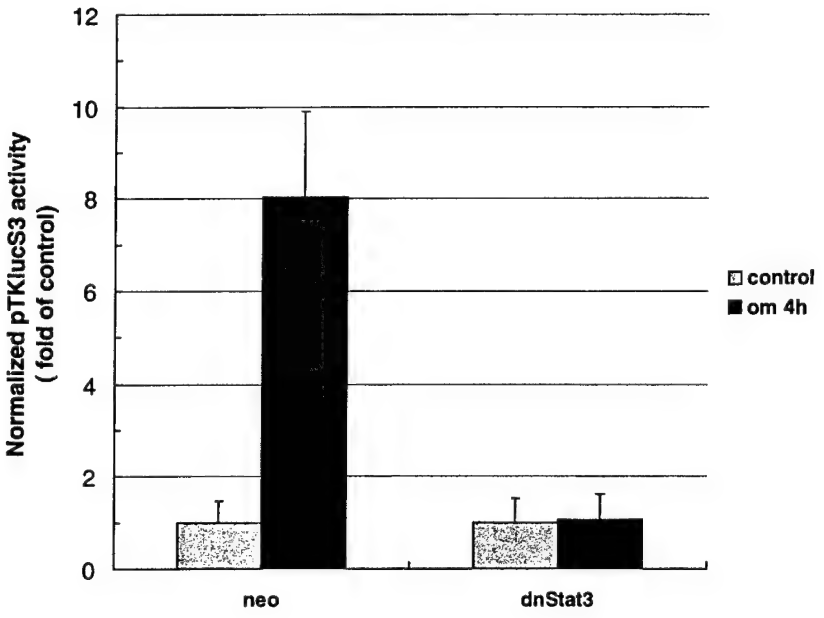
Normalized pTKlucS3 activity
(fold of control)
12
10
8
6
4
2
0
neo
dnStat3
control
om 4h

Figure 2

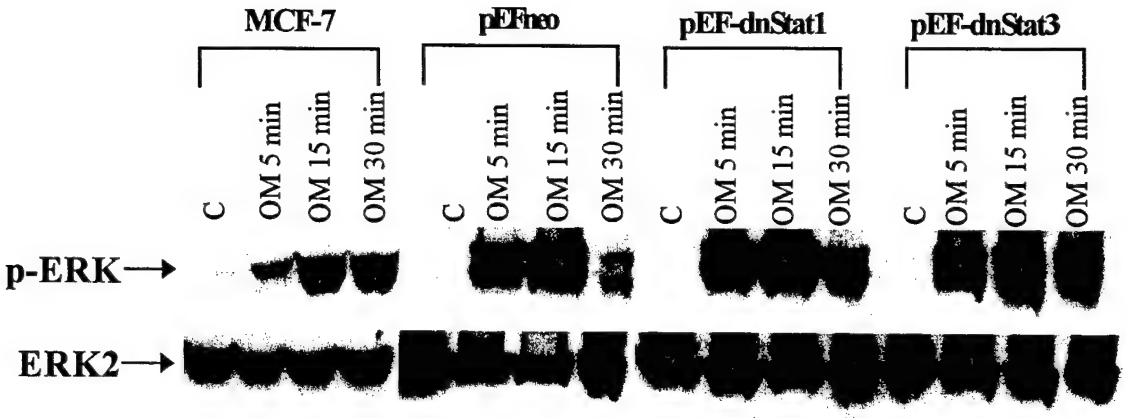
MCF-7
pEFneo
pEF-dnStat1
pEF-dnStat3
C
OM 5 min
OM 15 min
OM 30 min
p-ERK
ERK2

Figure 3

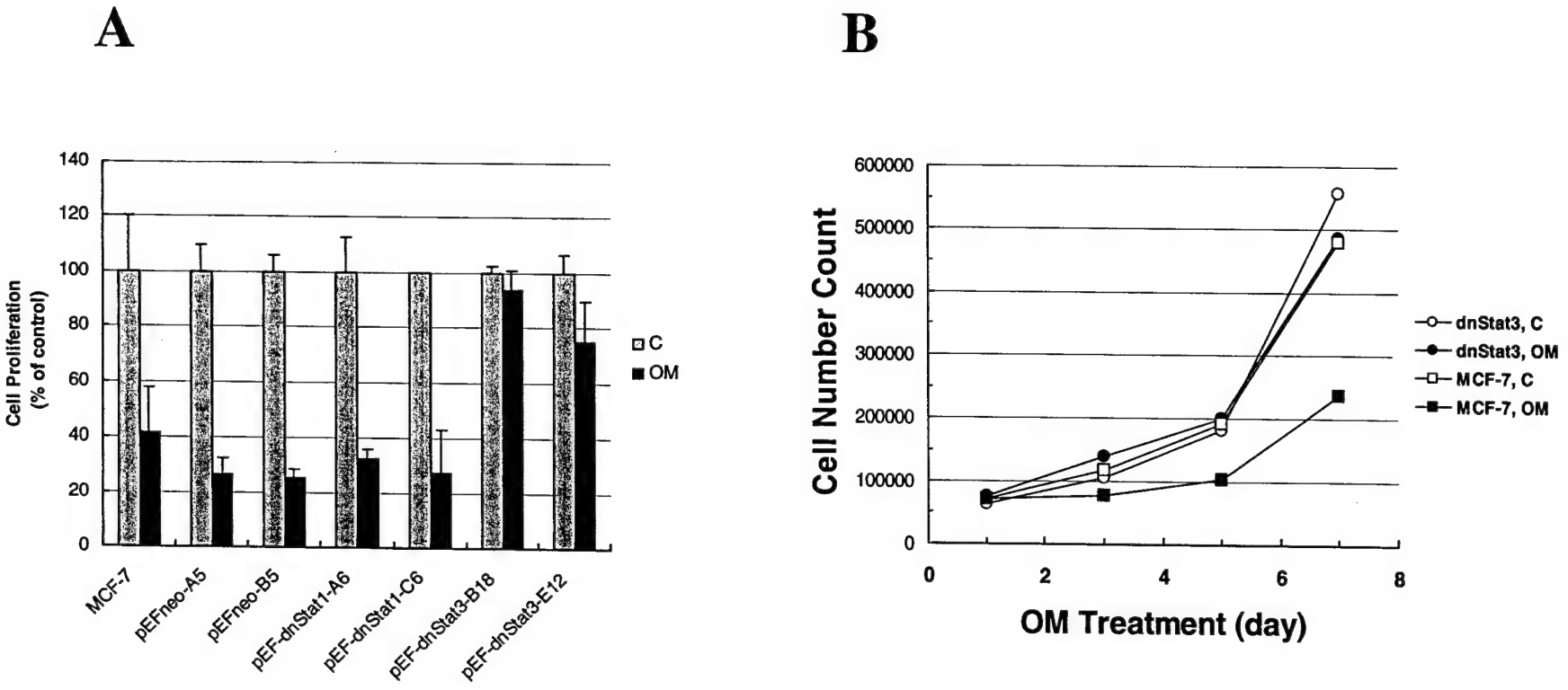
A
Cell Proliferation (% of control)
140
120
100
80
60
40
20
0
C
OM
MCF-7
pEFneo-A5
pEFneo-B5
pEF-dnStat1-A6
pEF-dnStat1-C6
pEF-dnStat3-B18
pEF-dnStat3-E12
B
Cell Number Count
600000
500000
400000
300000
200000
100000
0
0
2
4
6
8
OM Treatment (day)
dnStat3, C
dnStat3, OM
MCF-7, C
MCF-7, OM

Figure 4

A

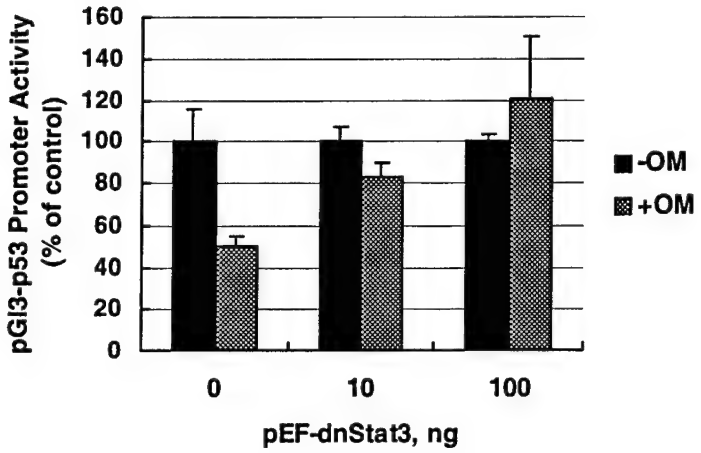
pGl3-p53 Promoter Activity
(% of control)
160
140
120
100
80
60
40
20
0
0
10
100
pEF-dnStat3, ng
-OM
+OM

B

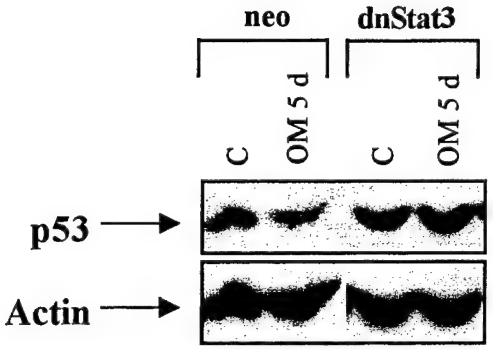
neo
dnStat3
C
OM 5 d
C
OM 5 d
p53
Actin

Figure 5

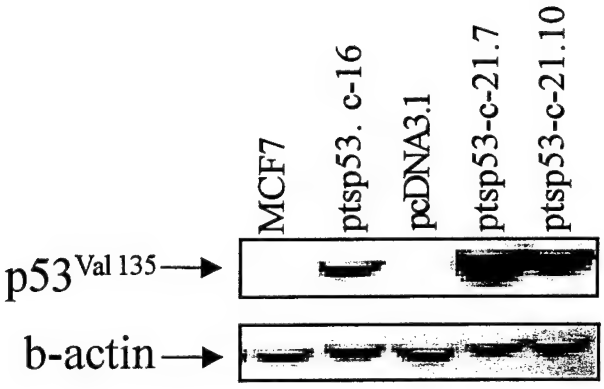
MCF7
ptsp53. c-16
pcDNA3.1
ptsp53-c-21.7
ptsp53-c-21.10
p53Val 135
b-actin

Figure 6

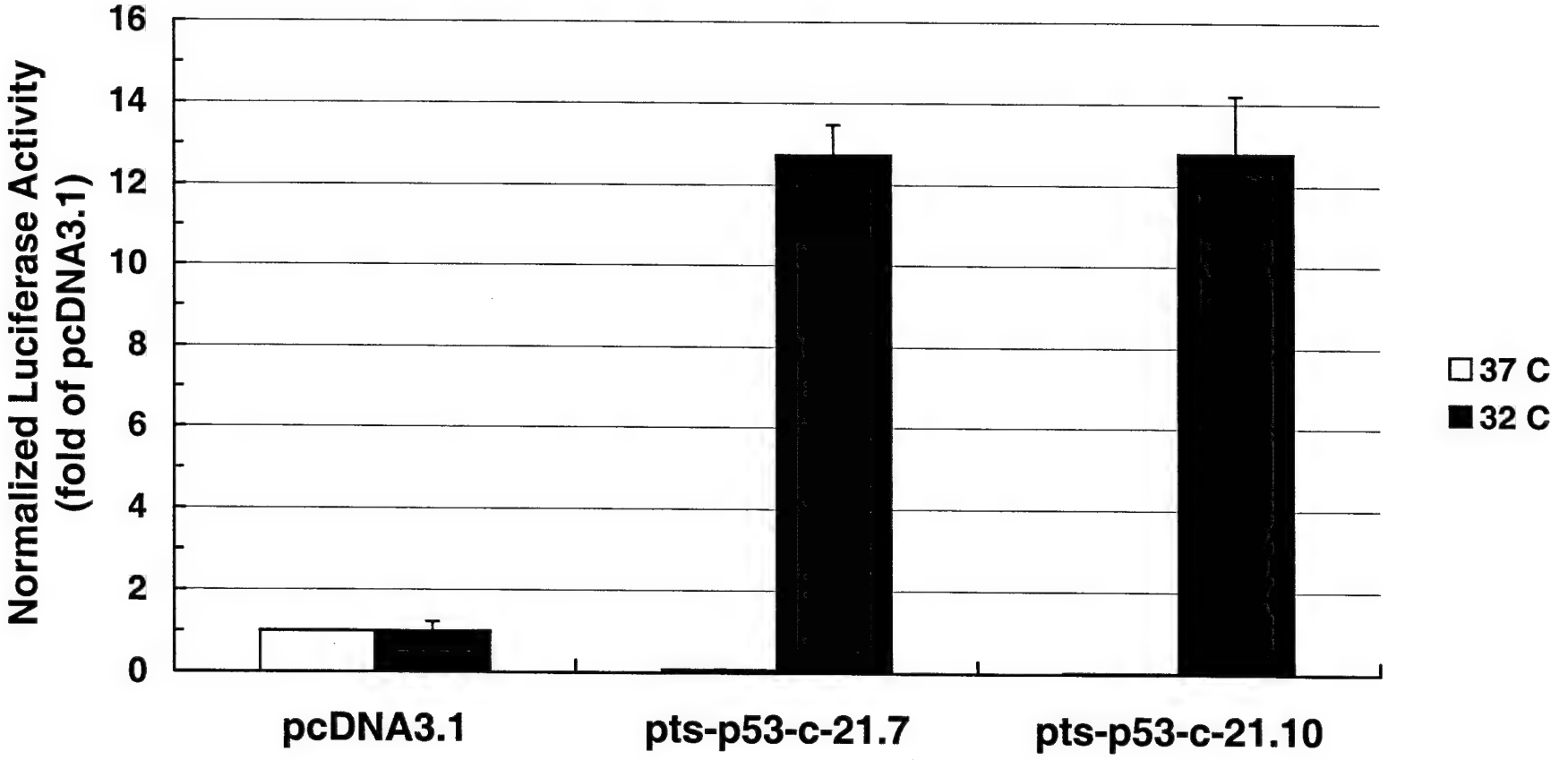
Normalized Luciferase Activity
(fold of pcDNA3.1)
16
14
12
10
8
6
4
2
0
pcDNA3.1
pts-p53-c-21.7
pts-p53-c-21.10
37 C
32 C

Figure 7

A: Viable Cell Number Count

37°C

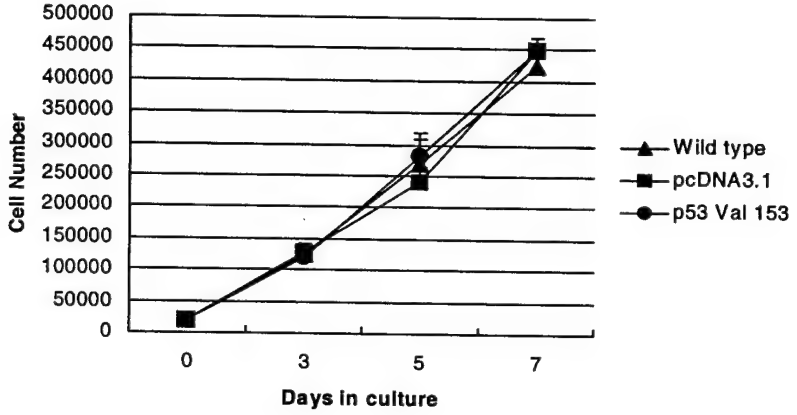

32°C

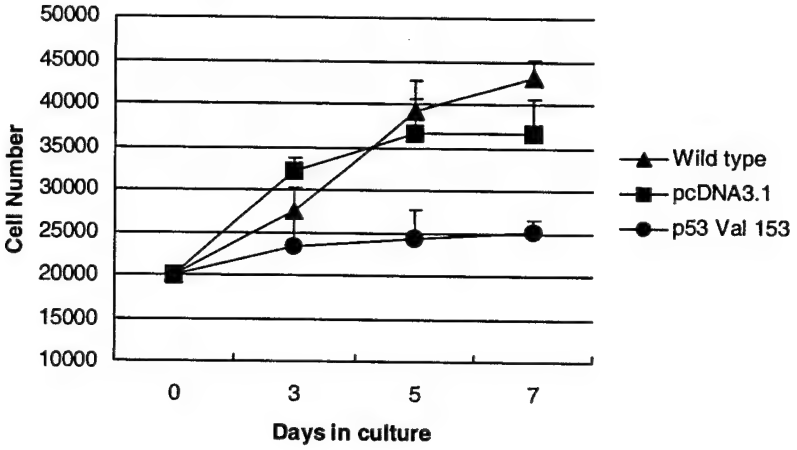

B: DNA Content

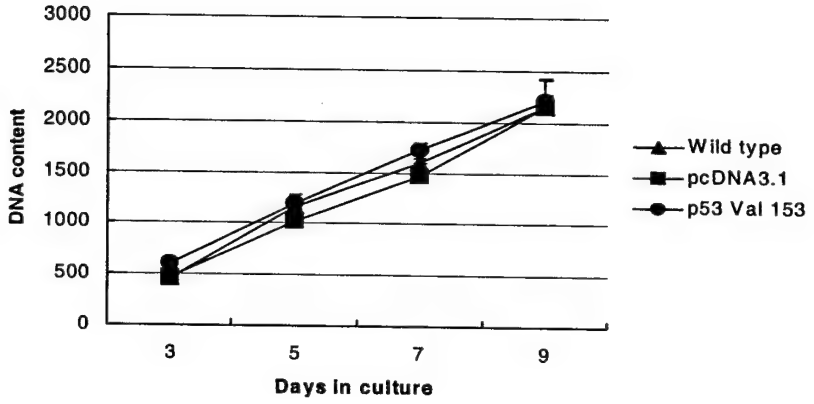

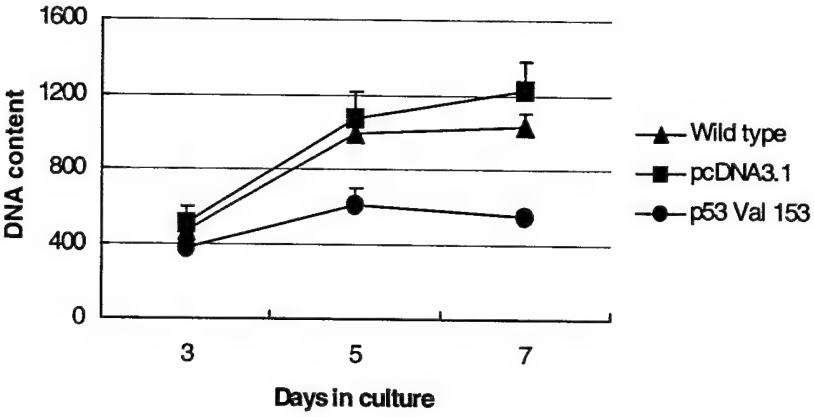

Figure 8

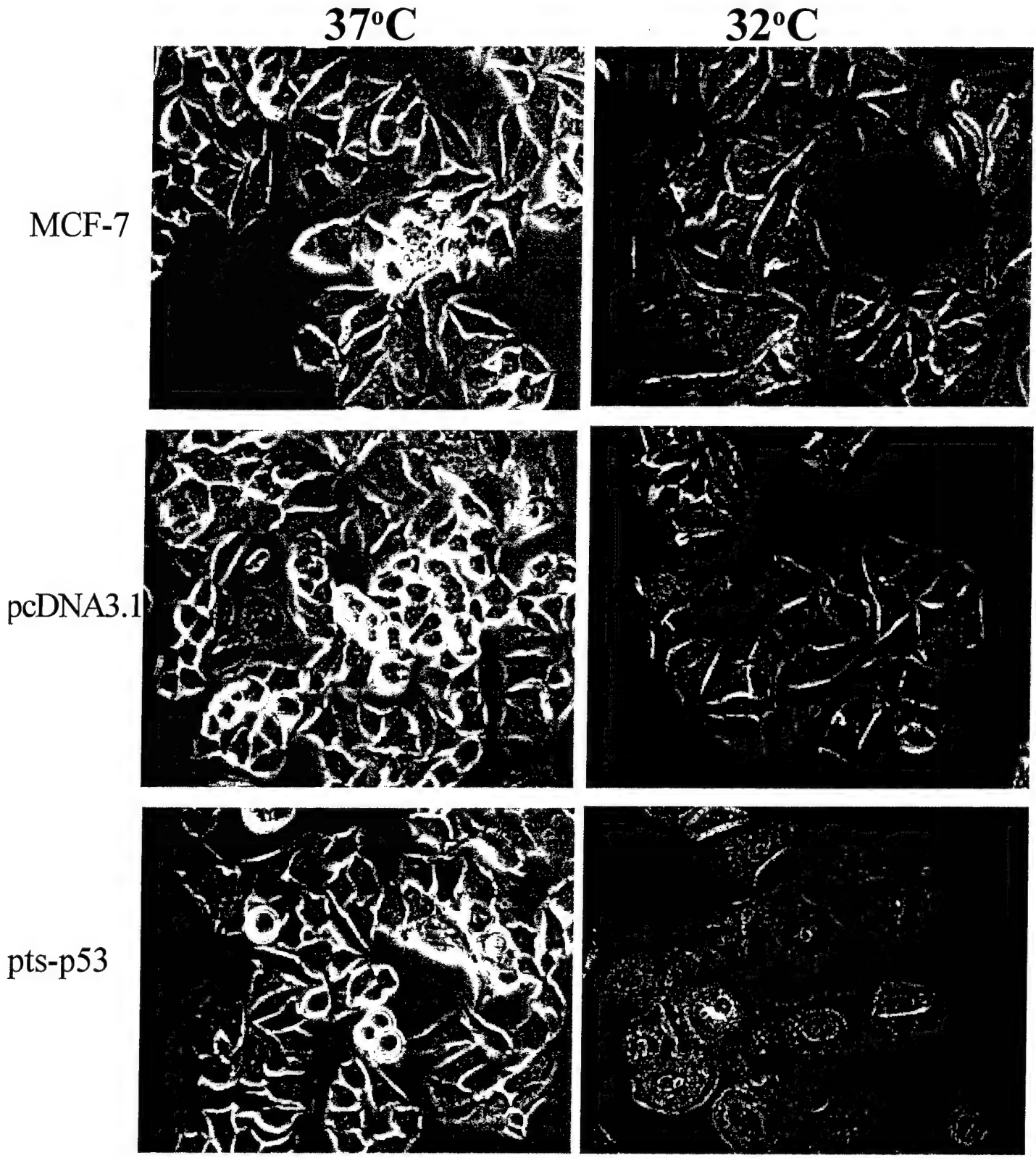

Figure 9

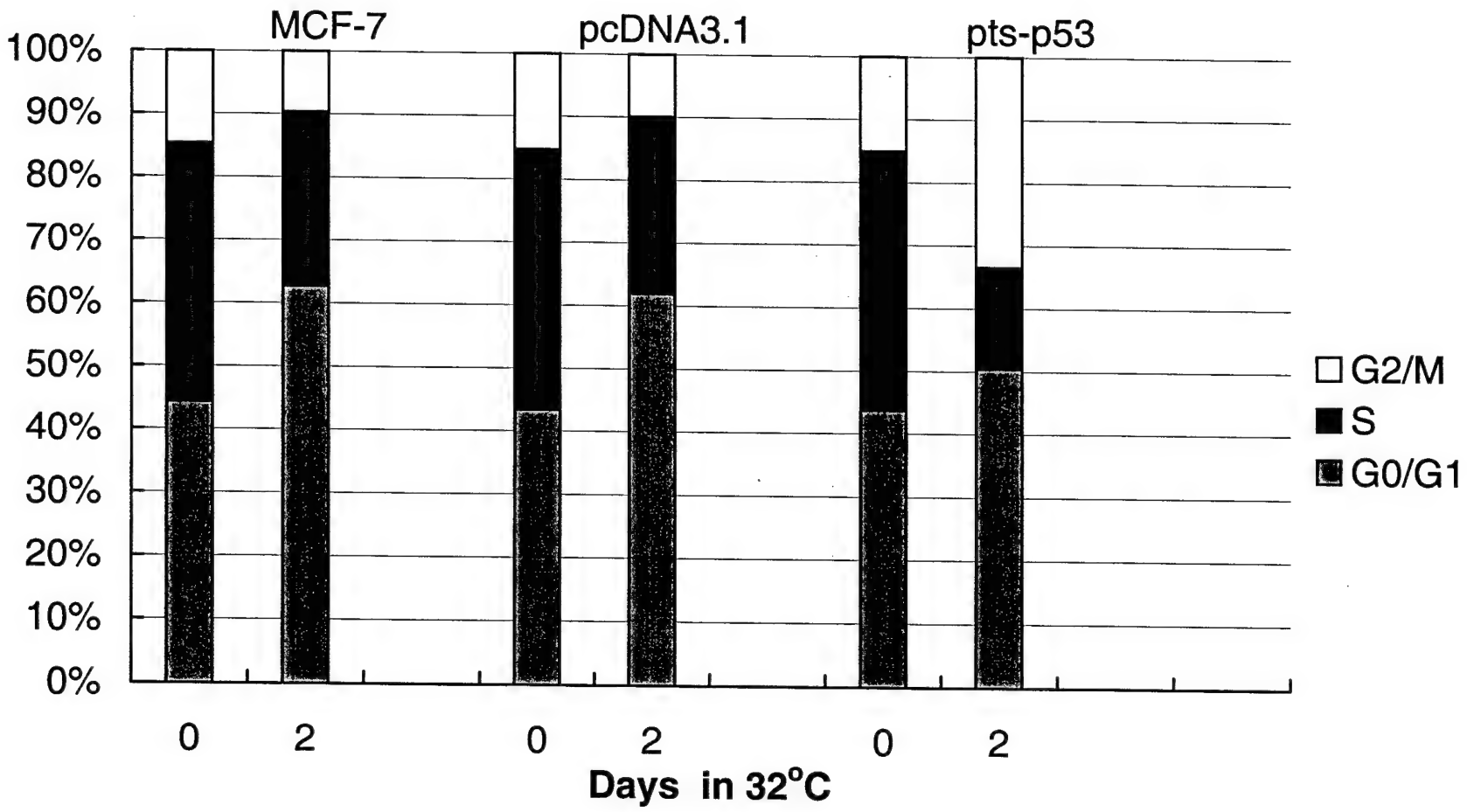
MCF-7
pcDNA3.1
pts-p53
100%
90%
80%
70%
60%
50%
40%
30%
20%
10%
0%
0
2
0
2
0
2
Days in 32°C
G2/M
S
G0/G1

APPENDICES

I. Reprints

II. Manuscript submitted to Oncogene

Oncogene (2001) 20, 8193–8202

www.nature.com/onc

The critical role of the PE21 element in oncostatin M-mediated transcriptional repression of the p53 tumor suppressor gene in breast cancer cells

Cong Li[1], Thomas E Ahlborn[1], Kazuhiko Tokita[2], Linda M Boxer[1,3], Asao Noda[4] and Jingwen Liu*,[1]

[1]*Department of Veterans Affairs Palo Alto Health Care System, Palo Alto, California, CA 94304, USA;* [2]*Third Department of Internal Medicine, Kyoto Prefectural University of Medicine, Kawaramachi-Hirokoji, Kamigyoku, Kyoto 602-8566, Japan;* [3]*Department of Medicine, Stanford University School of Medicine, Stanford, California, CA 94305, USA;* [4]*Department of Radiation Biophysics and Genetics, Kobe University School of Medicine, 7-5-1 Kusunokicho, Chuo-Ku, Kobe 650-0017, Japan*

Cytokine oncostatin M (OM) exerts growth-inhibitory and differentiative effects on breast cancer cells. Previously we showed that the transcription from the p53 gene in breast cancer cells was down regulated by OM. To elucidate the molecular mechanisms underlying the OM effect on p53 transcription, in this study, we dissected the p53 promoter region and analysed the p53 promoter activity in breast tumor cells. We showed that treatment of MCF-7 cells with OM induced a dose- and time-dependent suppression of p53 promoter activity. The p53 promoter activity was decreased to 35% of control at 24 h and further decreased to 20% at 48 h by OM at concentrations of 5 ng/ml and higher. Deletion of the 5′-flanking region of the p53 promoter from −426 to −97 did not affect the OM effect. However, further deletion to −40 completely abolished the repressive effect of OM. The p53 promoter region −96 to −41 contains NF-κB and c-*myc* binding sites, and a newly identified UV-inducible element PE21. Mutations to disrupt NF-κB binding or c-*myc* binding to the p53 promoter decreased the basal promoter activity without affecting the OM-mediated suppression, whereas mutation at the PE21 motif totally abolished the OM effect. We further demonstrated that insertion of PE21 element upstream of the thymidine kinase minimal promoter generated an OM response analogous to that of the p53 promoter. Finally, we detected the specific binding of a nuclear protein with a molecular mass of 87 kDa to the PE21 motif. Taken together, we demonstrate that OM inhibits the transcription of the p53 gene through the PE21 element. Thus, the PE21 element is functionally involved in p53 transcription regulated by UV-induction and OM suppression. *Oncogene* (2001) **20,** 8193–8202.

*Correspondence: J Liu, VA Palo Alto Health Care System, 3801 Miranda Avenue, Palo Alto, California, CA 94304, USA;
E-mail: Jingwen.Liu@med.va.gov
Received 13 June 2001; revised 19 September 2001; accepted 9 October 2001

Keywords: p53 tumor suppressor gene; transcriptional regulation; oncostatin M

Introduction

The p53 tumor suppressor protein is involved in several central cellular processes that are critical for maintaining cellular homeostasis, including gene transcription (Nakano *et al*., 2000; Xu *et al*., 2000), DNA repair (Kao *et al*., 2000; Zhu *et al*., 2000), cell cycling (Jeffy *et al*., 2000; Hirose *et al*., 2001), senescence (Peeper *et al*., 2001; Seluanov *et al*., 2001), and apoptosis (Uberti and Grilli, 2000; Zeng *et al*., 2000). Compared to the vast information and knowledge available regarding the regulation of p53 protein expression and function (Wang and Friedman, 2000; Ito *et al*., 2001; Wang *et al*., 2001), there is only a small amount of literature on transcriptional regulation of the p53 gene (Balint and Reisman, 1996; Benoit *et al*., 2000; Mokdad-Gargouri *et al*., 2001). However, control of p53 gene expression at the transcriptional level has been shown to play important roles in mitogenic stimulation or factor induced differentiation (Reich and Levine, 1984; Soini *et al*., 1992;). Moreover, the deregulated transcription of p53 accounts for at least in part, the elevated expression of mutant p53 in tumor cells (Balint and Reisman, 1996).

Since cloning of the human p53 promoter in 1989 (Tuck and Craword, 1989), several transcription factors have been identified that interact with specific regions of the p53 promoter to positively or negatively regulate transcription. The transcription factors shown to positively regulate p53 transcription include c-*myc* (Kirch *et al*., 1999; Lee and Rho, 2000), NF-κB (Pei *et al*., 1999; Benoit *et al*., 2000), YY1/NF1 (Lee *et al*., 1998, 1999; Nayak and Das, 1999), Ap1 (Kirch *et al*., 1999), and the HoxA5 homeobox containing gene product (Raman *et al*., 2000). Members of the PAX family are the only mammalian nuclear proteins shown to repress p53 transcription through a binding site present in the first non-coding exon (Stuart *et al*., 1995).

Recently, a novel 21 bp motif, named the PE21 element, was identified in the human p53 promoter that is located immediately upsteam of the NF-κB binding site (Noda *et al*., 2000). It was shown that the PE21 element covering the region of −79 to −59 is a primary determinant for the basal transcription of the p53 gene and the sequence required for UV-induced transcription in human fibroblasts. Mutations within this region drastically reduced the basal promoter activity and abolished the UV-induction. Interestingly, this 21 bp motif appears to have a function in initiation of transcription in a bi-directional manner. Insertion of multiple copies of PE21 in the sense or antisense orientiation into a promoterless luciferase reporter pGL2-basic initiated the transcription of the luciferase gene and generated an UV-inducible response as well. It remains to be elucidated whether the PE21 element has a functional role in p53 transcription regulated by cellular factors or other extracellular stimuli. Furthermore, the PE21 binding proteins need to be identified and characterized.

Oncostatin M (OM), a 28 kDa glycoprotein, is a cytokine produced by activated T lymphocytes and macrophages (Zarling *et al*., 1986). Previous studies showed that OM inhibits the growth of several breast cancer cell lines, including MCF-7, MDA-MB231, and H3922, which is a cell line derived from an infiltrating ductal carcinoma (Horn *et al*., 1990; Douglas *et al*., 1997, 1998; Liu *et al*., 1997; Spence *et al*., 1997). Breast cancer cells respond to OM treatment with reduced growth rates and the appearance of differentiated phenotypes. However, OM treatment does not appear to lead to apoptosis. Since the p53 tumor suppressor protein plays important roles in cellular proliferation and differentiation, we examined the effects of OM on p53 expression in breast cancer cells. Surprisingly, we found that p53 expression was down regulated by OM in MCF-7, MDA-MB231, and H3922 cells (Liu *et al*., 1999). Decreased levels of p53 protein and mRNA were detected after 1 day of OM treatment and reached maximal suppression of 10–20% of control after 3 days in H3922 cells. Nuclear run-on assays further demonstrated that OM decreased the number of actively transcribed p53 mRNA. These studies suggest that OM may repress p53 gene transcription. The effect of OM on p53 transcription appears to precede its effects on cell growth inhibition and induction of morphological changes, as the retardation of cell growth by OM as measured by [^{3}H]-thymidine incorporation could be detected after 2 days but a decrease in the level of p53 mRNA could be detected as early as 6–8 h.

In order to delineate the molecular mechanisms by which OM regulates p53 transcription and to understand the relationship between p53 expression and proliferation and differentiation of breast cancer cells, in this study we dissected the p53 promoter region to identify the *cis*-acting element that mediates the OM effect in MCF-7 cells. Our results demonstrate that the effect of OM is not mediated through the known repressor PAX binding site. Instead the PE21 element is responsible for OM-induced suppression of p53 transcription. Mutation of PE21 in the context of the p53 promoter completely abolished the inhibitory activity of OM on p53 transcription. By contrast, insertion of the PE21 motif into an OM-unresponsive TK promoter created a phenomenon of transcriptional suppression, resembling the p53 promoter.

Results

Deletion analysis to define the regulatory sequences involved in the basal transcriptional activity of the p53 promoter in breast tumor cells

The regulatory sequences that control p53 transcription in breast tumor cells have not been clearly defined, although a number of studies had examined p53 promoter activity in other cell types. Thus, initially in the present study, we generated a series of reporter constructs in which luciferase gene is driven by varying lengths of the 5′-flanking region of the p53 gene. These constructs were tested for activity in MCF-7 cells. A diagram of the deletion constructs is shown in Figure 1. Figure 2a compared the basal promoter activity of the deletion constructs with the activity of the full promoter construct pGL3-p53Luc that contains a 599 bp fragment of the p53 promoter (−426 to +172) (Liu *et al*., 1999). These results, representing 6–8 separate transfections, showed that deletion of the 5′-flanking region from −426 to −177 did not affect the p53 promoter activity, whereas deletion down to −97 (5′ Del-4) significantly lowered the basal activity to approximately 40% of the full promoter. Further deletion to −41 (5′ Del-5) to eliminate the binding sites for NF-κB and c-*myc* drastically reduced the basal promoter activity to a level below 5% of the full promoter. These data suggest that the transcription factors NF-κB and c-*myc* play critical roles in the basal transcriptional activity of the p53 gene in breast tumor cells, however, the promoter region covering −176 to −97 may contain a regulatory sequence that is responsible for the maximal basal transcriptional activity of the p53 gene in MCF-7 cells.

The p53 promoter region from −176 to −97 contains a stretch of CT rich sequence (CCCTCCTCCCC −174 to −164), a potential binding site for the transcription factor Sp1. To determine whether Sp1 interacts with this sequence, electrophoretic mobility shift assay (EMSA) was conducted with the nuclear extract isolated from MCF-7 cells and a ^{32}P-labeled double-stranded oligonucleotide, p53-Sp1, corresponding to the promoter region −183 to −154. Upon incubation of p53-Sp1 with nuclear extract, two DNA-protein complexes were detected (Figure 2b, lane 1). Formation of these complexes was inhibited by competition with a 100-fold molar excess of the unlabeled probe p53-Sp1 (lane 2), but was not inhibited by the oligonucleotide p53-mSp1 that contains mutations within the CT-stretch (lane 3).

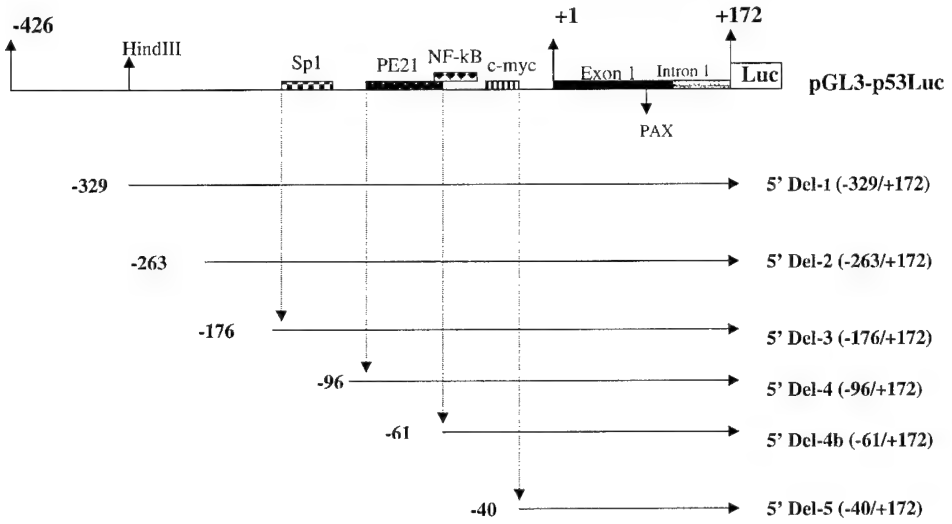

Figure 1 Schematic representation of p53 promoter luciferase reporter plasmid. A 599 bp fragment of the p53 gene covering −426 to +172 was inserted into 5′ *KpnI* and 3′ *Bgl*II sites of the promoter-less luciferase reporter pGL3-basic. The 5′ deletion fragments of the p53 promoter were synthesized by PCR using pGL3-p53Luc as the template. The p53 promoter fragments were inserted into 5′ *Sac*I and 3′ *Xho*I sites of pGL3-basic. The most 3′ end of the major transcription initiation site for the human p53 gene is defined as +1 and the locations of the 5′ ends of the promoters are indicated by the negative numbers of nucleotides relative to the transcription start site

The faster moving complex was supershifted by the anti-Sp3 antibody (lane 5), whereas the slower moving complex was partially supershifted by the anti-Sp1 antibody (lane 4). Inclusion of anti-Sp1 and anti-Sp3 antibodies together in the reaction mixture completely supershifted both complexes (lane 6). These data demonstrate that transcription factors Sp1 and Sp3 bind to this CT-rich region of the p53 promoter.

To determine the function of Sp1/Sp3 in mediating the p53 basal promoter activity, the Sp1 site in p53Luc was mutated (CCCTCCTCCCC to CGCTCGTCGCC) and the mutated reporter p53Luc-mSp1 along with the wild type vector p53Luc were transfected into MCF-7 cells. Figure 2c shows that mutation of this Sp1 site lowered the p53 promoter activity by approximately 50%, thereby suggesting that loss of the Sp1/Sp3 binding to the CT-rich region is primarily responsible for the diminished basal promoter activity of the deletion mutant 5′ Del-4. These results together demonstrate that Sp1 and Sp3 are positive trans-activators of p53 transcription and that their binding to the CT rich sequence contributes to the basal transcriptional activity of the p53 gene.

Dose-dependent and time-dependent responses of p53 transcription to OM

Next, the effect of OM on p53 promoter activity in MCF-7 cells was examined. The full promoter construct p53Luc was transiently transfected into MCF-7 cells along with the renilla luciferase expression vector pRL-TK. After transfection, cells were untreated or treated with OM at different concentrations for 48 h. Figure 3a shows that the suppressive effect of OM on p53 promoter activity was detected at 0.1 ng/ml, and a maximal suppression of 75–80% of p53 promoter activity was observed at 5 ng/ml. The inhibitory effect of OM on p53 transcription was also time-dependent. The p53 promoter activity was decreased to 67% of control by 8 h, lowered to 35% by 24 h, and further declined to 20% of control by 48 h after treating cells with a saturable concentration of OM. These results clearly demonstrate that OM represses p53 promoter activity in a dose-dependent and a time-dependent manner that is directly correlated with the effects of OM on p53 mRNA expression, as we previously reported (Liu *et al*., 1999).

The biological functions of OM can be mediated through two types of receptor complexes, the leukemia inhibitory factor (LIF)/OM shared receptor (type I) and the OM-specific receptor (type II). Previous studies have shown that MCF-7 cells express both the type I and the type II receptors of OM (Estrov *et al*., 1995). To determine which receptor complex mediates the effect of OM on p53 transcription, we compared the effect of OM with that of LIF on p53 promoter activity. As shown in Figure 4, in contrast to the strong inhibitory effect of OM, LIF at saturable concentrations (50 and 100 ng/ml) had no effect at all on the activity of p53 promoter p53Luc, thereby implying that OM regulates the transcription of the p53 gene mainly through the type II OM-specific receptor not the OM/LIF shared receptor type I complex.

Dissection of the p53 promoter to define the OM-responsive region

To define the OM-responsive region in the p53 promoter, the 5′ and 3′ deletion constructs of the p53

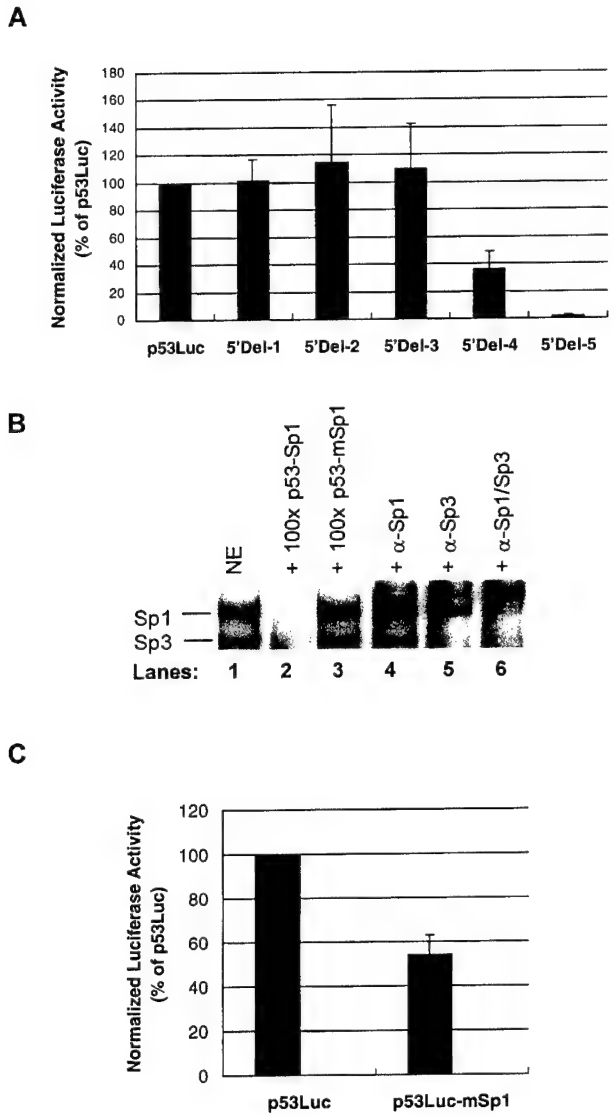

Figure 2 P53 promoter deletion and mutation analysis to define functional regulatory sequences that control the basal promoter activity of the p53 gene. (**a**) Deletion analysis: p53Luc and 5′ deletion constructs containing various lengths of the promoter were transfected into MCF-7 cells along with the vector pRL-TK. Cell lysate was harvested 40 h after transfection. The normalized luciferase activity of p53Luc is expressed as 100%. The data (mean ± s.d.) shown are derived from 6–8 separate transfection experiments in which triplicate wells were assayed. (**b**) EMSA: A double stranded oligonucleotide corresponding to the p53 promoter region −183 to −154, designated as p53-Sp1, was radiolabeled and incubated with 10 μg of nuclear extract prepared from MCF-7 cell in the absence (lane 1) or in the presence of 100-fold molar unlabeled competitors (lanes 2, 3), or in the presence of antibodies (lanes 4–6). The reaction mixture was loaded onto a 6% polyacrylamide gel and run in TGE buffer at 30 mA for 2.5 h at 4°C. (**c**) Mutation analysis: p53Luc-wt and p53Luc-mSp1 were transiently transfected into MCF-7 along with the vector pRL-TK. The normalized luciferase activity of p53Luc-wt is expressed as 100%. The p53Luc-mSp1 exhibited 54.1% activity compared with p53Luc-wt

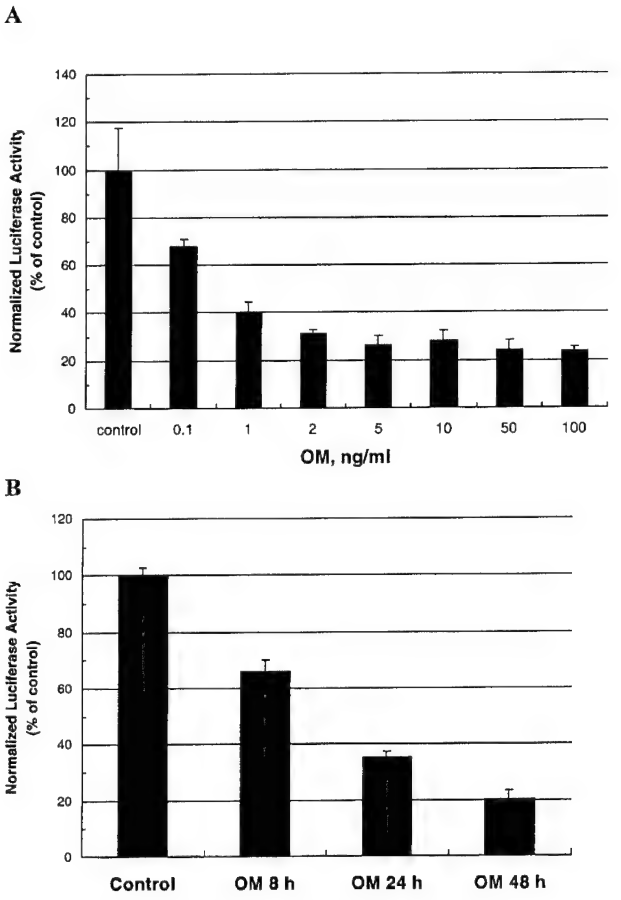

Figure 3 OM down-regulates p53 promoter activity in a dose-dependent and a time-dependent manner. MCF-7 cells were transfected with p53Luc along with the vector pRL-TK. (**a**) After addition of DNA into the medium, OM dilution buffer or OM at different concentrations were added to the cells and cells were harvested 40 h later. (**b**) After addition of DNA into the medium, OM at a saturable concentration (50 ng/ml) was added to the cells at different times and cells were harvested together after 48 h of transfection. The normalized luciferase activity of transfected cells that were untreated is expressed as 100%. The data (mean ± s.d.) shown are representative of three independent transfection experiments in which triplicate wells were transfected for each condition

promoter were transfected into MCF-7 cells. Then the transfected cells were untreated or treated with OM for 40 h prior to cell lysis. The results of 6–8 transfection assays using 5′ deletion constructs are summarized in Figure 5. These results showed that deletion of the 5′-flanking region from −426 to −97 did not affect the OM response. In contrast, further deletion to −41 (5′ Del-5) eliminated the OM effect. These data suggest that the promoter region covering −96 to −40 is not only important for the basal transcriptional activity as shown in Figure 2a but it may also contain the critical OM-responsive element. Furthermore, shortening of the 3′ region from +172 to +14 to delete the PAX binding site had no effect on OM-mediated suppression or the basal promoter activity, thereby excluding the involvement of the repressor PAX in OM-mediated down regulation of p53 transcription (data not shown).

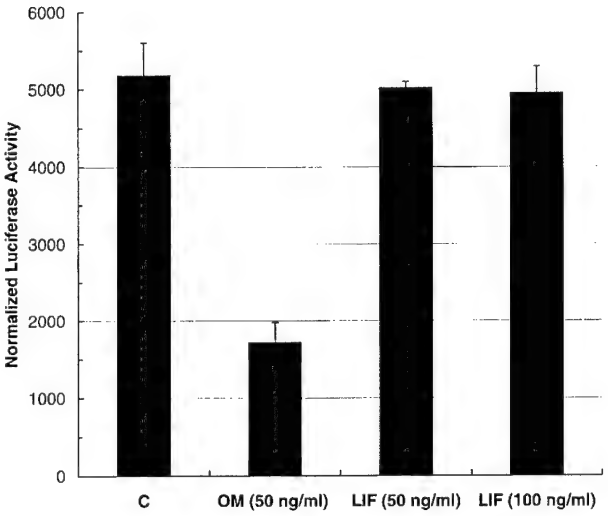

Figure 4 Comparison of inhibitory effect of OM and LIF on p53 promoter activity. MCF-7 cells were transfected with p53Luc along with the vector pRL-TK. After addition of DNA into the medium, OM or LIF at indicated concentrations were added to the cells and cells were harvested 40 h later

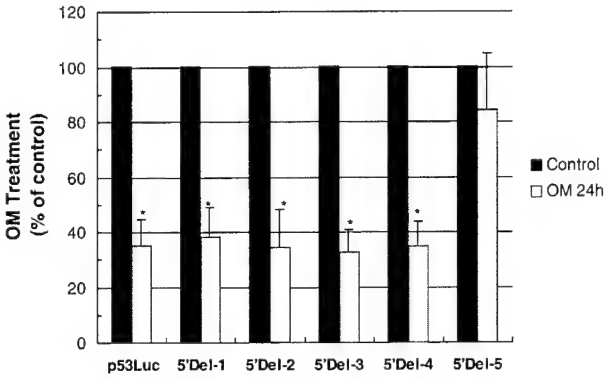

Figure 5 The proximal region of the p53 promoter contains an OM-responsive element. P53Luc and 5′ deletion constructs containing various lengths of the promoter were transfected into MCF-7 cells along with the vector pRL-TK. After transfection, cells were incubated in the presence or absence of OM 50 ng/ml for 24 h. The normalized luciferase activity of transfected cells that were untreated is expressed as 100%. The data (mean ± s.e.) shown were derived from 6–8 independent transfection assays. Differences in normalized luciferase activities between untreated and OM treated samples were evaluated using two tailed Student's *t*-test. A statistically significant difference ($P<0.05$) is indicated by an asterisk

Localization of the OM-responsive sequence to the PE21 element

The 5′ deletion analysis localized the OM-responsive sequence to the proximal region of the p53 promoter from −96 to −41. This region contains three important regulatory motifs including NF-κB, the E-box (c-*myc*), and the newly identified UV-inducible PE21 element. To investigate the role of these regulatory sequences in OM-mediated suppression, site-directed mutagenesis was conducted on the full promoter p53Luc to mutate each binding site individually. Figure 6 shows that mutation of the c-*myc* site lowered the basal promoter activity 75% without affecting the OM effect. Likewise, mutation of the NF-κB binding site decreased the basal promoter activity 85% with little effect on OM. By contrast, mutation at the PE21 element drastically reduced the basal promoter activity and rendered the p53 promoter unresponsive to OM. To confirm this finding, the PE21 element was mutated in the vector 5′ Del-4 that contains the minimal sequence for the basal transcription and the OM-mediated suppression. Again, the OM inhibitory effect was not observed in the PE21 mutant in the context of this short promoter fragment. Similarly, the suppressive effect of OM was not seen on the plasmid 5′ Del-4b in which the PE21 element was deleted.

Next, we were interested in determining whether OM could exert its effect on PE21 in the context of a heterologous promoter that contains the PE21 element without auxiliary sequences of p53 promoter. To test this, luciferase reporters containing different copies of PE21 in tandem inserted 5′ upstream of a minimal HSV tk promoter (pTKLuc) in either sense, pTKLuc-PE21 (S), or antisense, pTKLuc-PE21 (As) orientations were transfected into MCF-7 cells. The plasmid pTKLuc produced low but measurable luciferase activity in MCF-7 cells and OM treatment did not lower the activity. Inclusion of the PE21 sequence in either direction greatly increased luciferase activities from 20–400-fold of the pTKLuc. The fold increase of luciferase activity was correlated with the increase in PE21 copy number in most cases and showed a preference with the antisense orientation. Importantly, in contrast to the vector pTKLuc, the reporters containing the PE21 element clearly displayed responses to OM with luciferase activities reduced to 39 to 59% of control in the OM treated cells (Figure 7), comparable to the OM effect observed in the native p53 promoter. Together, our results presented in Figures 6 and 7 provide strong evidence that the PE21 element plays an important role in the basal transcription of the p53 gene and is also critically involved in the OM-induced transcriptional suppression of the p53 gene in breast cancer cells.

Characterization of nuclear proteins that interact with the PE21 element

To detect nuclear proteins in MCF-7 cells that specifically interact with the PE21 sequence, EMSA was conducted with ^{32}P-labeled oligonucleotide p53-PE21 containing the PE21 and flanking sequence, and nuclear extracts prepared from untreated or OM 40 h-treated cells. Figure 8 shows that three specific complexes were detected in both control and OM-treated nuclear extracts. The formation of these complexes was inhibited with 100-fold molar excess of unlabeled probe (lanes 2, 7) but was not inhibited by a 100-fold molar excess of an unrelated DNA containing an estrogen response element (lanes 5, 10). An oligonucleotide containing the NF-κB site of the p53

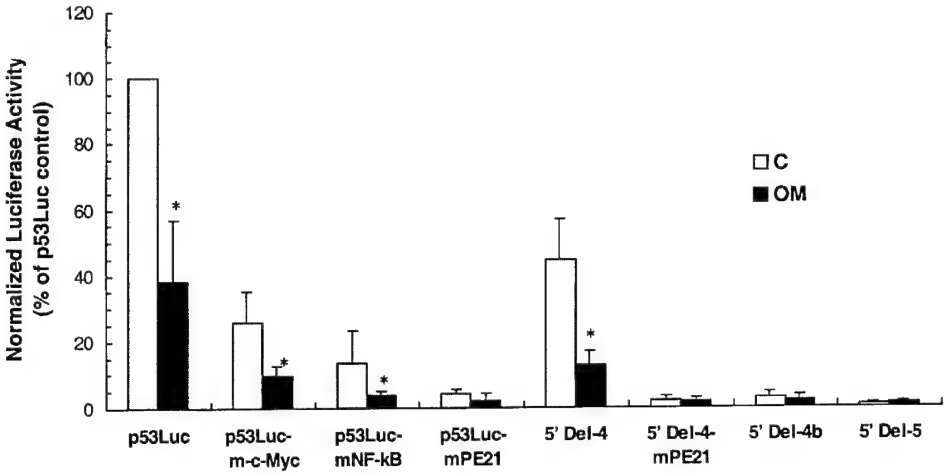

Figure 6 Localization of the OM response to the PE21 element in the human p53 promoter. P53 promoter reporter wild type and mutants were transfected into MCF-7 cells individually. After transfection, cells were incubated in the presence or absence of OM (50 ng/ml) for 40 h. The data represent the results of 6–8 independent transfections. The normalized luciferase activity of each vector was expressed as the per cent of luciferase activity of p53Luc wild type vector in untreated control cells. An asterisk sign indicates that there is a statistically significant difference between the untreated control and the OM treated sample

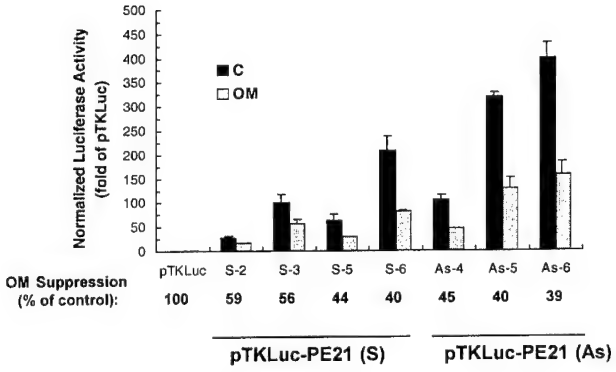

Figure 7 Effects of OM on heterologous promoter constructs containing the PE21 element. The pTKLuc-PE21 vectors were constructed by insertion of sequences of the PE21 element in tandem in sense (S) or antisense (As) orientation adjacent and upstream of the TATA box from the HSV tk promoter. The number indicates the number of repeat of the PE21 element in each construct. These vectors were transiently transfected into MCF-7 cells and examined for responses to OM treatment as described in Figure 5. The data shown are representative of 3–4 separate transfections

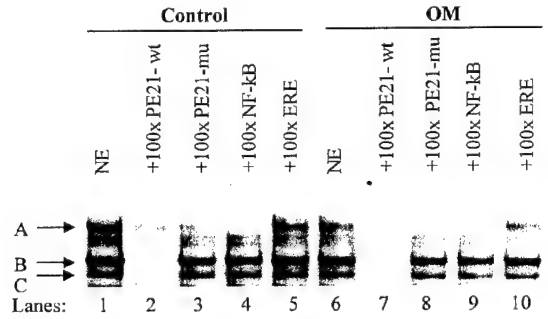

Figure 8 EMSA analysis of nuclear proteins interacting with the PE21 motif. A double stranded oligonucleotide, designated as p53-PE21, was radiolabeled and incubated with 10 μg of nuclear extracts prepared from untreated (lanes 1–5) or OM 40 h treated MCF-7 cell (lanes 6–10) in the absence (lanes 1, 6) or in the presence of 100-fold molar unlabeled competitors. The reaction mixture was loaded onto a 6% polyacrylamide gel and run in TGE buffer at 30 mA for 2.5 h at 4°C

promoter competed for the binding of complex A but not complexes B and C (lanes 4, 9). The binding of complex A was also competed by oligonucleotide p53-mPE21 that contains a 3 bp mutation within the PE21 sequence (lanes 3, 8). These data suggest that the complex A was formed at sequences that flank the PE21 core element. Thus, the identity of complex A was not further investigated in this study since the emphasis of this study is on the PE21 core element.

Complexes B and C are PE21 specific as the oligonucleotide p53-mPE21 lost the ability to compete with the binding of these two complexes to the labeled PE21 probe. Apparently OM treatment of 40 h did not altered the pattern of the complexes or the intensity of the binding signals. Similar results were obtained with the nuclear extracts treated with OM for different length of times including 6 and 24 h. These observations were consistent with previous results of UV-induction. It was shown that the binding of nuclear proteins of fibroblasts without or with UV-irradiation to the PE21 probe was not different (Noda *et al.*, 2000).

Previous studies conducted in human fibroblasts did not characterize the protein/DNA complex of the PE21 sequence. It is unknown whether a single DNA binding protein or multiple proteins interact with the PE21 motif. To characterize the MCF-7 nuclear proteins present in the PE21 DNA complexes, EMSA with MCF-7 nuclear extract and the labeled PE21 probe was followed by UV cross-linking. Complex B was excised from the gel and the protein components were analysed by denaturing SDS-polyacrylamide gel electrophoresis (SDS–PAGE).

Analysis of the SDS–PAGE revealed that one protein was crosslinked to the labeled PE21 probe (Figure 9). After correction for the bound oligonucleotide, the molecular mass of the protein appeared to be 87 kDa. A similar procedure was used to characterize complex C, but the UV-crosslinking experiments failed to detect any proteins present in the complex C, probably due to the low abundance of the complex and low efficiency of the UV-crosslinking.

Discussion

The PE21 element was originally discovered by searching for the sequence that was responsible for the UV-induced transcription of the p53 gene in human fibroblasts (Noda *et al*., 2000). Intriguingly, in this study, we found that the repressive effect of OM on p53 transcription was also mediated through this regulatory element. Our studies further highlight the importance of the PE21 element in the control of p53 gene transcription.

Our studies clearly demonstrate that the PE21 element is a critical sequence that controls p53 transcription in breast cancer cells, as mutation of this sequence produced the severest impact on p53 promoter activity in MCF-7 cells as compared to mutations on other functional sites such as NF-κB or the bHLH c-*myc* binding site. Mutations to disrupt the binding of NF-κB to its recognition sequence adjacent to PE21 lowered the basal promoter activity to 15% of the wild type promoter; mutation of the basic HLH site to interfere the binding of c-*myc* reduced the basal transcription by 75%. In contrast, alteration of 3 bp within the PE21 motif nearly eliminated the transcriptional activity of the p53 promoter. The promoter activity with the PE21 mutant was less than 5% of the wild type promoter. The ability of PE21 in activation of gene transcription was further demonstrated by its strong inducing effect on pTKLuc that contains a weak promoter composed a TATA box and one non-functional Sp1 site.

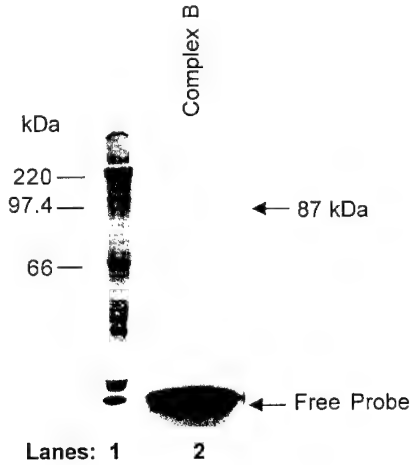

Figure 9 Denaturing SDS-polyacrylamide gel analysis of the UV cross-linked complex B formed with MCF-7 control nuclear extract and the PE21 probe. The positions of ^{14}C-labeled molecular mass markers are shown in lane 1, and the protein detected from complex B is shown in lane 2. After correction for the bound oligonucleotide, the molecular mass of the band is 87 kDa. A very faint signal, possibly caused by insoluble materials, was seen in the interface of the stacking gel and the separating gel

In this study we showed that mutations of the PE21 element in the context of the full p53 promoter (p53Luc) or in the context of the short promoter fragment (5′ Del-4) that retains 40% of the p53 promoter activity completely eliminated the inhibitory effect of OM on p53 transcription. In contrast, mutations at other functional sites including NF-κB or c-*myc* did not abolish the OM inhibitory activity. The critical role of the PE21 site in OM-mediated repression of p53 transcription is further supported by the results of transfection with the pTKLuc-PE21 reporters. OM had no effect on the promoter activity of pTKLuc. However, the promoter activities of pTKLuc-PE21 in either the sense or antisense orientation were clearly suppressed by OM to levels comparable to that observed in the p53 promoter. These results suggest that the PE21 element is the primary *cis*-acting sequence that mediates the OM-induced transcriptional repression of the p53 gene.

We were able to detect two DNA-protein complexes formed with the PE21 sequence from MCF-7 cells. Complex B was relatively more abundant than complex C. EMSA experiments followed by UV-cross linking and SDS–PAGE revealed that a nuclear protein with a molecular mass around 87 kDa was present in complex B. Interestingly, in an effort to purify the PE21 binding proteins, two proteins with molecular weights of 80 and 85 kDa were isolated from Molt 4 cells through PE21-sepharose affinity column. These two proteins were shown to specifically bind to the PE21 probe (Noda *et al*., unpublished data). It is possible that the 87 kDa protein present in the complex B is identical or related to one of these two PE21 binding proteins. The relationship between complexes B and C is presently unknown. It is highly likely that more than one nuclear protein binds to the PE21 sequence. Alternatively, the faster moving complex C may represent a degradation product of the protein in complex B.

OM treatment did not alter the binding of nuclear proteins to PE21; the same two complexes were detected in the OM-treated sample as in the control. This result is not totally surprising as the previous studies with UV-induction did not detect a different binding pattern with the PE21 sequence and nuclear extracts isolated from UV-irradiated and non irradiated fibroblasts (Noda *et al*., 2000). Our results combined with the prior study suggest that regulation of p53 transcription through the PE21 element by OM is mediated by mechanisms other than direct alteration of the DNA binding activity of the PE21 interacting proteins. It is possible that there are other cofactors associated with the PE21 binding protein. OM treatment could interfere with this

association. The inability to detect changes of DNA binding activities of transcription factors to a functional regulatory element by gel shift assays has been described in other promoter studies. For example, the transcription of $p21^{WAF1/CIP1}$ gene is activated by TGFβ, phobol esters, and histone deacetylase inhibitors through a Sp1 site proximal to the p21 promoter. However, none of these activators altered the DNA binding activity of Sp1 (Datto *et al*., 1995; Briggs *et al*., 1996; Nakano *et al*., 1997; Sowa *et al*., 1997; Huang *et al*., 2000).

Previous studies have defined the p53 promoter as a TATA-less and GC-rich less promoter, as the TATA-box and GC-rich sequence are not present in the proximal promoter region of the p53 gene (Tuck and Craword, 1989). However, our studies with deletion and mutation analysis identified a novel Sp1/Sp3 binding site that covers the regions −174 to −165 of the p53 promoter. This Sp1 binding site is expendable for OM-mediated suppression of p53 transcription but is important for the basal transcriptional activity of p53 gene. Mutation or deletion of this CT-rich sequence decreased p53 promoter activity by 50–60%. The involvement of Sp1/Sp3 in p53 transcription is further demonstrated by our EMSA supershift assay that clearly showed Sp1 and Sp3 binding to this region. Therefore, it is highly likely that Sp1 as a ubiquitously expressed transcription factor has a functional role in p53 gene transcription.

In summary, our studies demonstrate that p53 transcription is down regulated by OM in growth-inhibited and differentiated breast cancer cells. The PE21 element mediates this repressive effect. It is interesting to speculate that the activities of several different intracellular signal transduction pathways converge at the PE21 element. The UV-induced activation of p53 transcription is linked to a stress signal. The OM-induced suppression likely involves the MAP kinase ERK pathway, as we have found that the effects of OM on p53 protein expression and on p53 promoter activity can be partially blocked by the MEK inhibitor PD98059 (Liu *et al*., 1999). Further studies to identify and characterize the PE21 element binding proteins will greatly facilitate the understanding of the role of the PE21 site in the control of p53 transcription and its connection to intracellular signaling in normal cells as well as in tumor cells.

Materials and methods

Cells and reagent

The human breast cancer cell line MCF-7 was obtained from American Type Culture Collection (Manassas, VA, USA) and cultured in RPMI-1640 medium supplemented with 10% heat inactivated fetal bovine serum (FBS). Human recombinant OM and LIF were purchased from the R&D systems (Minneapolis, MN, USA).

P53 promoter luciferase reporters

pGL3-p53Luc contains a 599 bp fragment of the human p53 promoter region and exon 1 (−426 to +172) (Liu *et al*., 1999). To construct 5′ Del-1 (−329 to +172), the pGL3-p53Luc was digested with restriction enzyme *Hind*III. The DNA fragment was isolated and subcloned into the *Hind*III site of pGL3-basic vector. Additional 5′ and 3′ deletion constructs were made by PCR with pGL3-p53Luc as the template. Table 1 describes the primer sequence of oligonucleotides utilized in the deletion and mutation analysis, as well as in EMSAs.

Transient transfection and luciferase assay

MCF-7 cells were plated at a density of 80 000 cells/well in 24-well plates and incubated for 24 h. Cells were cotransfected with 90 ng of various p53 promoter reporter plasmids and 10 ng of a pRL-TK as a normalizing vector per well by using Effectene transfection reagent (Qiagen). Transfected cells were incubated with human recombinant OM at a saturable concentration of 50 ng/ml or the OM dilution buffer (BSA 1 mg/ml in PBS) for 40 h prior to cell lysis. Luciferase activities were measured using the Promega Dual Luciferase Assay System. All the measured fire fly luciferase activity of the plasmid constructs was divided by the renilla

Table 1 Sequences of p53 promoter specific primers. Mutated nucleotides are in boldface and the binding sites are underlined

Primer	*Nucleotide sequence 5′ to 3′*
5′ deletion PCR primers	
5′ Del-2 5′	GAGCTCAAGCTTCTGCCCTCACAGCTCTGGCTTGCAG
5′ Del-3	GAGCTCAAGCTTCACCCTCCTCCCCAACTCC
5′ Del-4	GAGCTCAAGCTTGCTTTTGTGCCAGGAGCCTCG
5′ Del-5	GAGCTCAAGCTTGCTCAAGACTGGCGCTAAAAGTT
3′	GAAAATACGGAGCCGAGAGCC
EMSA oligonucleotides	
P53-Sp1 5′	GCACCCTCCTCCCCAACTCC
P53-mSp1 5′	GACTCTGCAC**GC**TC**GT**C**G**CCAACTCCATTTCCTTTGC
P53-PE21 5′	CCTCGCAGGGGTTGATGGGATTGGGGT
P53-mPE21 5′	CCTCGCAGGGGTTGATG**A**G**CT**CGGGGT
Mutation primers	
P53Luc-mNFκB 5′	GGGGTTGATGGGATT**ATC**GTTTT**AAG**CTCCCATGTGC
P53Luc-m-c-*myc* 5′	GGGATTGGGGTTTTCCCCTCCC**T**TG**GA**CTCAAGACTGGC
P53Luc-mPE21 5′	GCCTCGCAGGGGTTGATG**A**G**CT**CGGGGTTTTCCCCTCCC

luciferase activity of pRL-TK to normalize the transfection efficiency.

Electrophoretic mobility shift assays (EMSA)

Nuclear extracts of MCF-7 cells were prepared as previously described (Liu *et al*., 2000). Ten micrograms of nuclear extract were incubated with a ^{32}P-labeled 27 bp oligonucleotide containing the PE21 sequence for 15 min at RT and loaded onto 6% polyacrylamide gels and run in TGE buffer at 30 mA for 2.5 h at 4°C. The gels were dried and visualized on a PhosphorImager. For UV-cross-linking, after electrophoresis, the wet gel was exposed to a short-wave UV box from a distance of 2–3 cm at 4°C for 1 h as previously described (Phan *et al*., 1996). Then, the wet gel was briefly exposed to a PhosphoImager screen to locate the complexes. The region of the gel containing complex B was cut out, and the proteins were eluted at room temperature overnight in elution buffer containing 50 mM Tris-HCL (pH 7.9), 0.1% SDS, 0.1 mM EDTA, 5 mM DTT, 150 mM NaCl, and 50 μg/ml gamma-globulin. The eluted protein was precipitated with four volumes of dry ice-cold acetone, washed with ethanol, and air-dried. After resuspension in Laemmili loading buffer and heating, SDS-polyacrylamide gel electrophoresis was performed and the labeled protein was visualized by a PhosphorImager.

Abbreviations

EMSA, electrophoretic mobility shift assay; FBS, fetal bovine serum; LIF, leukemia inhibitory factor; OM, oncostatin M; TK, thymidine kinase

Acknowledgments

This study was supported by the Department of Veterans Affairs (Office of Research and Development, Medical Research Service), by grant (1RO1CA83648-01) from National Cancer Institute, and by grant (BC990960) from the United States Army Medical Research and Development Command.

References

Balint E and Reisman D. (1996). *Cancer Research*, **56**, 1648–1653.

Benoit V, Hellin A, Huygen S, Gielen J, Bours V and Merville M. (2000). *Oncogene*, **19**, 4787–4794.

Briggs J, Kudlow J and Kraft A. (1996). *J. Biol. Chem.*, **271**, 901–906.

Datto M, Yu Y and Wang X. (1995). *J. Biol. Chem.*, **270**, 28623–28628.

Douglas A, Goss A, Sutherland R, Hilton D, Berndt M, Nicola N and Begley C. (1997). *Oncogene*, **14**, 661–669.

Douglas A, Grant S, Goss G, Clouston D, Sutherland R and Begley C. (1998). *Int. J. Cancer*, **75**, 64–73.

Estrov Z, Samal B, Kellokumpulehtinen P, Sahin AA, Kurzrock R, Talpaz M and Aggarwal BB. (1995). *J. Interferon Cytokine Res.*, **15**, 905–913.

Hirose Y, Berger M and Pieper R. (2001). *Cancer Research*, **61**, 1957–1963.

Horn D, Fitzpatrick W, Gompper P, Ochs V, Bolton-Hanson M, Zarling J, Malik N, Todaro G and Linsley P. (1990). *Growth Factors*, **2**, 157–165.

Huang L, Sowa Y, Sakai T and Bpardee A. (2000). *Oncogene*, **19**, 5712–5719.

Ito A, Lai C, Zhao X, Saito S, Hamilton M, Appella E and Yao T. (2001). *EMBO J.*, **20**, 1331–1340.

Jeffy B, Chen E, Gudas J and Romagnolo D. (2000). *Neoplasia*, **2**, 460–470.

Kao S, Lemoine F and Marriott S. (2000). *J. Biol. Chem.*, **275**, 35926–35931.

Kirch H-C, Flaswinkel S, Rumpf H, Brockmann D and Esche H. (1999). *Oncogene*, **18**, 2728–2738.

Lee M, Song H, Park S and Park J. (1998). *Biol. Chem.*, **379**, 1333–1340.

Lee M, Song H, Yu S, Lee K and Park J. (1999). *Biochem. Cell. Biol.*, **77**, 209–214.

Lee S and Rho H. (2000). *Oncogene*, **19**, 468–471.

Liu J, Spence M, Wallace P, Forcier K, Hellstrom I and Vestal R. (1997). *Cell. Growth Differ.*, **8**, 667–676.

Liu J, Li C, Ahlborn T, Spence M, Meng L and Boxer L. (1999). *Cell. Growth Differ.*, **5**, 15–18.

Liu J, Ahlborn T, Briggs M and Kraemer F. (2000). *J. Biol. Chem.*, **275**, 5214–5221.

Mokdad-Gargouri R, Belhadj K and Gargouri A. (2001). *Nucleic Acids Res.*, **29**, 1222–1227.

Nakano K, Balint E, Ashcroft M and Vousden K. (2000). *Oncogene*, **19**, 4283–4289.

Nakano K, Mizuno T, Sowa Y, Orita T, Okuyama Y, Fujita T, Ohtani F, Matsukawa Y and Tokino T. (1997). *J. Biol. Chem.*, **272**, 22199–22206.

Nayak B and Das B. (1999). *Mol. Biol. Rep.*, **26**, 223–230.

Noda A, Toma-Aiba Y and Fujiwaba Y. (2000). *Oncogene*, **19**, 21–31.

Phan SC, Feeley B, Withers D and Boxer LM. (1996). *Mol. Cell. Biol.*, **16**, 2387–2393.

Peeper D, Dannenberg J, Riele H and Bernards R. (2001). *Nat. Cell. Biol.*, **3**, 198–203.

Pei X, Nakanish Y, Takayama K, Bai F and Hara N. (1999). *J. Biol. Chem.*, **274**, 35240–35246.

Raman V, Martensaen S, Reisman D, Evron E, Odenwald W, Faffee M and Sukumar S. (2000). *Nature*, **405**, 974–978.

Reich N and Levine A. (1984). *Nature*, **308**, 199–201.

Seluanov A, Gorbunova V, Falcovitz A, Sigal A, Milyavsky M, Zurer I, Shohat G and Goldfinger N. (2001). *Mol. Cell. Biol.*, **21**, 1552–1564.

Soini Y, Kamel D, Nuorva K, Lane D and Vahakangsa K. (1992). *Pathol. Anat. Histopathol.*, **421**, 415–420.

Sowa Y, Orita T, Minamikawa S, Nakano K, Mizuno T, Normura H and Sakai T. (1997). *Biochem. Biophys. Res. Comm.*, **241**, 142–150.

Spence M, Vestal R and Liu J. (1997). *Cancer Research*, **57**, 2223–2228.

Stuart E, Haffner R, Oren M and Gruss P. (1995). *EMBO J.*, **14**, 5638–5645.

Tuck S and Craword L. (1989). *Mol. Cell. Biol.*, **9**, 2163–2172.

Uberti D and Grilli M. (2000). *Amino Acids*, **19**, 253–261.

Wang J and Friedman E. (2000). *Mol. Carcinog.*, **29**, 179–188.

Wang X, Ongkeko W, Lau A, Leung K and Poon R. (2001). *Cancer Research*, **61**, 1598–1603.

Xu D, Wang Q, Gruber A, Bjorkholm M, Chen Z, Zaid A, Selivanova G, Peterson C, Wiman K and Pisa P. (2000). *Oncogene*, **19,** 5123–5133.

Zarling J, Shoyab M, Marquardt H, Hanson M, Lionbin M and Todaro G. (1986). *Proc. Natl. Acad. Sci. USA*, **83,** 9739–9743.

Zeng X, Keller D, Wu L and Lu H. (2000). *Cancer Research*, **60,** 6184–6188.

Zhu Q, Wani M, El-Mahdy M, Wani G and Wanni A. (2000). *Mol. Carcinog.*, **28,** 215–224.

Breast Cancer Research and Treatment 1913: 1–11, 2001.

66 : 111- 121, 20

Report

Oncostatin M–induced growth inhibition and morphological changes of MDA-MB231 breast cancer cells are abolished by blocking the MEK/ERK signaling pathway

Cong Li, Thomas E. Ahlborn, Fredric B. Kraemer, and Jingwen Liu
Department of Veterans Affairs Palo Alto Health Care System, 3801 Miranda Avenue, Palo Alto, CA 94304

Key words:

Summary

Cytokine oncostatin M (OM) has profound effects on proliferation and differentiation of breast cancer cells. OM treated cells show reduced growth rate and differentiated phenotypes. The mechanisms underlying the OM growth-inhibitory activity in breast cancer cells have not been fully elucidated. In this study, we investigated the OM-elicited signaling pathways in breast cancer cell lines MDA-MB231 and MCF-7. We show that OM rapidly activates the extracellular signal-regulated kinase (ERK) and the signal transducer and activator of transcription (STAT) 1 and 3 in both cell lines. Intriguingly, OM-induced growth inhibition and morphological changes in MDA-MB231 cells are completely abolished by inhibitors to ERK upstream kinase MEK (nitrogen/extracellular-regulated protein kinase kinase), but the MEK inhibitors have little effects on OM growth-inhibitory activity in MCF-7 cells. In addition, expressions of the cyclin kinase inhibitors p21 and p27 are strongly induced by OM in MCF-7 cells, but their expression is only slightly increased by OM in MDA-MB231 cells. These data together demonstrate that the growth-inhibitory activity of OM can be mediated by different signaling pathways in a cell line-specific manner. While the MEK/ERK pathway is the predominant signaling pathway that leads to the growth inhibition of MDA-MB231 cells, activation of additional signaling pathways are necessary for OM to exert its growth-inhibitory activity in MCF-7 cells.

Introduction

Breast cancer is the most common malignancy among women. It has been predicted that one of every nine women in the United States will get this disease in their lifetime. A clear understanding at the molecular and cellular levels of factors that regulate the growth and differentiation of breast cancer cells would provide insights into this complicated disease and may open new avenues for developing alternative treatments.

Oncostatin M (OM), a cytokine produced by activated T-lymphocytes and macrophages [1–3], has been shown to inhibit the growth of a number of breast cancer cell lines and primary breast tumor cells [4–7]. The ability of OM to inhibit growth and to induce differentiation of breast cancer cells was demonstrated through several lines of investigation. First, the proliferation of cells in monolayer culture and the clonogenecity in soft agar was decreased by OM treatment [4–6]. This decrease in growth rate was caused for the most part by decreased cell cycle progression, as exposure of breast cancer cells to OM resulted in a decreased proportion of cells in the S phase and an increased proportion of cells in the G_0/G_1 phase of the cell cycle [5]. Second, the growth arrest caused by OM was accompanied by cellular phenotypic changes [5, 6]. OM-treated cells typically showed a more heterogeneous morphology. Cells were enlarged, elongated, less tightly associated and developed vacuolation in the cytoplasm. Third, differentiation markers were detected in OM-treated breast cancer cells. In breast cancer cells, one characteristic feature of differentiation is the accumulation of cytoplasmic lipid droplets that form components of milk. OM induced lipid droplet formation in MCF-7 cells as evidenced by the positive staining of the lipophilic dye Oil-Red-O [5]. Furthermore, cells under extended treatment of OM increased expression of

epithelial membrane antigen (EMA) [8], a component of milk fat globule protein [9]. Last, exposure of breast cancer cells to OM altered transcription of specific genes whose protein products are involved in cell proliferation and differentiation such as proto oncogene *c-myc* [6, 7], estrogen receptor [5], the tumor suppressor gene *p53* [10], and the breast cancer specific gene1 (*BCSG1*) [11].

Binding of OM to its cell surface receptors immediately activates several signaling transduction pathways including the signal transduction and activation of transcription (STAT) pathway [12–16], the MAP kinase MEK/ERK pathway [17–21], and the PI 3-kinase pathway [22]. Previous studies have examined the signaling pathways of OM in Ba/F3 cells [23], myoleukemia M1 cells [24, 25], and osteoblast MG63 cells [16]. In Ba/F3 cells, stimulation of gp130 leads to cell proliferation. This proliferative response depends on both STAT activation and the activation of nitrogen activated protein (MAP) kinase extracellular signal-regulated kinase (ERK). However, in M1 cells, introducing a dominant negative form of STAT3 totally abolished interleukin 6 (IL-6) induced growth arrest, whereas introducing a mutant gp130 missing the SHP-2 docking tyrosine, that is absolutely required for ERK activation, did not affect IL-6 activity. These observations suggest that ERK is not involved in M1 cell differentiation induced by the IL-6 family of cytokines. Similarly, IL-6 and OM-induced differentiation of osteoblast MG63 cells depends on STAT3 activation, whereas inhibition of ERK activation with nitrogen/extracellular regulated protein kinase kinase (MEK) inhibitors had no effect. These studies demonstrate that different signaling pathways can be utilized by OM to regulate cell growth in a cell-type specific manner. In this study, we examine the possible involvement of the ERK signaling pathway in OM-induced growth inhibition and differentiation of breast cancer cell line MDA-MB231 and MCF-7. We demonstrate that inhibition of activation of the ERK signaling pathway completely abrogated OM exerted growth-inhibitory activity in MDA-MB231 cells, whereas blocking this ERK signaling pathway had little effect on OM activity in MCF-7 cells.

Materials and methods

Cells and reagents

Human breast cancer cell lines MDA-MB231 and MCF-7 were obtained from American Type Culture Collection (Manassas, VA). MDA-MB231 cells were cultured in Iscoves Modified Dulbecco's Medium (IMDM) supplemented with 10% heat inactivated fetal bovine serum (FBS). MCF-7 cells were cultured in RPMI-1640 medium supplemented with 10% FBS. Purified human recombinant OM was obtained from Bristol-Myers Squibb Pharmaceutical Research Institute (Princeton, NJ). MEK inhibitor U0126 was obtained from Du Pont Merck Pharmaceutical. MEK inhibitor PD 98059 was purchased from New England Biolabs (Beverly, MA). Rabbit polyclonal antibodies against activated ERK1 and ERK2 were obtained from Promega, Inc. (Madison,WI). Rabbit polyclonal antibodies to detect inactive ERK2, p21, and p27 were purchased from Santa Cruz Biotechnology. The specific antibodies to detect STAT1 and STAT3 in supershift assays were also obtained from Santa Cruz Biotechnology. The anti-β-actin mAb was obtained from Sigma, Inc. (St. Louis, MO).

Cell growth

Cell proliferation was measured in monolayer culture in 24-well Costar cluster plates. Cells were plated at an initial density of 2.5×10^3 cells/well in 0.5 ml medium supplemented with 2% FBS. Both OM and MEK inhibitors were added 24 h after initial seeding. The culture media were replenished every 2 days. After 6–7 days of treatment, cells were trypsinized and then viable cell numbers were counted using a hemocytometer.

Western blot

For detection of activated ERK, cells were cultured in medium containing 0.5% FBS or 2% FBS for over night. Cells in 60-mm culture dishes were lysed with 0.2 ml of cold lysis buffer (20 mM Hepes, pH7.4, 30 mM p-nitrophenyl phosphate, 10 mM NaF, 10 mM $MgCl_2$, 2 mM EDTA, 5 mM dithiothreitol, 0.1 mM Na3VO4, 0.1 mM Na2MnO4, 10 mM Sodium B-glycerolphosphate, 10 nM Okadiac acid, 10 nM cypermethrin, 1 mM phenylmethylsulfonyl fluoride, 5 μg/ml aprotinin, 1 μg/ml leupeptin, and 1.25 μg/ml pepstatin). Approximately 10 μg protein of total cell lysate per sample was separated on 10% SDS-polyacrylamide gel electrophoresis (SDS PAGE), transferred to nitrocellulose membrane, blotted with rabbit anti-activated ERK antibodies using an enhanced chemiluminescence (ECL) detection system (Amersham). Membranes were stripped and reblotted with anti-inactivated ERK2 monoclonal antibody.

The signals were quantitated with a BioRad Fluor-S MultiImager System. Densitometric analysis of autoradiographs in these studies included various exposure times to ensure linearity of signals.

For detection of cycline kinase inhibitors p21 and p27, cells were cultured in medium containing 2% FBS with or without OM for various lengths of time.

Preparation of nuclear extracts and electrophoresis mobility shift assays (EMSA)

MDA-MB231 and MCF-7 cells were seeded at 5–8×10^6 cells/100 mm and cultured in medium containing 0.5% FBS over night. Then cells were untreated or treated with U0126 (5 μM) for 1 h prior to stimulation of cells with OM for 15 min. Nuclear extracts were prepared by the method of Dignam et al. [26] except that the buffer A was supplemented with 1 mM Na_3VO_4 and 1 μg per ml of each of pepstatin and leupeptin. Nuclear extracts were quick frozen by liquid nitrogen and stored in aliquots. Protein concentrations were determined using a modified Bradford assay using BSA as a standard (Pierce). Protein concentrations of nuclear extracts from different preparations were typically 2–3 mg/ml.

Each binding reaction was composed of 10 mM HEPES, pH 7.8, 0.5 mM $MgCl_2$, 1 mM DTT, 100 mM KCL, 10% glycerol, 1 μg of poly (dI-dC), 1 μg BSA, and 10 μg nuclear extract in a final volume of 20 μl. Nuclear extracts were incubated with 0.2–0.5 ng of ^{32}P-labeled double-stranded synthetic oligonucleotide probe ($40–80 \times 10^3$ cpm) for 10 min at room temperature. The reaction mixtures were loaded onto a 6% polyacrylamide gel and run in TGE buffer (50 mM Tris base, 400 mM glycine, 1.5 mM EDTA, pH 8.5) at 180 V for 3 h at 4°C. The gels were dried and visualized on a PhosphorImager. In competition analysis, nuclear extracts were incubated with 100-fold molar excess of unlabeled competitor DNA for 5 min prior to the addition of the labeled probe. For supershift assay, antibody was incubated with nuclear extract for 30–60 min at room temperature prior to the addition of the probe.

The sequence for STAT oligonucleotide (5′CTAGGATTTACGGGAAATG-3′) was derived from the high affinity Stat-binding site (m67) from the *c-fos* gene promoter [27]. The sequence for Sp1 oligonucleotide (5′TTCGAAACTCCTCCCCCTGCTAG3′) was derived from the Sp1 binding site identified in the low density lipoprotein receptor gene [28]. The binding sites for STAT and Sp1 are underlined.

RNA isolation and northern blot analysis

Cells were lysed in Ultraspec RNA lysis solution (Biotecxs Laboratory, Houston, Texas) and total cellular RNA was isolated according to the vendor's protocol. Approximately 15 μg of each total RNA sample was used in northern blot analysis as previously described. The *p21* mRNA was detected with a 1.6 kb cDNA probe isolated from plasmid pCMV-Cip1(ATCC). The glyceraldehyde-3-phosphate dehydrogenase (*GAPDH*) mRNA was detected with a plasmid containing a human *GAPDH* cDNA. Differences in hybridization signals of northern blots were quantitated by a PhosphorImager.

Results

Although activation of ERK by OM has been shown in several cell types, it is unknown whether OM could induce ERK activation in breast cancer cells. Thus, two OM-responsive cell lines MDA-MB231 and MCF-7 were examined. Cells were cultured over night in medium containing 0.5% serum and then stimulated with OM for different lengths of time in the presence or the absence of U0126 which is a specific inhibitor of the ERK upstream kinase MEK [29]. Total cell lysates were isolated and 1 μg soluble protein per sample was separated by SDS-PAGE and transferred to nitrocellulose membrane. Detections of inactive nonphosphorylated and the activated double phosphorylated ERK1 and ERK2 were performed by immunoblotting. As shown in Figure 1A, neither OM nor U0126 treatment altered the expression level of the inactived ERK. In contrast, the detectable levels of activated ERK1 and ERK2 were rapidly increased by OM stimulation. In MCF-7 cells, a 7.8-fold increase was detected at 5 min, reached a maximal level of 8.3-fold of control at 15 min, and slowly declined to baseline after 1 h. Similarly, a strong induction of ERK activation by OM (approximately 10-fold) was observed in MCF-7 cells that were cultured in 2% serum. In MDA-MB231 cells, a significant amount of activated ERK was readily detected in untreated cells as compared to that seen in untreated MCF-7 cells. OM stimulation moderately increased the level of activated ERK1 and ERK2 to a maximum of 3.3-fold of control in 0.5% serum and at 15 min. A similar moderate induction of ERK activation was seen in cells cultured in 2% serum by OM (Figure 1B). Prior treatment of cells with U0126 lowered the levels of activated ERK in both untreated

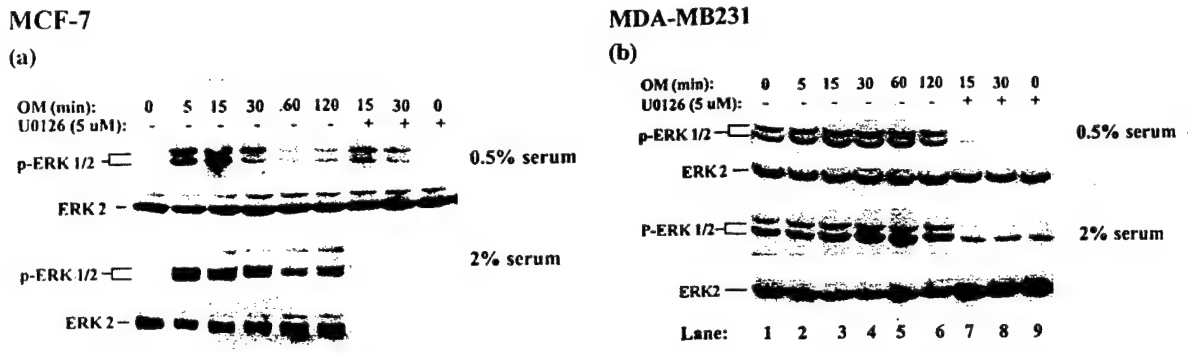

Figure 1. Time course of activation of MAP kinases ERK1 and ERK2 by OM. Breast cancer cells MCF-7 (A) and MDA-MB231 (B) cultured in medium containing 0.5% or 2% FBS were stimulated with 50 ng/ml OM in the absence(−) or the presence(+) of U0126 (5 μM). At the indicated times, the cells were scraped into lysis buffer and cell extracts were prepared. Soluble proteins (10 μg/lane) were applied to SDS-PAGE. Detections of nonphosphorylated and phosphorylated ERK1 and ERK2 were performed by immunoblotting.

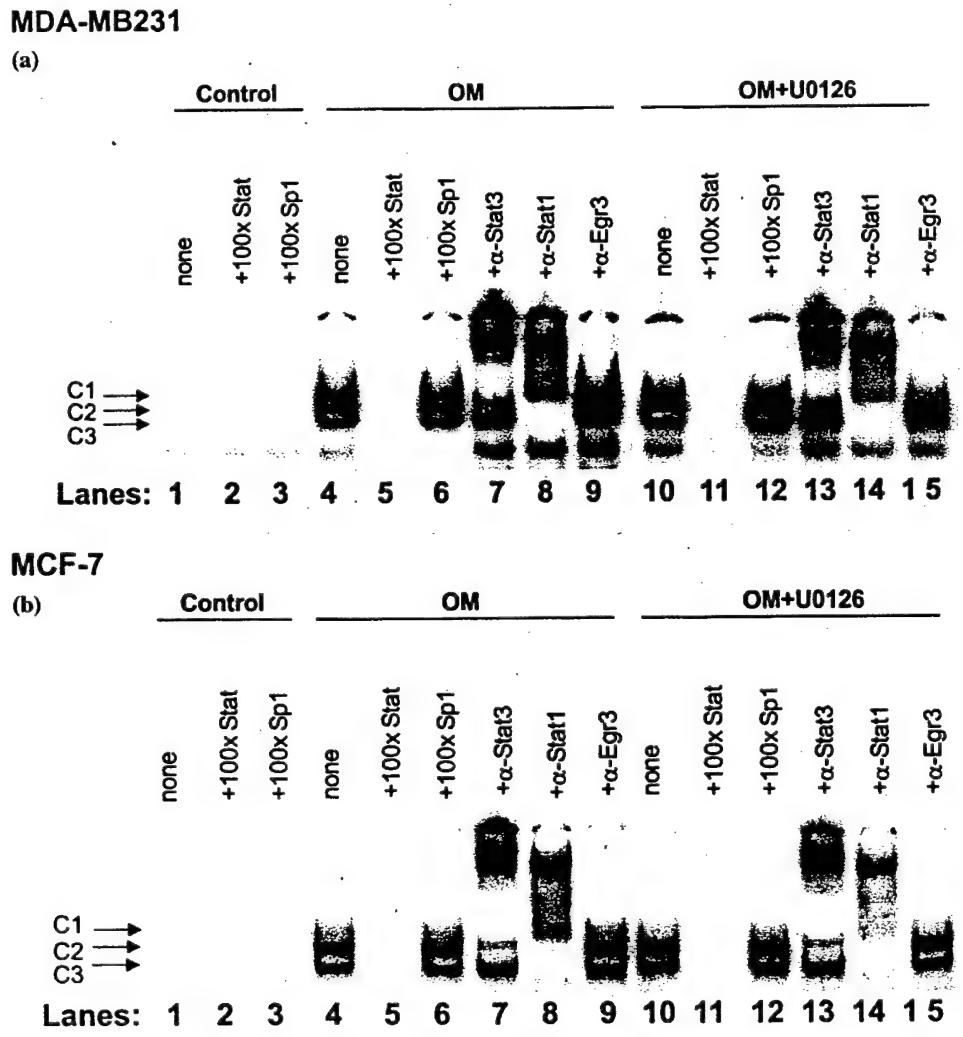

Figure 2.

and OM-stimulated cells. The detection of the activated ERK in unstimulated MDA-MB231 cells is consistent with a recent report showing that some tumor cells, including MDA-MB231, constitutively express activated ERK [30].

It has been shown that activation of STAT3 is essential for OM to induce growth arrest and differentiation of the osteoblast cell line MG63 [16]. To determine whether OM-induced growth arrest in breast cancer cells is preceded by activation of STAT, gel shift assays using a ^{32}P-labeled oligonucleotide probe (STAT), containing the high affinity STAT binding site of *c-fos* gene promoter [27], were performed with nuclear extracts prepared from untreated and OM-treated MDA-MB231 cells. As shown in Figure 2A, three specific DNA-protein complexes were formed only from the OM-stimulated cells (lane 4). Formation of these complexes were inhibited by a 100-fold molar excess of the unlabeled oligonucleotide STAT (lane 5), but was not inhibited by an oligonucleotide containing the binding site for Sp1 (lane 6), demonstrating the specificity of the binding. Supershift assays with antibodies specific to STAT1 or to STAT3 showed that the complex C3 was completely supershifted by anti-STAT1 antibody (lane 8), suggesting that C3 is the homodimer of STAT1. The C2 complex was supershifted by both anti-STAT1 and anti-STAT3 (lane 7), thereby demonstrating that C2 is the heterodimer of STAT1 and STAT3. The low intensity band C1 was completely supershifted by anti-STAT 3 antibody (lane 7), demonstrating its identity as the STAT3 homodimer. In contrast to anti-STAT antibodies, an unrelated antibody to the transcription factor Egr3 had no effect on the formation of these three complexes. These results clearly demonstrate that both STAT1 and STAT3 are activated by OM in MDA-MB231 cells. Treating these cells with U0126 at concentrations (5–10 μM) that effectively inhibited ERK activation did not affect the formation of these complexes (lanes 10–15), suggesting that activation of the STAT signaling pathway by OM in these cells was not affected by the MEK inhibitor. The electrophoresis mobility shift assays (EMSA) with nuclear extract prepared from MCF-7 cells showed a similar result (Figure 2B). These data together demonstrate activation of STAT1 and STAT3 by OM in both breast cancer cell lines.

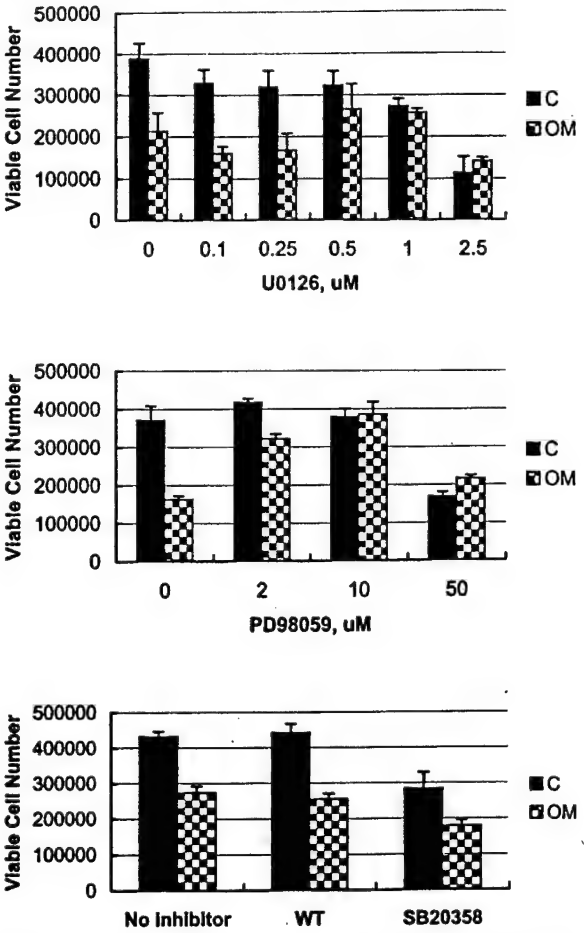

Figure 3. Abrogation of OM growth-inhibitory activity in MDAMB-231 cells by MEK inhibitors. Cells were cultured in 24-well culture plates at a density of 2.5×10^3 cells/well in 0.5 ml IMDM containing 2% FBS with or without 50 ng/ml of OM in the absence or the presence of different doses of U0126 (Top Panel), PD98059 (Middle Panel), or Wortmannin (100 nM), an inhibitor to PI 3-kinase, or SB23058 (20 μM), an inhibitor to p38 kinase (Bottom Panel). Six days later, cells were trypsinized and viable cells (trypan blue excluding cells) were counted. Values are mean ± standard deviation of triplicate wells. The figure shown is representative of 4–5 separate experiments.

Figure 2. EMSA analyses of nuclear proteins interacting with the STAT binding site. Cells were cultured in medium containing 0.5% FBS over night. Nuclear extracts were prepared from MDA-MD231 cells (A) or MCF-7 cells (B) that were untreated (lanes 1–3), or treated with OM (15 min) (lanes 4–9), or, treated with 5 μM U0126 for 1 h then stimulated with OM for 15 min (lanes 10–15). A double-stranded oligonucleotide, designated as STAT, containing the STAT binding sequence from *c-fos* gene promoter was radiolabeled and incubated with 10 μg of nuclear extract per reaction for 10 min at 22°C in the absence (lanes 1, 4, 10) or the presence of 100-fold molar amounts of unlabeled competitor DNA (lanes 2, 3, 5, 6, 11, 12). For supershift, antibodies were incubated with nuclear extracts at 22°C for 30–60 min prior the addition of the probe (lanes 7–9, 13–15). The reaction mixtures were loaded onto a 6% polyacrylamide gel and run in TGE buffer at 180 V for 3 h at 4°C.

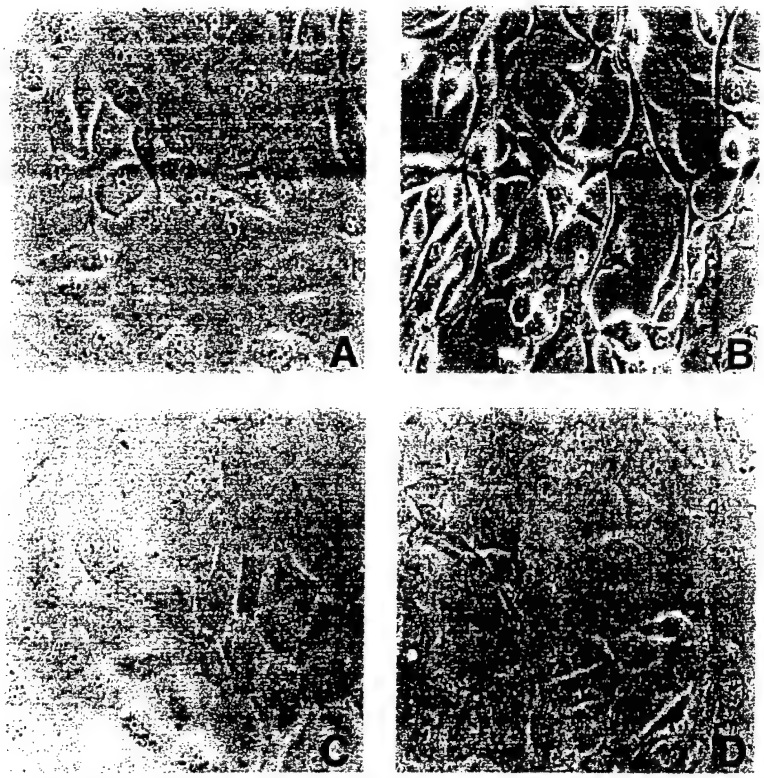

Figure 4. Morphological changes of MDA-MB231 cells induced by OM in the absence or the presence of U0126. Cells were cultured in IMDM containing 2% FBS with or without OM and in the presence or the absence of U0126 (5 μM). Photographs were taken after 3 days of initial culturing (400 × magnification). A, control; B, OM; C, OM+U0126; D, control+U0126.

Since MEK inhibitor U0126 was able to specifically block ERK activation, U0126 was utilized to assess the role of the MEK/ERK pathway in OM-induced growth inhibition. MDA-MB231 cells cultured in monolayer were treated with OM for 6 days in the absence or the presence of different doses of U0126. As determined by viable cell number count, U0126 itself has a notable growth inhibitory effect. At 1 μM, the cell number was decreased by 30%. In the absence of U0126, OM decreased the cell number to 50% of control. In the presence of U0126, this OM inhibitory activity was abolished in a U0126 dose-dependent manner (Figure 3, top panel). Similar results were obtained with another MEK inhibitor PD98059 [31] (Figure 3, middle panel). In contrast to the MEK inhibitors, inhibitors of p38 kinase (SB-203580, 20 μM) [32] and PI 3-kinase (wortmannin, 100 nM) [33] at their effective concentrations did not reverse OM growth inhibitory activity (Figure 3, bottom panel).

In addition to a decreased growth rate, morphology of MDA-MB231 cells was markedly altered by OM. In comparison with control cells (Figure 4A), OM-treated cells were elongated, and became spindle-shaped. The tight cell to cell junction was severely disrupted (Figure 4B). These phenotypic changes were clearly seen after 2 days of OM treatment. Co-incubation of cells with OM and U0126 (5 μM) totally prevented these changes (Figure 4C). Incubation of cells with U0126 alone did not significantly change cell morphology (Figure 4D). The results presented from Figure 3 and 4 together suggest that activation of ERK by OM is a critical event in the signaling pathway that leads to growth inhibition and morphological changes in MDA-MB231 cells.

We next investigated the involvement of the MEK/ERK pathway in OM-induced growth inhibition of MCF-7 cells. OM has a stronger inhibitory effect on growth of MCF-7 cells than MDA-MB231 cells. After 6–7 days of treatment with OM, the viable cell number decreased approximately 80–90% as compared to untreated cells. The decrease in cell number by OM was not associated with induction of apoptosis, as staining cells with Annexin V reagent did not detect

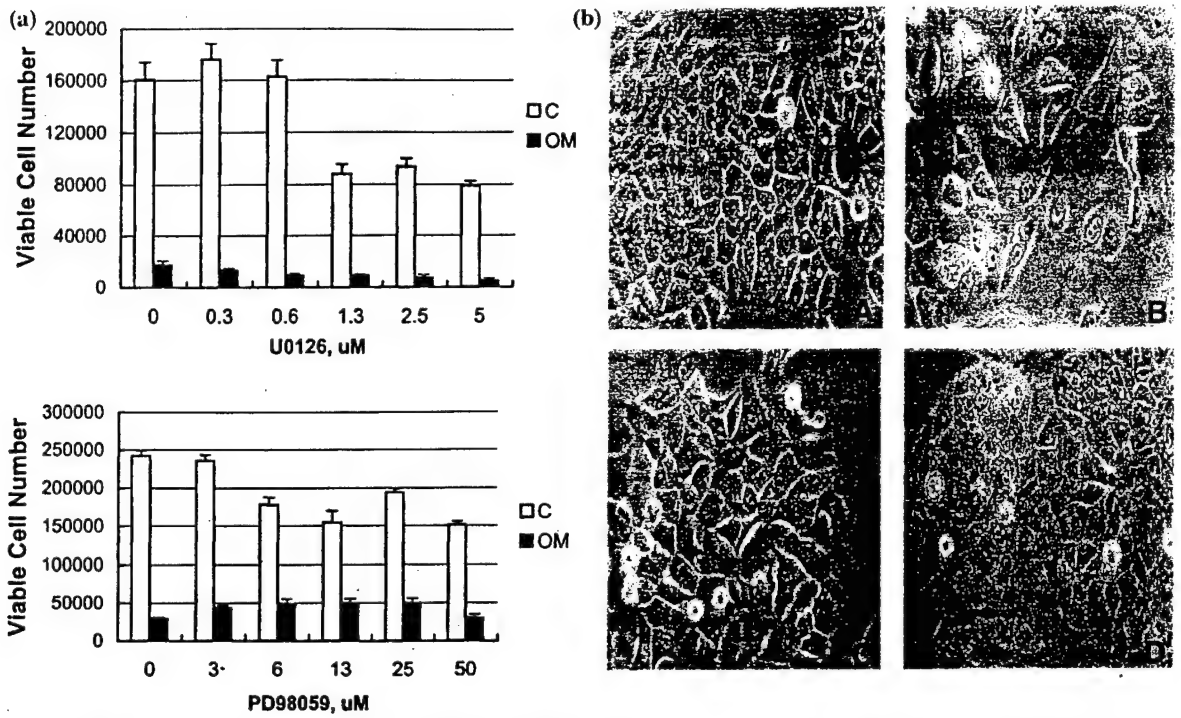

Figure 5. OM-induced growth inhibition and morphological changes in MCF-7 were not effectively inhibited by MEK inhibitors. (A) MCF-7 cells cultured in medium containing 2% FBS were treated with OM in the absence or the presence of different doses of U0126 (Upper Panel) or PD98059 (Lower Panel). Seven days later, cells were trypsinized and viable cells (trypan blue excluding cells) were counted. Values are mean ± standard deviation of triplicate wells. The figure shown is representative of 4–5 separate experiments. (B) Cells were cultured in medium containing 2% FBS with or without OM and in the presence or the absence of U0126 (5 μM). Photographs were taken after 3 days of initial culturing (400x magnification). A, control; B, OM; C, OM+U0126; D, control+U0126. Same results were obtained from cells treated with PD98059.

a significant increase in the number of apoptotic cells during the entire treatment (data not shown). Surprisingly, neither U0126 nor PD98059 blocked the OM growth inhibitory activity (Figure 5A), despite of the strong induction of ERK activation by OM in these cells. Consistent with the lack of effect on cell growth, U0126 or PD98059 did not effectively prevent the OM-induced morphological changes seen in MCF-7 cells (Figure 5B).

The difference in cellular responses of MCF-7 versus MDA-MB231 cells to the MEK inhibitors suggest that OM inhibits the growth of these two cell lines by different mechanisms. It is possible that the STAT1/3 activation and ERK activation lead to activation of different genes in these two cell lines. To explore this possibility, we examined expressions of cyclin kinase inhibitors p21 and p27, as it was previously shown that OM inhibits proliferation of MG63 cells via mechanisms involving induction of p21 [34], and an increased expression of p27 is correlated with growth inhibition in OM-treated A375 melanoma cells [35]. Western blot analysis show that in MCF-7 cells, the level of p21 protein was increased 5.4-fold by OM at 4 h, 20-fold at 24 h, and further increased to more than 30-fold by 48 h treatment. In comparison with p21, the expression of p27 protein was increased 4-fold by OM at 4 h and was continuously maintained at that level through the period of 48 h treatment (Figure 6A). In contrast to MCF-7 cells, expression level of p21 and p27 in MBA-MB231 cells were not changed by OM during 24 h treatment, and moderate increases (2–3-fold) were only seen after 48 h (Figure 6A). We were interested to determine whether the marked increase in p21 protein expression induced by OM in MCF-7 cells correlates with an increased mRNA expression, northern blot was performed to detect p21 mRNA in untreated and OM-treated MCF-7 cells. As shown in Figure 6B, the level of p21 mRNA was only moderately increased by OM to a maximal of 3-fold of control, suggesting that OM may regulate p21 expression through both transcriptional and post transcriptional mechanisms. The differential ef-

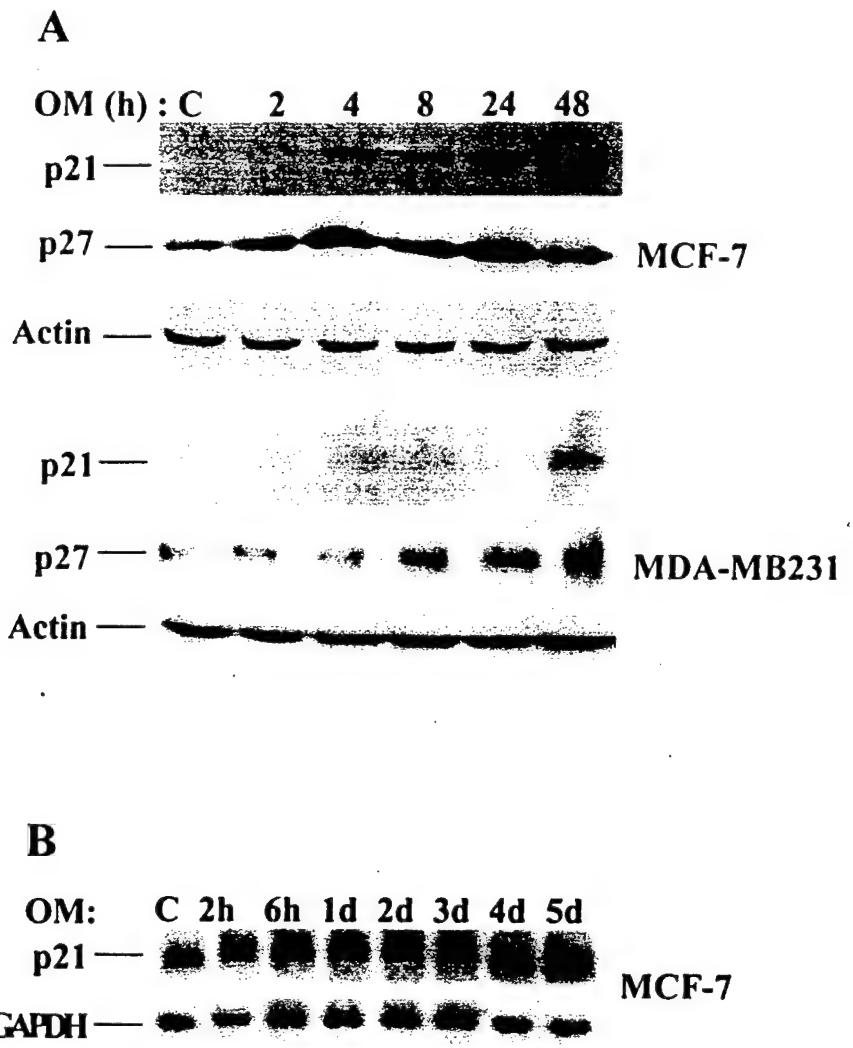

Figure 6. Analyses of p21 and p27 protein expressions and p21 mRNA expression. (A) Western blot analysis of expression of cycline kinase inhibitors p21 and p27 in MCF-7 and MBA-MB231 cells. Cells cultured in medium containing 2% FBS were incubated with 50 ng/ml OM for the indicated times and total cell lysate was harvested at the end of treatment. Soluble proteins (50 μg/lane) were applied to SDS-PAGE. Detections of p21, p27, and β-actin were performed by immunoblotting and autoradiography. (B) Northern blot analysis of p21 mRNA expression in MCF-7 cells. Total RNA was isolated from untreated control cells or OM treated MCF-7 cells, and 15 μg per sample was analyzed for *p21* mRNA by northern blot. The membrane was stripped and hybridized to a human *GAPDH* probe. The figure shown is a representative of two separate experiments.

fects of OM on p21 and p27 induction further suggest that different signaling pathways are utilized by OM in MCF-7 cells versus MDA-MB231 cells.

Discussion

Previous studies conducted by our laboratory and other investigators have established a functional role of OM in growth inhibition and differentiation of breast cancer cells. The present studies attempt to identify and characterize the pathways that transduce the OM-elicited signals from the cell membrane to the nucleus that slow down the proliferation process in malignant mammary epithelial cells.

In this study, we demonstrated that OM was able to activate both the STAT pathway and the MEK/ERK pathway in two OM-responsive cell lines MCF-7 and MDA-MB231. In both cell lines, the DNA binding activity of activated STAT was not detectable in untreated control cells. OM stimulation caused a rapid induction of STAT DNA binding activity, as demon-

strated by EMSA. Supershift assays demonstrate that both STAT1 and STAT3 were activated by OM in MCF-7 and MDA-MB231 cells. The sequence for STAT probe used in these experiments was identical to the high affinity STAT binding site, referred as the sis-inducible element (SIE), present in the promoter of *c-fos* proto oncogene [27]. Previously it has been shown that EMSA using this probe and nuclear extracts of 86HG39 glioblastoma cells that were treated with OM detected 3 DNA-protein complexes [36], similar to the complexes detected in OM-treated breast cancer cells. In contrast to STAT, the level of activated ERK was very low in untreated MCF-7 cells, but was constitutively expressed in MDA-MB231 cells. The fact that OM induced a more than 8-fold increase in activated ERK in MCF-7 cells, as compared to a 2–3-fold increase of activated ERK in MDA-MB231 cells, may reflect the difference in the basal levels of activated ERK in these two cell lines.

Activation of the MEK/ERK pathway has been shown to occur in response to mitogenic stimulations. ERK activity is elevated in response to many different growth factors [37]. Upon activation, ERK translocates to the nucleus where it phosphorylates a number of transcription factors that function as positive regulators of cell proliferation, including ELK, *c-jun*, and *c-myc* [38–40]. Phosphorylation of ELK by ERK potentiates the DNA binding of ELK and the formation of a ternary complex at the serum response element of the *c-fos* gene promoter, resulting in an immediate activation of transcription of the *c-fos* gene (40). However, there is increasing evidence to show that ERK is also activated during the process of cell differentiation and growth arrest. For example, retinoic acid-induced differentiation and growth arrest of HL-60 cells requires ERK activation [41]. Currently, little is known regarding the substrates of ERK that may negatively regulate cell growth.

In mammalian cells ERK1 and ERK2 are activated by their upstream kinase MEK by inducing phosphorylation of threonine and tyrosine residues in ERK [42]. This signaling cascade can be specifically blocked by the MEK inhibitors (U0126 and PD98059) [29, 31]. Therefore, these inhibitors have been used successfully in evaluating roles of MAP kinase cascade in cellular functions. In MDA-MB231 cells, OM-induced growth inhibition and differentiation were completely abolished by U0126 or PD98059, suggesting that in this cell line OM activity may be predominantly transduced through the MEK/ERK signaling cascade. However, these data do not completely rule out the possibility that other signaling pathways are also involved. In contrast to MDA-MB231 cells, MEK inhibitors have little effects in blocking OM growth inhibitory activity in MCF-7 cells. There could be several reasons to explain this discrepancy. First, the level of endogenous activated ERK and/or activated MEK may influence the usage of the MAP kinase cascade. Second, the cellular substrates of ERK may be different in MCF-7 cells than in MDA-MB231 cells. Third, the targeted genes of STAT3 activation may be differently regulated in MCF-7 cells than in MDA-MB231 cells. This speculation is supported by the observation of differential inductions of p21 and p27 by OM in these two cell lines. The expression of p21 and p27 is strongly and rapidly induced by OM in MCF-7 cells, but is only slightly induced by OM after 2 days in MDA-MB231 cells. It is possible that the STAT pathway is critically involved in OM induced growth inhibition in MCF-7 cells. Currently, the function of STAT signaling pathway in OM-induced growth inhibition of MCF-7 cells is under further investigation.

In summary, these studies show that OM-induced growth inhibition of breast cancer cells is preceded by the activation of MAP kinase ERK and STAT1 and STAT3. Activation of the ERK signaling pathway is important for OM to inhibit the growth of MDA-MB231 cells, but is not critical for OM to inhibit the growth of MCF-7 cells. Further investigations to identify the down stream effectors of ERK in these cells will be needed to link ERK activation with control of cell growth.

Acknowledgements

This study was supported by the Department of Veterans Affairs (Office of Research and Development, Medical Research Service), by grant (1RO1CA83648-01) from National Cancer Institute, and by grant (BC990960) from the United States Army Medical Research and Development Command.

References

1. Zarling JM, Shoyab M, Marquardt H, Hanson MB, Lionbin MN, Todaro GJ: Oncostatin M: a growth regulator produced by differentiated lymphoma cells. Proc Natl Acad Sci USA 83: 9739–9743, 1986
2. Brown TJ, Lionbin MN, Marquardt H: Purification and characterization of cytostatic lymphokines produced by activated

human T- lymphocytes: Synergistic antiproliferative activity of transforming growth factor β1, interferon γ and oncostatin M for human melanoma cells. J Immunol 139: 2977–2983, 1987

3. Grove RI, Mazzucco CE, Allegretto N, Kiener PA, Spitalny G, Radka SF, Shoyab M, Antonaccio M, Warr GA: Macrophages-derived factors increase low-density lipoprotein uptake and receptor number in cultured human liver cells. J Lipid Res 32: 1889–1897, 1991
4. Horn D, Fitzpatrick WC, Gompper PT, Ochs V, Bolton-Hanson M, Zarling JM, Malik N, Todaro GJ, Linsley PS: Regulation of cell growth by recombinant oncostatin M. Growth Factors 2: 157–165, 1990
5. Douglas AM, Grant SL, Goss GA, Clouston DR, Sutherland RL, Begley CG: Oncostatin M induces the differentiation of breast cancer cells. Int J Cancer 75: 64–73, 1998
6. Liu J, Spence MJ, Wallace PM, Forcier K, Hellstrom I, Vestal RE: Oncostatin M-specific receptor mediates inhibition of breast cancer cell growth and down-regulation of the *c-myc* proto-oncogene. Cell Growth Differ 8: 667–676, 1997
7. Spence MJ, Vestal RE, Liu J: Oncostatin M-mediated transcriptional suppression of the *c-myc* gene in breast cancer cells. Cancer Res 57: 2223–2228, 1997
8. Grant SL, Begley CG: The oncostatin M signalling pathway: reversing the neoplastic phenotype? Mol Med Today 5: 406–412, 1999
9. Guibaud NF, Gas N, Puont MA, Valette A: Effects of differentiation-inducing agents on maturation of human MCF-7 breast cancer cells. J Cell Physiol 145: 162–172, 1990
10. Liu J, Li C, Ahlborn TE, Spence MJ, Meng L, Boxer LM: The expression of p53 tumor suppressor gene in breast cancer cells is down-regulated by cytokine oncostatin M. Cell Growth Differ 5: 15–18, 1999
11. Liu J, Spence MJ, Zhang YL, Jia T, Liu YE, Shi YE: Transcriptional suppression of synuclein gamma (SNCG) expression in human breast cancer cells by the growth inhibitory cytokine oncostatin M. Breast Cancer Res Treat (in press)
12. Stahl N, Boulton TG, Farruggella T, Ip NY, Davis S, Witthuhn BA, Quelle FW, Silvennoinen O, Barbieri G, Pellegrini S, Ihle JN, Yancopoulos GD: Association and activation of Jak-Tyk kinase by CNTF-LIF-OSM-IL-6 β receptor components. Science 263: 92–95, 1994
13. Darnell JE, Kerr IM, Stark GR: Jak-STAT pathways and transcriptional activation in response to INFs and other extracellular signaling proteins. Science 264: 1415–1420, 1994
14. Zhao Y, Nichols JE, Bulun SE, Mendelson CR, Simpson ER: Aromatase P450 gene expression in human adipose tissue: role of a JAK/STAT pathway in regulation of the adipose-specific promoter. J Biol Chem 270: 16449–16457, 1995
15. Heinrich PC, Behrmann I, Muller-Newen G, Schaper F, Graeve L: Interleukin-6-type cytokine signaling through the gp130/Jak/STAT pathway. Biochem J 334: 297–314, 1998
16. Bellido T, Borba VZC, Roberson P, Manolagas SC: Activation of the Janus Kinase/STAT (signal transduction and activator of transcription) signal transduction pathway by interleukin-6 type cytokines promotes osteoblast differentiation. Endocrinology 138: 3666–3676, 1997
17. Thoma B, Bird TA, Friend DJ, Gearing DP, Dower SK: Oncostatin M and leukemia inhibitory factor trigger overlapping and different signals through partially shared receptor complexs. J Biol Chem 269: 6215–6222, 1994
18. Yin T, Yang Y: Mitogen-activated protein kinases and ribosomal S6 protein kinases are involved in signaling pathways shared by interleukin-11, interleukin-6, leukemia inhibitory factor, and oncostatin M in mouse 3T3-L1 cells. J Biol Chem 269: 3731–3738, 1994
19. Stancato LF, Yu C, Petricoin III EF, Larner AC: Activation of Raf-1 by interferon γ and oncostatin M requires expression of the Stat1 transcription factor. J Biol Chem 273: 18701–18704, 1998
20. Korzus E, Nagase H, Rydell R, Travis J: The mitogen-activated protein kinase and JAK-STAT signaling pathways are required for an oncostatin M-responsive element-mediated activation of matrix metalloproteinase 1 gene expression. J Biol Chem 272: 1188–1196, 1997
21. Stancato LF, Sakatsume M, David M, Dent P, Dong F, Petricoin EF, Krolewski JJ, Silvennoinen O, Saharinnen P, Pierce J, Marshall CJ, Sturgill T, Finbloom DS, Larner AC: Beta interferon and oncostatin M activate Raf-1 and mitogen-activated protein kinase through a JAK1-dependent pathway. Mol Cell Biol 17: 3833–3840, 1997
22. Porter A, Vaillancourt R: Tyrosine kinase receptor-activated signal transduction pathways which lead to oncogenesis. Oncogene 17: 1343–1352, 1998
23. Fukada T, Hibi M, Yamanaka Y: Two signals are necessary for cell proliferation induced by a cytokine receptor gp130: involvement of STAT3 in anti-apoptosis. Immunity 5: 449–460, 1996
24. Minami M, Inoue M, Wei S, Takeda K, Matsumoto M, Kishimoto T, Akira S: Stat3 activation is a critical step in gp130-mediated terminal differentiation and growth arrest of a myeloid cell line. Proc Natl Acad Sci USA 93: 3963–3966, 1996
25. Yamanaka Y, Nakajima K, Fukada T: Differentiation and growth arrest signals are generated through the cytoplasmic region of gp130 that is essential for STAT3 activation. EMBO J 15: 1557–1565, 1996
26. Dignam JD, Lebovitz RM, Roeder RC: Accurate transcription initiation by RNA polymerase II in a soluble extract from isolated mammalian nuclei. Nucleic Acids Res 11: 1475–1489, 1983
27. Wagner BJ, Hayes TE, Hoban CJ, Cochran BH: The SIF binding element confers sis/PDGF inducibility onto the *c-fos* promoter. EMBO J 13: 4477–4484, 1990
28. Liu J, Streiff R, Vestal E, Briggs M: Novel mechanism of transcriptional activation of hepatic LDL receptor by oncostatin M. J Lipid Res 38: 2035–2048, 1997
29. Favata MF, Horiuchi KY, Manos EJ, Daulerio AJ, Stradley DA, Feeser WS, Van Dyk DE, Pitts WJ, Earl RA, Hobbs F, Copeland RA, Magolda RL, Scherle PA, Trzaskos JM: Identification of a novel inhibitor of mitogen-activated protein kinase kinase. J Biol Chem 263: 18623–18632, 1998
30. Hoshino R, Chatani Y, Yamori T, Tsuruo T, Oka H, Yoshida O, Shimada Y, Ari-i S, Wada H, Fujimoto J, Kohno M: Constitutive activation of the 41/43-kda mitogen-activated protein kinase signaling pathway in human tumors. Oncogene 18: 813–822, 1999
31. Alessi DR, Cuenda A, Cohen P, Dudley DT, Saltiel AR: PD 098059 is a specific inhibitor of the activation of mitogen-activated protein kinase kinase *in intro* and *in vivo*. J Biol Chem 270: 27489–27494, 1995
32. Cuenda A, Rouse J, Doza YN, Meier R, Cohen P, Gallagher TF, Young PR, Lee JC: SB 203580 is a specific inhibitor of a MAP kinase homologue which is stimulated by cellular stresses and interleukin-1. FEBS Lett 364: 229–233, 1995
33. Oh H, Fujio Y, Kunisada K, Hirota H, Matsui H, Kishimoto T, Yamauchi-Takihara K: Activation of phosphatidylinositol

Delineating an oncostatin M-activated STAT3 signaling pathway that coordinates the expression of genes involved in cell cycle regulation and extracellular matrix deposition of MCF-7 cells

Fang Zhang[1], Cong Li[1], Hartmut Halfter[2], and Jingwen Liu[1*]

1. Department of Veterans Affairs Palo Alto Health Care System, Palo Alto, CA 94304, USA
2. Department of Neurology and Internal Medicine A (Oncology), Westfälische Wilhelms-Universität Münster, Münster, Germany

Running Title

STAT3 mediates oncostatin-M induced growth arrest and migration of MCF-7 breast cancer cells

Key Words

Oncostatin M, STAT3, Cell growth, Cell migration, Extracellular matrix

Send reprints request to: Jingwen Liu, Ph.D. (154P), VA Palo Alto Health Care System, 3801 Miranda Avenue, Palo Alto, CA 94304
Phone: (650) 493-5000, extension 64411
FAX: (650) 849-0251
Email: Jingwen.Liu@med.va.gov

ABSTRACT

A number of studies have demonstrated that the STAT pathway is an important signaling cascade utilized by the IL-6 cytokine family to regulate a variety of cell functions. However, the downstream target genes of STAT activation that mediate the cytokine-induced cellular responses are largely uncharacterized. The aims of the current study are to determine whether the STAT signaling pathway is critically involved in the OM-induced growth inhibition and morphological changes of MCF-7 cells and to identify STAT3-target genes that are utilized by OM to regulate cell growth and morphology. We show that expression of a dominant negative (DN) mutant of STAT3 in MCF-7 cells completely eliminated the antiproliferative activity of OM, whereas expression of DN STAT1 had no effect. The growth inhibition of breast cancer cells was achieved through a concerted action of OM on cell cycle components. We have identified 4 cell cycle regulators including c-myc, cyclin D1, c/EBPδ, and p53 as downstream effectors of the OM-activated STAT3 signaling cascade. The expression of these genes is differentially regulated by OM in MCF-7 cells but is unaffected by OM in MCF-7-dnStat3 stable clones. We also demonstrate that the OM-induced morphological changes are correlated with increased cell motility in a STAT3-dependent manner. Expression analysis of extracellular matrix (ECM) proteins leads to the identification of fibronectin as a novel OM-regulated ECM component. Our studies further reveal that STAT3 plays a key role in the robust induction of fibronectin expression by OM in MCF-7 cells. These new findings provide a molecular basis for the mechanistic understanding of the effects of OM on cell growth and migration.

INTRODUCTION

STAT proteins are important signaling molecules for many cytokines, such as IL-6 family cytokines (Hirano *et al.*, 1997; Heinrich *et al.*, 1998), and numerous growth factors, including EGF (Leaman *et al.*, 1996). STAT proteins possess duel functions that not only transmit a signal from the cell surface to the nucleus after cytokine engagement of cognate cell surface receptors but also regulate gene expression by direct binding to STAT-recognition sequence in the promoter region of the target genes (Bowman *et al.*, 2000). Although seven members of the STAT family have been characterized in mammalian cells, in general only a single STAT protein or a subset of family members is specifically activated by individual cytokines.

STAT3 and STAT1 are the main STAT proteins activated by the IL-6 cytokine family in a variety of cell types including hepatocytes (Kiuchi *et al.*, 1999; Li *et al.*, 2002; Marsters *et al.*, 2002), chondrocytes (Catterall *et al.*, 2001), astrocytes (Schaefer *et al.*, 2000), endothelial cells (Mahboubi and Pober, 2002), glioblastoma cells (Halfter *et al.*, 2000), melanoma cells (Kortylewski *et al.*, 1999), and breast cancer cells (Badache *et al.*, 2001; Li *et al.*, 2001; Grant *et al.*, 2002). A number of recent studies have shown that activation of STAT3 and STAT1 by the same cytokine, such as oncostatin M (OM), leads to different biological outcomes in different cell types, suggesting that the expression of genetic programs initiated by STAT activation is heavily influenced by cellular context.

OM is a member of IL-6 cytokine family produced by activated T cells and macrophages (Zarling *et al.*, 1986; Brown *et al.*, 1987; Grove *et al.*, 1991). Similar to IL-6 or LIF, OM is pleiotropic and participates in diversified cellular processes such as wound healing (Duncan *et al.*, 1995; Bamber *et al.*, 1998), inflammatory response (Wahl and Wallce, 2001), and cellular proliferation and differentiation (Horn *et al.*, 1990; Grove *et al.*, 1993; Zhang *et al.*, 1994; Liu *et al.*, 1997; Douglas *et al.*, 1997; Halfter *et al.*, 1998). OM manifests its function through specific binding to OM receptors, including the OM specific receptor (OSMR) and the LIF receptor (LIFR). Additions of OM to cells in culture immediately induce the dimerization of receptor subunits, OSMRβ and GP130. This results in phosphorylation and activation of receptor-associated JAK family kinases, leading to activation of several intracellular signaling pathways. Although the STAT1 and STAT3 proteins and the MAP kinase ERK are co-activated simultaneously by OM in every cell types that express the OM-high affinity receptor (OSMR), there are conflict reports as which signaling cascade is critically linked to a defined OM-induced cellular functional change.

Previously, we have shown that the OM-induced growth suppression and morphological changes of breast cancer cell line MDA-MB231 can be totally abrogated by blocking ERK activation with the MAP kinase kinase-1 (MEK-1) inhibitors (Li *et al.*, 2001). By contrast, MEK inhibitors, PD98059 and U0126 were not able to abolish the OM antiproliferative activity or to reverse the morphological changes in MCF-7 cells, implying that other signaling pathways activated by OM in MCF-7 cells are responsible for its actions.

It has been reported in several studies that the OM antiproliferative activity is accompanied by the induction of morphological changes of breast cancer cells (Liu *et al.*, 1997; Spence *et al.*, 1997; Douglas *et al.*, 1998; Halfter *et al.*, 1998). In general the OM treated cells displayed disrupted intercellular cell junctions. Cells became scattered. The morphological changes could be partially attributed to cellular differentiation, as the accumulation of neutral lipid, a marker of differentiation, was detected in OM-treated MCF-7 cells (Douglas *et al.*, 1998; Grant *et al.*, 2002). However, a recent study conducted in T47D cells has suggested that the

scattered phenotype is associated with an increased cell migration towards OM (Badache and Hynes, 2001). OM, acted as a chemoattractant, induced T47D cells to migrate in the absence of STAT3 activation. The mechanisms that underlie the effect of OM on cell migration of T47D cells remain elusive.

The aims of the current study are to determine whether the STAT signaling pathway is critically involved in the OM-induced growth inhibition and morphological changes of MCF-7 cells and to identify STAT3-target genes that are utilized by OM to regulate cell growth and motility.

RESULT

Blockade of OM-induced STAT3 and STAT1 transactivation by dominant negative STAT mutant proteins

OM activates both STAT3 and STAT1 in MCF-7 cells. To determine whether STAT3 or STAT1 activation is a key event in the OM-induced growth inhibition of MCF-7 cells, we established stable MCF-7 clones that express a dominant negative STAT3 mutant (dnStat3, Y705F) or a dominant negative STAT1 mutant (dnStat1, Y701F). MCF-7 clones (neo) transfected with the empty vector (pEFneo) were also generated and were used in this study as negative controls to access possible side effects associated with antibiotic selection.

To determine the effect of mutant STAT proteins on OM-induced STAT DNA binding activity, gel shift and supershift assays using a ^{32}P-labeled oligonucleotide probe (c-FosSIE), containing the high affinity STAT3 binding site of c-fos gene promoter, were performed with nuclear extracts prepared from MCF-7 stable clones that were untreated or treated with OM for 15 min. As shown in Figure 1A, in MCF-7-neo cells, OM induced the formation of 3 specific DNA-protein complexes (lane 2). Supershift assays with antibodies specific to STAT1 or to STAT3 showed that the complex C3 was completely supershifted by anti-STAT1 antibody (lane 3), suggesting that C3 is the homodimer of STAT1. The C2 complex was supershifted by both anti-STAT1 and anti-STAT3 (lane 5), thereby demonstrating that C2 is the heterodimer of STAT1 and STAT3. The low intensity band C1 was completely supershifted by anti-STAT 3 antibody (lane 4), demonstrating its identity as the STAT3 homodimer. The OM-induced STAT binding activity was markedly reduced in clones of dnStat3 (lanes 8-11) and dnStat1 (lanes 12-15) as compared to the neo clone (lanes 1-7) and untransfected MCF-7 cells (data not shown).

To further demonstrate a blockade of STAT3 transactivating activity by the mutant dnStat3 a STAT3 luciferase reporter (pTKlucS3) was transiently transfected into MCF-7-neo and dnStat3 clones. Forty h after transfection, cells were treated with OM for 4 h and luciferase activities were measured. As shown in Figure 1B, OM induced 8-fold increase in the promoter activity of pTKlucS3 in the neo clone, but this induction was completely abolished in the clone of dnStat3.

We next examined the effect of OM on ERK activation in MCF-7 and stable clones. Western blot analysis detected comparable levels of activated ERK in parental MCF-7 cells and stable clones (Figure 2). These results clearly demonstrate that expression of the DN STATs specifically abolished STAT DNA binding and transactivating activity without subverting the OM-induced MEK/ERK signaling pathway.

Expression of dnStat3 but not dnStat1 abolished the antiproliferative activity of OM

The impact of dnStat3 or dnStat1 expression on OM-induced growth suppression was first evaluated by cell proliferation assays that measured the binding of a fluorescent dye to cellular nucleic acids which produces fluorescent signals in proportion to the cell number. Figure 3A shows that the cellular proliferation of MCF-7, the neo clones, and the clones expressing dnStat1 was inhibited by 60-75% as compared to control after incubation with OM for 5 days, whereas the growth rate of dnStat3 clones were unaffected by OM. To further verify the blocking effect of DN STAT3 on OM growth inhibitory activity, a time course of cell growth rate in the absence or the presence of OM was conducted by direct accounting of the viable cell numbers of MCF-7 cells and the dnStat3 clone. Figure 3B shows that OM exerted a time-dependent inhibitory effect on MCF-7 cells. By 7 days of the OM treatment, the number of viable cells was decreased by more than 50% as compared to control. Consistent with the results of Fig. 3A, the growth of dnStat3 cells was not inhibited by OM through the entire duration of

the experiment. These results demonstrate that expression of the dominant negative mutant of STAT3 but not STAT1 blocked the OM-mediated growth arrest in MCF-7 cells.

OM regulates c-myc gene expression through STAT3-dependent and independent mechanisms

c-Myc is a potent oncogene, the expression level of which is directly correlated with cellular growth status (Kelly *et al.*, 1983; Carroll *et al.*, 2002). Recent studies further identify c-myc as a target gene of STAT3 (Kiuchi *et al.*, 1999; Bowman *et al.*, 2001). OM and IL-6 regulates c-myc mRNA expression in a biphasic manner with an early induction and a subsequent suppression (Liu *et al.*, 1992; Minami *et al.*, 1996; Liu *et al.*, 1997; Spence *et al.*, 1997). To determine the role of STAT3 in OM-regulated transcription of c-myc, northern blot analysis was conducted to detect levels of the c-myc mRNA after short and long exposures to OM in MCF-7 and stable clones. Figure 4A shows that OM treatment over a 3-day time course decreased the levels of c-myc mRNA by 60-80% in MCF-7, neo, and dnStat1 clones but not in dnStat3 clones. Interestingly, in contrary to the long exposure, the transient induction of c-myc mRNA by OM was not abolished by overexpression of dnStat3 or dnStat1 (Figure 4B). A brief incubation of cells with OM stimulated c-myc expression to comparable levels (2-4 fold) in MCF-7, neo, dnStat1, and the dnStat3 clones. These results suggest that OM downregulates c-myc transcription through a STAT3-dependent mechanism whereas the immediate effect of OM on upregulation of c-myc is independent of the STAT3 signaling cascade.

Identification of STAT3 target genes c/EBPδ and cyclin D1 as novel OM-regulated genes that participate in OM-mediated growth repression

Previous investigations have shown that OM treatment resulted in an accumulation of breast cancer cells in the G_0/G_1 phase of the cell cycle (Douglas *et al.*, 1998; Grant *et al.*, 2002). The molecular mechanisms underlying the OM effects on cell cycle have not been clearly defined. Since cyclin D1 (Sinibaldi *et al.*, 2000; Sauter *et al.*, 2002) and c/EBPδ (Yamada *et al.*, 1997) are known target genes of STAT3 activation and their gene products are important regulators in the G_0/G1 phase of the cell cycle, we sought to determine whether OM regulates cyclin D1 and c/EBPδ in MCF-7 cells and whether this regulation requires STAT3 activity. Figure 5 shows that OM reciprocally modulates cyclin D1 and c/EBPδ expression. OM increased c/EBPδ protein expression to levels of 3-5 fold of control in MCF-7, the neo, and dnStat1 clones, whereas the c/EBPδ expression in dnStat3 cells was not induced by OM (Figure 5A). The expression of cyclin D1 was inhibited by OM in MCF-7 cells and this inhibition was abrogated by overexpression of dnStat3 (Figure 5B). These results demonstrate that OM exerts its effect on cell growth by direct regulation of critical cell cycle components through the STAT3 signaling pathway.

STAT3 participates in OM-mediated downregulation of p53

OM downregulates p53 expression in MCF-7 cells by inhibiting the gene transcription (Liu *et al.*, 1999; Li *et al.*, 2001). Since blocking the MEK/ERK pathway only partially reversed the OM inhibitory effect on p53 protein expression, it is possible that other signaling pathways could also be involved. To evaluate the role of STAT3 in p53 transcription, a p53 promoter luciferase reporter construct pGL3-p53 was cotransfected with pEF-dnStat3 or with a control vector (pEFneo) into MCF-7 cells along with pRL-SV40 for normalization of variations in transfection efficiency. Cells were treated with OM or OM dilution buffer for 40 h and duel luciferase activities were measured in total cell lysates. The p53 promoter activity was decreased by 50% in OM treated cells in the absence of pEF-dnStat3. Expression of dnStat3 reversed the OM inhibitory effect on p53 promoter activity (Figure 6A). We further examined p53 protein levels in MCF-7 neo and dnStat3 clones untreated or treated with OM. Western blot analysis

shows that while OM treatment lowered p53 protein level to 35% of control in the neo clone, the level of p53 protein in the dnStat3 clone was not decreased by OM treatment (Figure 6B). Taken together, these results demonstrate that activation of STAT3 signaling pathway is a necessary step in the OM-mediated regulation of p53 transcription.

OM-induced morphological changes are associated with increased cell motility and expression of fibronectin in a STAT3-dependent manner

Figure 7 shows OM-induced morphological changes appeared in MCF-7, neo clone, and dnStat1 clone, but not in dnStat3 clones. The tight cell to cell junctions in MCF-7 cells was severely disrupted by OM. Cells became flat and larger, and also developed cell extensions and membrane protrusions. These changes subtly surfaced after 1 day of OM treatment and were predominant after 3 days. However, in dnStat3 clones morphological changes were not readily detected even after 5 days. After a longer period of culture (7 days) in the presence of OM, slight morphological changes were noticed. The OM-induced morphological changes were reversible, as cells slowly resumed original cell shape after withdrawal of OM from the culture medium.

We were interested to know whether the OM-induced phenotype is a sign of increased cell motility. Boyden chamber assays were performed to examine the direct effect of OM on cell motility. MCF-7 cells were pretreated with OM for different days, trypsinized, counted, and seeded onto the top chamber; cells were then allowed to migrate through the membrane in the absence of any chemoattractant. As shown in Figure 8A, OM induced a time-dependent increase in the number of migrated cells. After a 2-day treatment, the number of migrated cells increased more than 12-fold of control. In order to understand the mechanisms underlying the OM-induced cell migration, using western blot analysis, we examined several extracellular matrix (ECM) proteins including P-cadeherin, E-cadeherin, and fibronectin that are known to play important roles in cell migration. We found that the protein level of E-cadeherin was not changed by OM and the level of P-cadeherin was only slightly increased after OM treatment (data not shown). In contrast, OM induced a robust expression of fibronectin with a kinetic similar to that of OM-induced cell migration (Figure 8B). To determine the involvement of STAT3 in this newly discovered property of OM the migration assay was conducted using DN STAT3 cells that were untreated or treated with OM. Figure 8C shows that the cell motility of dnStat3 clones was not stimulated at all even after 6 days of OM treatment. Moreover, the ability of OM to induce fibronectin expression was significantly impaired in the cells expressing the STAT3 mutant (Figure 8B). These results strongly suggest that fibronectin is a downstream effector of the STAT3 signaling cascade and its robust expression contributes to the increased cell motility after OM treatment.

Previously, using OM as a chemoattractant added to the bottom chamber, Badache et al. has shown that expression of DN STAT3 did not affect the migration of T47D cells (Badache and Hynes, 2001). To determine whether DN STAT3 expression in MCF-7 cells is able to block the cell migration towards OM, MCF-7 and the dnStat3 clone were directly seeded onto the top chambers without prior exposure to OM. OM or its dilution buffer as control was added to the bottom chambers. Cells were allowed to migrate for 24 h and the migrated cells were stained and counted. Figure 8D shows that OM as a chemoattractant induced the migration of dnStat3 clone and MCF-7 to similar extents. This corroborated the observation made in T47D cells. Thus, our results, for the first time, demonstrate that OM affects the intrinsic cell motility through a STAT3-dependent mechanism whereas the mechanism of chemoattraction mediated by OM is independent of STAT signaling pathway.

DISCUSSION

The STAT pathway and the MEK/ERK pathway are two major signaling cascades utilized by IL-6 cytokine family to elicit a variety of biological response (Heinrich *et al.*, 1998). Depending on cell types, activation of the same pathway can lead to different biological outcomes. It is conceivable that the downstream targets of ERK or STAT are differentially activated in different cell lines. Each signaling pathway may regulate a unique set of genes whose functions dictate the outcome induced by the cytokine in a cell line-specific manner. From this point of view, identification of target genes of a specific signaling cascade is of importance. It can provide insight to understand the mechanisms of cytokine's action at the molecular levels and may help predict outcomes in an uncharacterized system.

In this study, by utilizing dominant negative mutants of STAT3 and STAT1 we demonstrate that STAT3 but not STAT1 activation is a critical event in the OM-mediated growth inhibition of MCF-7 cells. Our results are consistent with the finding in A375 melonoma cells whose growth was strongly inhibited by OM in a STAT3 but not a STAT1-depdendent mechanism (Kortylewski *et al.*, 1999). While it has been shown that STAT1 activation by IL-4 results in reduced growth rates in human colon carcinoma cell lines (Chang *et al.*, 2000), it appears that activation of Stat1 by OM alone does not lead to changes in gene transcription and cell function.

Recent investigations have identified c-myc as the downstream effector of STAT3 signaling (Kiuchi *et al.*, 1999; Bowman *et al.*, 2001). By using the dnStat3 clone, we found that the OM-induced biphasic regulation of c-myc is both STAT3-dependent and STAT3-independent. Our finding that dnStat3 blocks the OM-induced suppression of c-myc transcription recapitulates the observation obtained previously in M1 cells (Minami *et al.*, 1996). It was shown that IL-6 induced downregulation of c-myc in M1 cells was obviated by dnStat3 expression. Unexpectedly, the rapid induction of c-myc mRNA expression by OM in MCF-7 cells was not affected by dnStat3. The induction of c-myc mRNA (3-4 fold of control) by OM was completely abolished by actinomycin D (data not shown), implying a nature of transcriptional activation. The E2F binding site of the c-myc promoter, located at +98 to +106 bp, was shown to interact with STAT3 and to mediate the inducing activity of IL-6 on c-myc promoter activity (Kiuchi *et al.*, 1999). We have analyzed a series of c-myc promoter luciferase reporters that contain the wildtype E2F or the mutated E2F sites in a transient transfection system of MCF-7 cells. We did not observe a significant induction of the c-myc promoter activity by OM regardless the status of the E2F site (our unpublished data). Our results suggest that OM may stimulate c-myc transcription through some regulatory mechanisms such as chromatin remodeling that might not be readily accessed by the transient transfection of plasmid DNA. The mechanisms underlying the STAT3-independent activation of c-myc transcription by OM is currently under investigation in our laboratory.

In addition to c-myc, we have identified another two cell cycle regulators, c/EBPδ and cyclin D1, that function in the G_0/G1 phase of the cell cycle. c/EBPδ has an important role in the induction of G_0 growth arrest in mammary epithelial cells (Hutt *et al.*, 2000) and cyclin D1 expression promotes cell cycle progression (Sherr and Roberts, 1999). OM through the STAT3 signaling cascade coordinately regulates the expression of c/EBPδ and cyclin D1. Although the direct role of these proteins individually in the OM-mediated growth arrest of MCF-7 cells has not been demonstrated in this study, we postulate that the reduced growth rate of MCF-7 cells results from a concerted regulatory action of OM on several cell cycle components, leading to an accumulation of cells at the G_0/G1 phase.

Recently, there is emerging information to link STAT3 signaling pathway with p53. It was shown that expression of the wildtype p53 in breast cancer cells inhibited STAT3-dependent transcriptional activity (Lin *et al.*, 2002). Another reporter showed that Hep3B cells stably expressing a temperature-sensitive p53 species (p53-Val-135) displayed a reduced response to IL-6 when cultured at the wildtype p53 permitting temperature (Rayanade *et al.*, 1997). Later studies revealed that the reduction of cellular response to IL-6 was due to a p53-caused masking of STAT3 and STAT5, but not STAT1 (Rayanade *et al.*, 1998). In this study we showed that blocking STAT3 activity by dnStat3 reversed the OM inhibitory effect on p53 transcription, demonstrating an involvement of STAT3 in OM-mediated negative regulation of the p53 transcription. Our previous investigation has identified the regulatory sequence (PE21) of p53 promoter as the OM-responsive element that mediates the OM effect on p53 transcription (Li *et al.*, 2001). The motif of PE21 is not related to the STAT canonical sequence (Noda *et al.*, 2000). Thus, different from the regulation of c/EBPδ and cyclin D1 where STAT3 directly bind to the SIE elements of the gene promoters, the effect of STAT3 on p53 transcription is likely indirect and might be mediated through other downstream effectors of STAT3. Nevertheless, our novel finding that STAT3 participates in p53 transcription brings new insight into the interaction between the STAT signaling machinery and p53. It is possible that a reciprocal interaction exists: p53 regulates STAT3 phosphorylation and transactivating activity and the STAT3 affects p53 function by controlling p53 transcription.

OM has been implicated in the process of wound healing which involves cell proliferation, migration, and remodeling of ECM. In dermal fibroblasts, OM stimulates the production of ECM components such as collagen and glycosaminoglycan (Duncan *et al.*, 1995). OM has been reported to stimulate the synthesis of tissue inhibitor of metalloproteinases 1 and 3 (Kerr *et al.*, 1999; Li, *et al.*, 2001). In endothelial cells, OM-promoted cell migration is associated with induction of the urokinase plasminogene activator (uPA) and uPA receptor (Strand *et al.*, 2000). In this study, we provide the first evidence that OM strongly induces fibronectin protein production. Analysis of fibronectin mRNA in untreated and OM-treated cells showed that OM increased the levels of fibronectin mRNA to the order of 20-30 fold (data not shown). The induction at this order of magnitude is likely to be transcriptional. Fibronectin is a multifunctional adhesive glycoprotein (Makogonenko *et al.*, 2002). It affects the cell adhesion and migration. The OM-induced cell migration is likely to be mediated through the interaction of fibronectin with other ECM components. In MCF-7 cells, the OM-induced morphological changes, increased intrinsic cell motility, and production of fibronectin are all inhibited by DN STAT3. Our studies suggest that STAT3 signaling cascade may play important roles in ECM remodeling in breast cancer cells.

In summary, our studies have defined c-myc, cyclin D1, c/EBPδ, and p53 as the downstream effectors of the OM-activated STAT3 signaling cascade that participate in the process of growth regulation. Furthermore, we have unraveled the importance of STAT3 activation in OM-induced migration of breast cancer cells and identified a new OM-regulated ECM component fibronectin. These results provide a better understanding of the molecular mechanisms whereby OM regulates cell growth and differentiation.

MATERIALS AND METHODS

Cells and reagents- Human breast cancer cell line MCF-7 was obtained from American Type Culture Collection (Manassas, VA) and cultured in RPMI-1640 medium supplemented with 10% heat inactivated fetal bovine serum (FBS). The plasmids pEFneo and pEFneo-dnStat1 (Y701F) (Chang *et al.*, 2000) were obtained from Dr. Xin-Yuan Fu at Yale University. The plasmid pEF-dnStat3 (Y705F) (Minami *et al.*, 1996) was provided by Dr. Shizuo Arika at Osaka University. The specific STAT3 luciferase reporter plasmid pLucTKS3 (Zhang *et al.*, 1996) and the control reporter pLucTK were provided by Dr. Richard Jove at University of South Florida College of Medicine, Tampa, Florida. Antibodies directly to STAT3, STAT1, ERK2, cyclin D1, c/EBPδ, p53, c-myc, and fibronectin were obtained from Santa Cruze and the anti phosphorylated ERK was obtained from Cell Signaling Technology.

Generation of stable clones for STAT3 and STAT1 mutant proteins- To generate stable MCF-7 clones that constitutively express a FLAG-tagged dominant negative (DN) form of STAT3 (Y705F), plasmid pEF-dnStat3 and a empty vector containing a neomycin resistant gene (pEFneo) were co-introduced into MCF-7 cells using the transfection reagent Effectene (Qiagen, Valencia, CA). Cells were selected in 300 μg/ml G418. Several clones were picked, expanded in the presence of G418, and analyzed for dnSTAT3 expression with anti-FLAG antibody by immunostainning. To generate MCF-7 clones expressing a DN form of STAT1 (Y701F), plasmid pEFneo-dnStat1 was transfected into MCF-7 cells and several independent clones were selected and characterized for dnStat1 expression by western blot. MCF-7-neo clones were established by introducing the empty vector pEFneo into MCF-7 cells. These clones were used as negative controls in this study.

For each stable cell lines, at least two independent clones were analyzed by western blot analysis for expression of mutant STAT proteins, by gel shift for STAT DNA binding activity, and by growth assays to determine the response to OM treatment. Significant clonal variations were not observed.

Electrophoresis mobility shift assays (EMSA) to detect STAT DNA binding activity in cells expressing the wild-type or the mutant STAT proteins- MCF-7 stable clones were seeded at 5-8 $x10^6$ cells/100 mm and cultured in medium containing 0.5% FBS overnight. Cells were then untreated or treated with OM for 15 min. Nuclear extracts were prepared by the method of Dignam et al. (Dignam *et al.*, 1983) except that the buffer A was supplemented with 1 mM Na_3VO_4 and 1 μg per ml of each of pepstatin and leupeptin. Nuclear extracts were quick frozen by liquid nitrogen and stored in aliquots. Protein concentrations were determined using a modified Bradford assay using BSA as a standard (Pierce). EMSA and supershift assays were conducted as previously described (Li *et al.*, 2001) using a double-stranded oligonucleotide probe (c-FosSIE) containing the high affinity STAT-binding site (m67) derived from the c-fos gene promoter (Wagner *et al.*, 1990). A double-stranded oligonuleotide probe containing a SP1 binding site was used in the assay for the assessment of nonspecific bindings.

Transfection and reporter assays- Cells cultured in 24-well plates at a density of $0.12x10^6$ cells per well were transiently transfected with a total of 200 ng of reporter DNA and 2 ng of pRL-SV40 (Renilla, Promega) per well mixed with the Effectene reagent. Twenty-four h after transfection, cells were switched to medium containing 0.5% FBS overnight, stimulated with OM for indicated length of time, and harvested. Luciferase activities in total cell lysates were measured using the Promega Dual Luciferase Assay System. Absolute firefly luciferase activity was normalized against renilla luciferase activity to correct for transfection efficiency. Triplicate wells were assayed for each transfection condition and at least three independent transfection

assays were performed for each reporter construct. The STAT3 luciferase reporter constructs contains 7 copies of specific STAT3 binding sites corresponding to the region -123/-85 of the c-Reactive protein (CRP) promoter (Zhang *et al.*, 1996). The p53 promoter luciferase reporter pGL3-p53 contains a 599 bp fragment of the human p53 promoter region and exon 1 (-426 to + 172) (Li *et al.*, 2001).

Cell growth assay- Cell number count was conducted in monolayer culture in 24-well Costar culture plates. Cells were plated at an initial density of $7x10^3$ cells/well in 0.5 ml medium supplemented with 2% FBS. OM was added 24 h after initial seeding. The culture media were replenished every 2 days. At the end of treatment, cells were trypsinized and then viable cell numbers were counted using a hemocytometer. Cell proliferation assay conducted in 96-well culture plates with an initial seeding of $2x10^3$ cells/well was measured using CyQUANT Cell Proliferation Assay Kit (C-7026) obtained from Molecular Probes and a fluorescence microplate reader with the parameters of 480 nm excitation and 520 nm emission.

Western blot analysis- For detection of activated ERK, cells were cultured in medium containing 0.5% FBS for overnight prior to OM stimulation. For detection of cycline D1, c/EBPδ, p53, and fibronectin expression, cells were cultured in medium containing 2% FBS with or without OM for various lengths of time. Cells in 60-mm culture dishes were lysed with 0.1 ml of cold lysis buffer (20 mM Hepes, pH 7.4, 30 mM p-nitrophenyl phosphate, 10 mM NaF, 10 mM $MgCl_2$, 2 mM EDTA, 5 mM dithiothreitol, 0.1 mM Na3VO4, 0.1 mM Na2MnO4, 10 mM Sodium B-glycerolphosphate, 10 nM Okadiac acid, 10 nM cypermethrin, 1 mM phenylmethylsulfonyl fluoride, 5 μg/ml aprotinin, 1 μg/ml leupeptin, and 1.25 μg/ml pepstatin). Approximately 50 μg protein of total cell lysate per sample was separated on 10-15% SDS PAGE, transferred to nitrocellulose membrane, followed by western blot analysis. The signals detected using an enhanced chemiluminescence (ECL) detection system were quantitated with a BioRad Fluor-S MultiImager System. Densitometric analysis of autoradiographs in these studies included various exposure times to ensure linearity of signals.

RNA isolation and northern blot analysis- Cells were lysed in Ultraspec RNA lysis solution (Biotecxs Laboratory, Houston, Texas) and total cellular RNA was isolated according to the vendor's protocol. Approximately 15 μg of each total RNA sample was used to analyze c-myc mRNA. The RNA blots were first hybridized to a 2 Kb human c-myc cDNA probe that was ^{32}P-labeled using the Primer-It II Random Primer Labeling kit (Stratagene) and then stripped and reprobed with a ^{32}P-labeled human GAPDH probe to ensure that equivalent amounts of RNA were being analyzed. Hybridization signals were visualized by a BioRad PhosphorImager and were quantified by the Quantity One program.

Analysis of OM-induced morphological changes- MCF-7 and stable clones were cultured in the absence or presence of OM. At indicated times, cell morphology was examined under a phase contrast microscope equipped with a Penguin 600CL digital camera.

Migration assays- Cell motility was examined in a Boyden chamber assay using 8-μm-pore polycarbonate membrane. The migrated cells were fixed and stained using the kit Hema 3 manual staining system obtained from Fisher Scientific. Cells were counted under an inverted microscope in 10 different 100X-power fields in triplicate wells.

ACKNOWLEDGMENTS

We thank Dr. Shizuo Arika for providing us with the plasmid pEF-dnStat3, Dr. Xin-Yuan Fu for providing the plasmids pEFneo and pEFneo-dnStat1, and Dr. Richard Jove for providing the Stat3 reporter plasmid. These vectors are key reagents for this investigation.

FOOTNOTES

1. Corresponding address: Jingwen Liu, Ph.D. (154P), VA Palo Alto Health Care System, 3801 Miranda Ave., Palo Alto, CA 94304. Phone: (650) 493-5000, ext. 64411, FAX: (650) 849-0251, email: Jingwen.Liu@med.va.gov

2. This study was supported by the Department of Veterans Affairs (Office of Research and Development, Medical Research Service), by grant (1RO1CA83648-01) from National Cancer Institute, and by grant (BC990960) from the United States Army Medical Research and Development Command.

3. The abbreviations used are:

ECM	=	extracellular matrix
EMSA	=	electrophoretic mobility shift assay
ERK	=	extracellular signal regulated kinase
GAPDH	=	glyceraldehyde-3-phosphate dehydrogenase
IL-6	=	interleukin-6
OM	=	oncostatin M
STAT	=	signal transducer and activator of transcription

REFERENCES

1. Badache A and Hynes N. (2001). *Cancer Research,* **61**, 383-391.

2. Bamber B, Reife R, Haugen H, and Clegg C. (1998). *J. Mol. Med.,* **76**, 61-69.

3. Bowman T, Broome M, Sinibaldi D, Wharton W, Pledger W, Sedivy J, Irby R, Yeatman T, and Courtneidge,SJR. (2001). *Proc. Natl. Acad. Sci. USA,* **98**, 7319-7324.

4. Bowman T, Garcia R, Turkson J, and Jove R. (2000). *Oncogene,* **19**, 2474-2488.

5. Brown TJ, Lionbin MN, and Marquardt H. (1987). *J. Immunol.,* **139**, 2977-2983.

6. Carroll J, Swarbrick A, Musgrove E, and Sutherland R. (2002). *Cancer Research,* **62**, 3126-3131.

7. Catterall J, Carrere S, Koshy P, Degnan B, Shingleton W, Brinckerhoff C, Rutter J, Cawston T, and Rowan A. (2001). *Arthritis&Rheumatism,* **44**, 2296-2310.

8. Chang TL, Peng X., and Fu X. (2000). *J. Biol. Chem.,* **275**, 10212-10217.

9. Dignam JD, Lebovitz RM, and Roeder RC. (1983). *Nucleic Acids Res.,* **11**, 1475-1489.

10. Douglas AM, Goss GA, Sutherland RL, Hilton DJ, Berndt MC, Nicola NA, and Begley CG. (1997). *Oncogene*,**14**, 661-669.

11. Douglas AM, Grant SL, Goss GA, Clouston DR, Sutherland RL, and Begley CG. (1998). *Int. J. Cancer,* **75**, 64-73.

12. Duncan MR, Hasan A, and Berman B. (1995). *J. Invest. Dermatol.,* **104** , 128-133.

13. Grant SL, Hammacher A, Douglas AM, Goss GA, Mansfield R, Heath J, and Begley C. (2002). *Oncogene,* **21**, 460-474.

14. Grove RI, Eberthardt C, Abid S, Mazzucco CE, Liu J, Todaro GJ, Kiener PA, and Shoyab M. (1993). *Proc. Natl. Acad. Sci. USA.,* **90**, 823-827.

15. Grove RI, Mazzucco CE, Allegretto N, Kiener PA, Spitalny G, Radka SF, Shoyab M, Antonaccio M, and Warr GA. (1991). *J. Lipid Res.,* **32**, 1889-1897.

16. Halfter H, Lotfi R, Westermann R, Young P, Ringelstein E, and Stögbauer F. (1998). *Growth Factors,* **15**, 135-147.

17. Halfter H, Stögbauer F, Friedrich M, Serve S, Serve H, and Ringelstein E. (2000). *J. Neurochem.,* **75**, 973-981.

18. Heinrich PC, Behrmann I, Muller-Newen G, Schaper F, and Graeve L. (1998). *Biochem. J.,* **334**, 297-314.

19. Hirano T, Nakajima K, and Hibi M. (1997). *Cytokine Growth Factor Rev.,* **8**, 241-252.

20. Horn D, Fitzpatrick WC, Gompper PT, Ochs V, Bolton-Hanson M, Zarling JM, Malik N, Todaro GJ, and Linsley PS. (1990). *Growth Factors,* **2**, 157-165.

21. Hutt J, O'Rourke J, and DeWille J. (2000). *J. Biol. Chem.,* **275**, 29123-29131.

22. Kelly K, Cochran BH, Stiles CD, and Leder P. (1983). *Cell,* **35**, 603-610.

23. Kerr C, Langdon C, Graham F, Gauldie L, Hara T, and Richard CD. (1999). *J. Interferon Cytokine Res.,* **19**, 1195-1205.

24. Kiuchi N, Nakajima K, Ichiba M, Fukada T, Narimatsu M, Mizuno K, Hibi M, and Hirano T. (1999). *J. Exp. Med.,* **189**, 63-73.

25. Kortylewski M, Heinrich P, Mackiewicz A, Schniertshauer U, Klingmüller U, Nakajima K, Hirano T, Horn F, and Behrmann I. (1999). *Oncogene,* **18**, 3742-3753.

26. Leaman D, Leung S, Li X, and Stark G. (1996). *FASEB J.,* **10**, 1578-1588.

27. Li C, Ahlborn TE, Kraemer FB, and Liu J. (2001). *Breast Cancer Research and Treatment,* **66**, 111-121.

28. Li C, Ahlborn TE, Tokita K, Boxer L, Noda A, and Liu J. (2001). *Oncogene,* **20**, 8193-8202.

29. Li W, Liang X, Kellendonk C, Poli V, and Taub R. (2002). *J. Biol. Chem.*, **1**, 1-10.

30. Li W, Dehnade F, and Zafarullah M. (2001). *J. Immunol.*, **166**, 3491-3498.

31. Liu J, Clegg JC, and Shoyab M. (1992). *Cell Growth & Differ.*, **3**, 307-313.

32. Lin J, Jin X, Rothman K, Liu H, Tang H, and Burke W. (2002). *Cancer Res.,* **62**, 376-380.

33. Liu J, Li C, Ahlborn TE, Spence MJ, Meng L, and Boxer LM. (1999). *Cell Growth & Differ.,* **5**, 15-18.

34. Liu J, Spence MJ, Wallace PM, Forcier K, Hellstrom I, and Vestal RE (1997). *Cell Growth & Differ.*, **8**, 667-676.

35. Mahboubi K and Pober J. (2002). *J. Biol. Chem.*, **277**, 8012-8021.

36. Makogonenko E, Tsurupa G, Ingham K, and Medved L. (2002). *Biochemistry*, **41**, 7907-7913.

37. Marsters P, Morgen K, Morley S, Gent D, Hejazi A, Backx M, Thorpe E, and Kalsheker N. (2002). *Biochem. J.*, **1**, 1-10.

38. Minami M, Inoue M, Wei S, Takeda K, Matsumoto M, Kishimoto T, and Akira S. (1996). *Proc. Natl. Acad. Sci. USA.,* **93**, 3963-3966.

39. Noda A, Toma-Aiba Y, and Fujiwaba Y. (2000). *Oncogene*, **19**, 21-31.

40. Rayanade RJ, Ndubuise MI, Etlinger JD, and Sehgal PB. (1998). *J. Immunol.*, **161**, 325-334.

41. Rayanade RJ, Patel K, Ndubuise M, Sharma S, Omura S, Etlinger JD, Pine R, and Sehgal PB. (1997). *J. Biol. Chem.*, **272**, 4659-4662.

42. Sauter E, Yeo U, SteMM A, Zhu W, Litwin S, Tichansky D, Pistritto G, Nesbit M, PiNkel D, Herlyn M, and Bastian B. (2002). *Cancer Res.*, **62**, 3200-3206.

43. Schaefer L, Wang S, and Schaefer T. (2000). *Cytokine*, **12**, 1647-1655.

44. Sherr C and Roberts J. (1999). *Genes Dev.*, **13**, 1501-1512.

45. Sinibaldi D, Wharton W, Turkson J, Bowman T, Pledger W, and Jove R. (2000). *Oncogene*, **19**, 5419-5427.

46. Spence MJ, Vestal RE, and Liu J. (1997). *Cancer Research,* **57**, 2223-2228.

47. Strand K, Murray J, Aziz S, Ishida A, Rahman S, Patel Y, Cardona C, Hammond W, Savidge G, and Wijelath E. (2000). *J. Cell. Biochem.*, **79**, 239-248.

48. Wagner B, Hayes T, Hoban C, and Cochran B. (1990). *EMBO J.*, **13**, 4477-4484.

49. Wahl A and Wallace PM. (2001). *Ann Rheum Dis.*, **60**, iii75-iii80

50. Yamada T, Tobita K, Osada S, Nishihara T, and Imagawa M. (1997). *J. Biochem.*, **121**, 731-738.

51. Zarling JM, Shoyab M, Marquardt H, Hanson MB, Lionbin MN, and Todaro GJ. (1986). *Proc. Natl. Acad. Sci. USA.*, **83**, 9739-9743.

52. Zhang D, Sun M, and Samols D. (1996). *J. Biol. Chem.*, **271**, 9503-9509.

53. Zhang XG, Gu JJ, Lu ZY, Yasukawa K, Yancopoulos GD, Turner K, Shoyab M, Taga T, Kishimoto T, Bataille R, and Klein B. (1994). *J. Exp. Med.*, **179**, 1343-1347.

FIGURE LEGENDS

Figure 1. Blocking STAT DNA binding and transactivation by STAT mutant proteins.

(A) EMSA analyses of nuclear proteins interacting with the STAT binding site. Nuclear extracts were prepared from MCF-7-neo clone, pEFneo-dnStat1 clone, and pEF-dnStat3 clone that were untreated (lanes 1), or treated with OM (15 min) (lanes 2-15). A double-stranded oligonucleotide, designated as c-FosSIE, was radiolabeled and incubated with 10 μg of nuclear extract per reaction for 10 min at 22°C in the absence (lanes 1,2,8,12) or the presence of 100-fold molar amounts of unlabeled competitor DNA (lanes 6,7). For supershift, antibodies were incubated with nuclear extracts at 22°C for 30 min prior the addition of the probe (lanes 3-5, 9-11, 13-15). The reaction mixtures were loaded onto a 6% polyacrylamide gel and run in TGE buffer at 30 mA for 3 h at 4°C.

(B) Analysis of STAT3 reporter luciferase activity. The STAT3 reporter pLucTKS3 was cotransfected with pRL-SV40 into neo or dnStat3 clones. Forty h after transfection, cells were treated either with OM (50 ng/ml) or with OM dilution buffer for 4 h prior to harvesting cell lysates. Luciferase activities in total cell lysates were measured using the Promega Dual Luciferase Assay System. Absolute firefly luciferase activity was normalized against renilla luciferase activity to correct for transfection efficiency. The normalized luciferase activity is expressed as the fold of luciferase activity in untreated control cells. The data presented are derived from 3 separate transfections in which triplicate wells were used in each condition.

Figure 2. Activation of MAP kinases ERK1 and ERK2 by OM in MCF-7 and stable clones. MCF-7, neo, dnStat1 and dnStat3 clones cultured in medium containing 0.5% FBS were stimulated with 50 ng/ml OM. At the indicated times, cells were scraped into lysis buffer and cell extracts were prepared. Soluble proteins (30 μg/lane) were applied to SDS-PAGE. Detection of phosphorylated ERK1 and ERK2 and the nonphosphorylated ERK2 was performed by immunoblotting.

Figure 3. Abrogation of OM antiproliferative activity by expression of DN STAT3 in MCF-7 cells.

(A) Untransfected parental MCF-7, 2 independently isolated neo clones, dnStat1 clones, and dnStat3 clones were cultured in 96-well plates at a density of 2000 cells/well in 0.1 ml RPMI containing 2% FBS with or without 50 ng/ml OM for 5 days. The medium was removed and cells were washed with PBS. Two hundred microliters of Cyquant GR dye mixed with cell lysis buffer were added to each well. The fluorescent signals were then measured using a fluorescence microplate reader

(B) Cells of MCF-7 and dnStat3 clone were cultured in 24-well culture plates at a density of $7x10^3$ cells/well in 0.5 ml RPMI containing 2% FBS with or without 50 ng/ml of OM for different days. At the indicated time, cells were trypsinized and viable cells (trypan blue excluding cells) were counted. Values are mean of triplicate wells. The figure shown is representative of 4 to 5 separate experiments.

Figure 4. Detection of c-myc mRNA expression in MCF-7, neo, dnStat1, and dnStat3 clones by northern blot analysis. Cells cultured in 60 mm dishes were treated with OM for 1 to 3 days (A) or for a short period of times (B). By the end of treatment, cells were lysed and total RNA was isolated. Total RNA of 15 μg per sample was analyzed for c-myc mRNA by northern blot. The membrane was stripped and rehybridized to a human GAPDH cDNA probe. The figure shown is representative of 3 separate experiments.

Figure 5. Western blot analyses of c/EBPδ and cyclin D1 protein expressions in MCF-7 and stable clones. Cells cultured in medium containing 2% FBS were incubated with 50 ng/ml OM for the indicated times and total cell lysate was harvested at the end of treatment. Soluble proteins (50 μg/lane) were applied to SDS-PAGE. Detections of c/EBPδ (A) and cyclin D1 (B) were performed by immunoblotting and autoradiography. Immunoblotting of the membranes with anti-β-actin mAb was conducted to normalize the amounts of protein being analyzed.

Figure 6. Evaluation of the role of STAT3 in OM-mediated downregulation of p53 promoter activity and protein expression.

(A) The p53 promoter reporter pGL3-p53 was cotransfected with pEF-dnStat3 or with pEFneo into cells along with the normalizing vector pRL-SV40. Transfected cells were treated either with OM (50 ng/ml) or with OM dilution buffer for 40 h prior to harvesting cell lysates. The normalized luciferase activity is expressed as the percentage of luciferase activity in untreated control cells.

(B) Cells were cultured in the presence or absence of OM for 5 days and harvested. Western blot analysis of p53 protein expression was conducted using total cell lysates.

Figure 7. Detection of OM-induced morphological changes in MCF-7, neo and dnStat1 clones but not in the dnStat3 clone. Cells were cultured in medium containing 2% FBS with or without OM for 3 to 5 days. Photographs were taken at the indicated time of OM treatment by using the Penguin 600CL digital camera at a magnification of 200.

Figure 8. OM induces cell migration and stimulates fibronectin production through the STAT3-signaling cascade. The effects of OM on cell motility and expression of fibronectin were examined in MCF-7 and the dnStat3 clone. In A, MCF-7 cells were pretreated with OM for different days at a concentration of 50 ng/ml. At the end of treatment, cells were trypsinized and counted. Cells were then seeded onto the top chamber at a density of 0.15×10^6 per chamber. The top chamber and the bottom chamber both contained 2% FBS RPMI. Migrated cells were counted after 6 h. In B, MCF-7 and dnStat3 clone were treated with OM. At the indicated time, cell was harvested and total cell lysates of 50 μg per sample were used to analyze fibronectin expression by western blot analysis. In C, cells were cultured in the absence (control) or the presence of OM for 6 days. The ability of cell to migrate was determined as described in A. In D, cells without prior exposure to OM were seeded onto the top chamber which contained 2% FBS RPMI. OM at a concentration of 50 ng/ml was added to the bottom chamber that contained 2% FBS RPMI. Cells were allowed to migrate towards OM for 24 h. The migrated cells were fixed, stained, and counted. Data are expressed as fold increase relative to control.

Figure 1

A

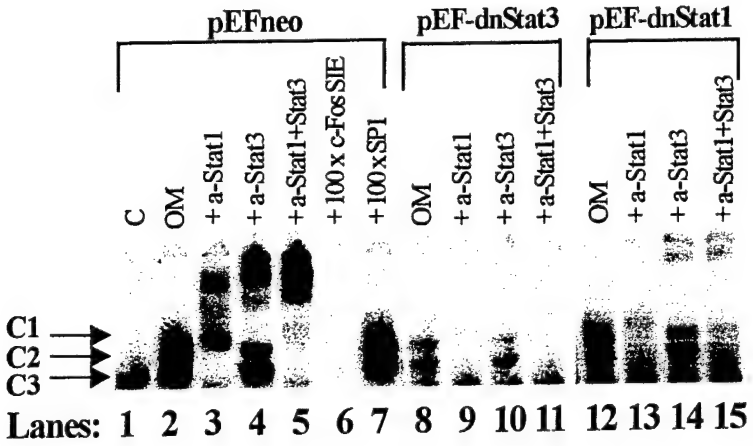
pEFneo
pEF-dnStat3
pEF-dnStat1
C
OM
+a-Stat1
+a-Stat3
+a-Stat1+Stat3
+100x c-Fos SIE
+100xSP1
OM
+a-Stat1
+a-Stat3
+a-Stat1+Stat3
OM
+a-Stat1
+a-Stat3
+a-Stat1+Stat3
C1
C2
C3
Lanes: 1 2 3 4 5 6 7 8 9 10 11 12 13 14 15

B

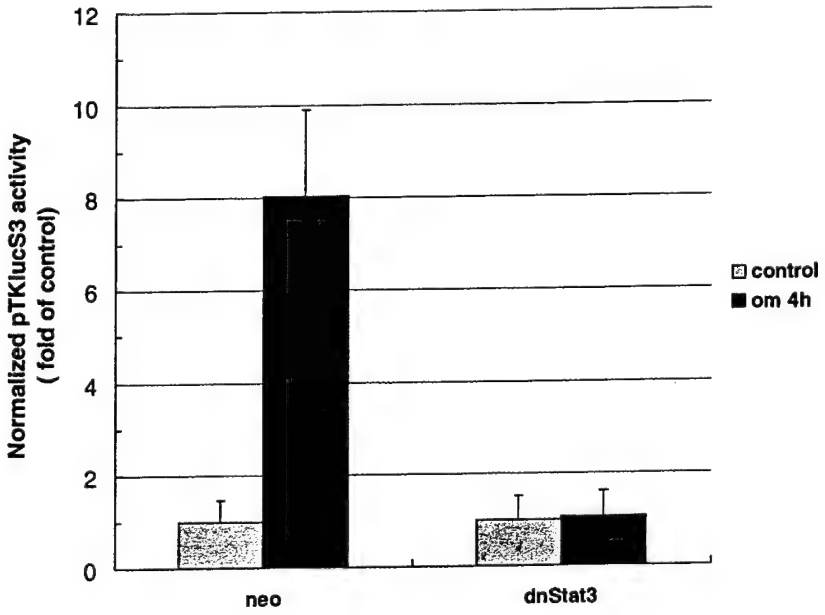
Normalized pTKlucS3 activity
(fold of control)
12
10
8
6
4
2
0
neo
dnStat3
control
om 4h

Figure 2

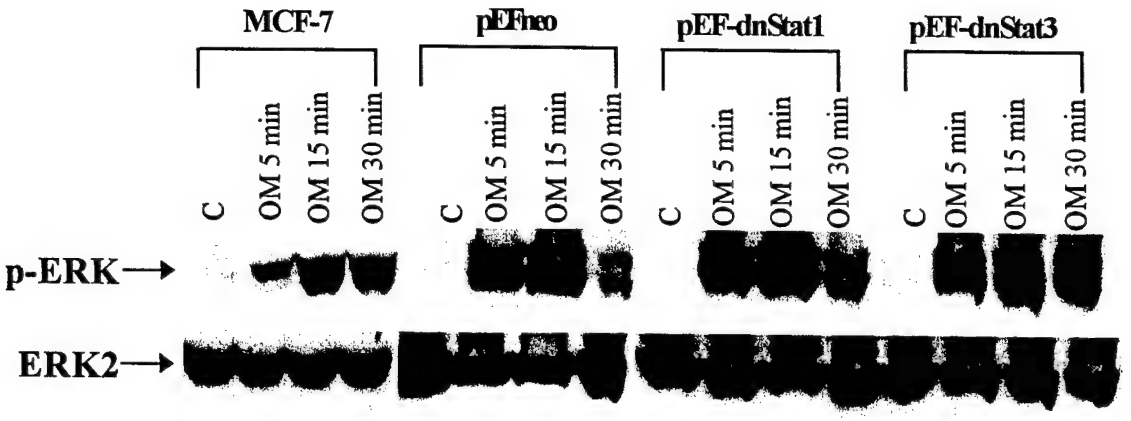
MCF-7
pEFneo
pEF-dnStat1
pEF-dnStat3
C
OM 5 min
OM 15 min
OM 30 min
p-ERK
ERK2

Figure 3

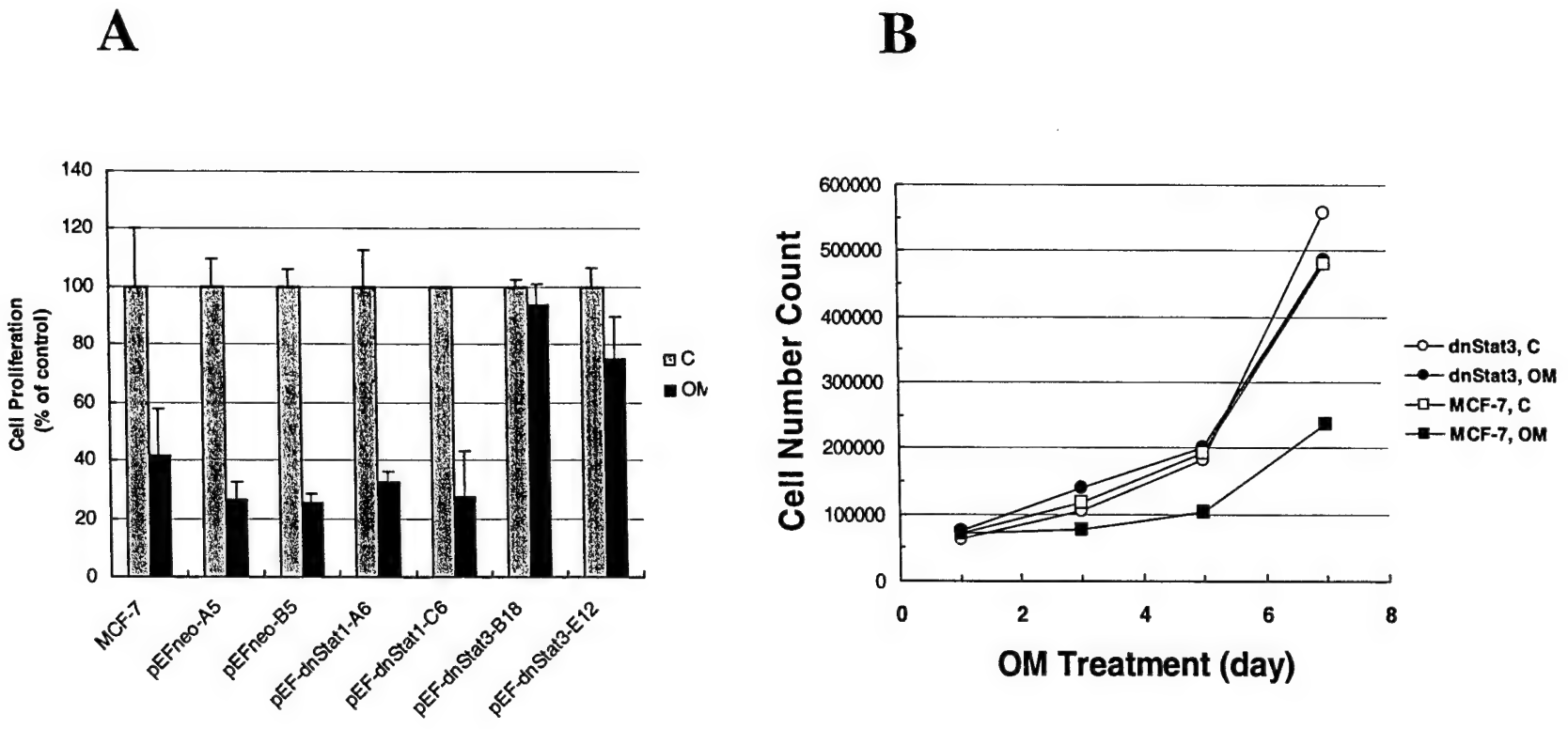
A
B
Cell Proliferation (% of control)
140
120
100
80
60
40
20
0
C
OM
MCF-7
pEFneo-A5
pEFneo-B5
pEF-dnStat1-A6
pEF-dnStat1-C6
pEF-dnStat3-B18
pEF-dnStat3-E12
Cell Number Count
600000
500000
400000
300000
200000
100000
0
0
2
4
6
8
OM Treatment (day)
dnStat3, C
dnStat3, OM
MCF-7, C
MCF-7, OM

Figure 4

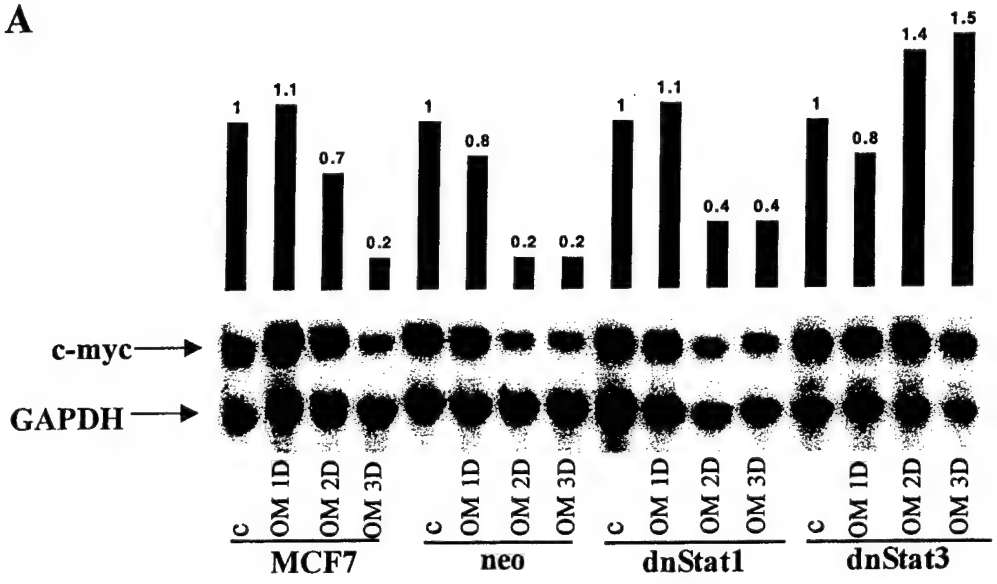
A
1
1.1
0.7
0.2
1
0.8
0.2
0.2
1
1.1
0.4
0.4
1
0.8
1.4
1.5
c-myc
GAPDH
c
OM 1D
OM 2D
OM 3D
MCF7
neo
dnStat1
dnStat3

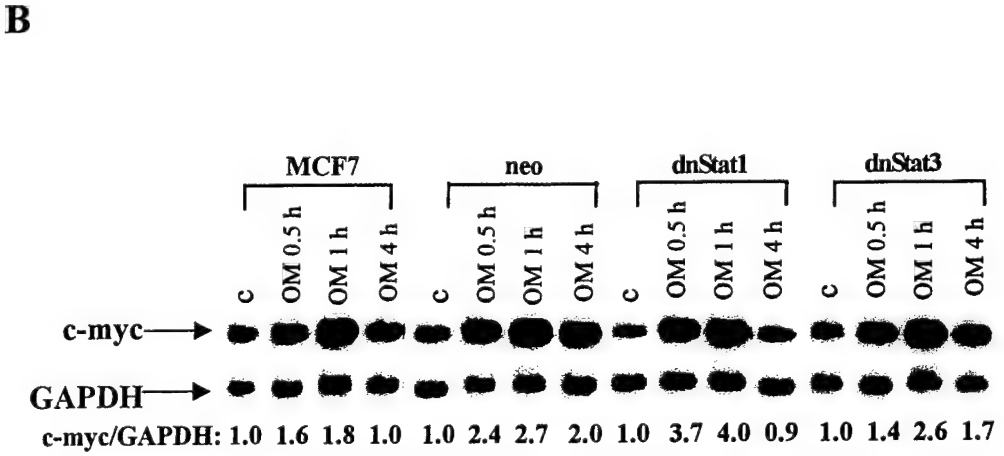
B
MCF7
neo
dnStat1
dnStat3
c
OM 0.5 h
OM 1 h
OM 4 h
c-myc
GAPDH
c-myc/GAPDH: 1.0 1.6 1.8 1.0 1.0 2.4 2.7 2.0 1.0 3.7 4.0 0.9 1.0 1.4 2.6 1.7

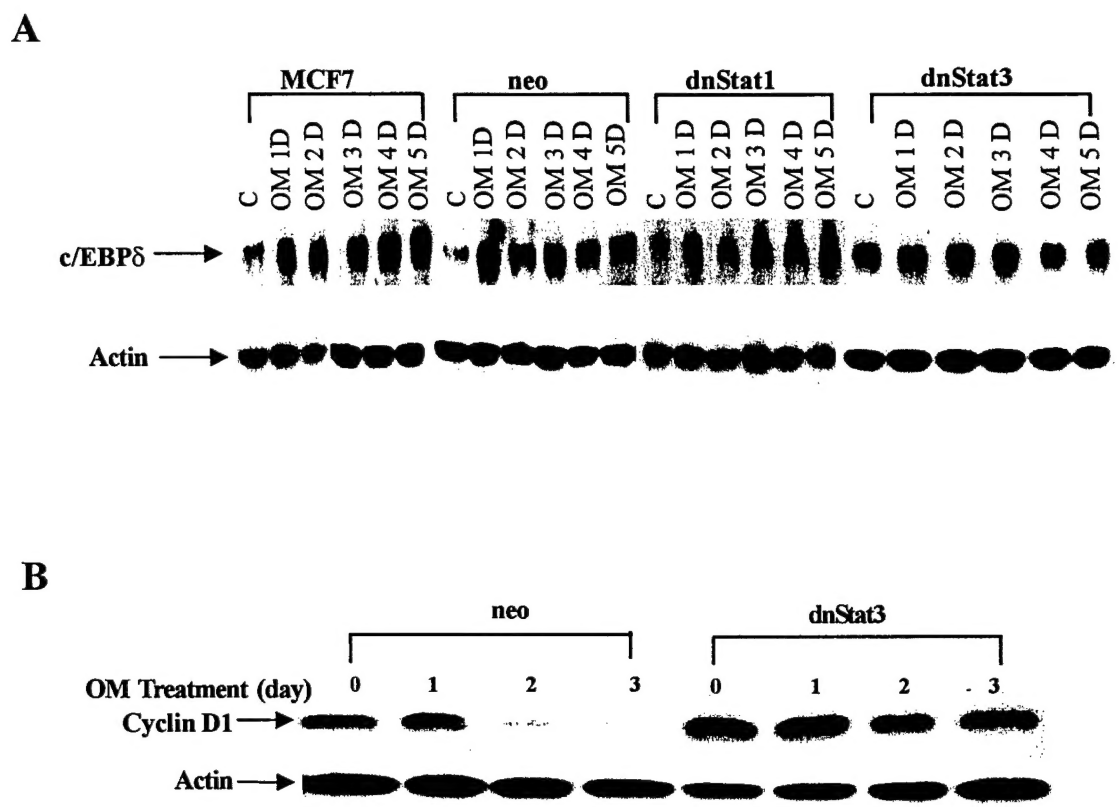
A
MCF7
neo
dnStat1
dnStat3
C
OM 1D
OM 2D
OM 3D
OM 4D
OM 5D
c/EBPδ
Actin
B
neo
dnStat3
OM Treatment (day)
0
1
2
3
Cyclin D1
Actin

Figure 5

Figure 6

A

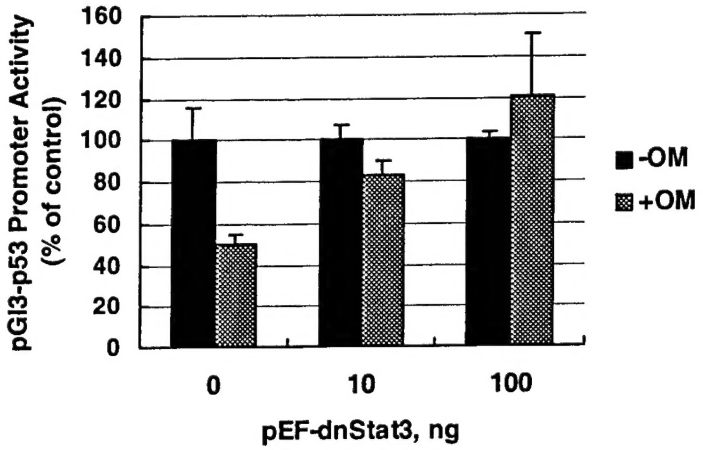
pGl3-p53 Promoter Activity
(% of control)
160
140
120
100
80
60
40
20
0
0
10
100
pEF-dnStat3, ng
-OM
+OM

B

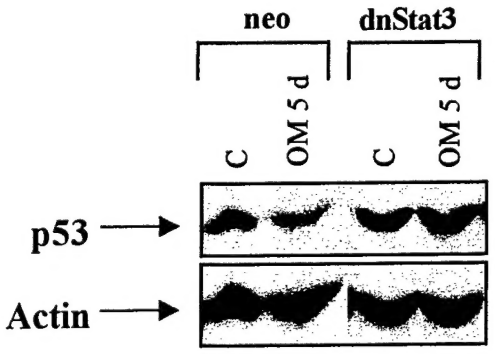
neo
dnStat3
C
OM 5 d
C
OM 5 d
p53
Actin

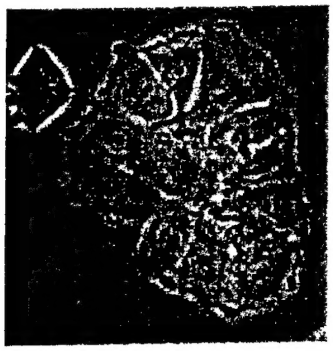

MCF7 control

MCF7 OM3D

MCF7 OM5D

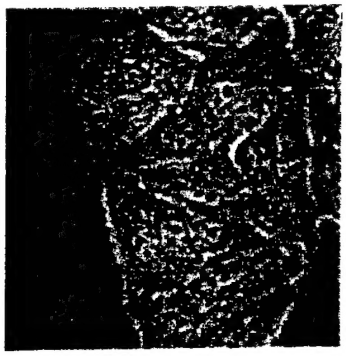

neo control

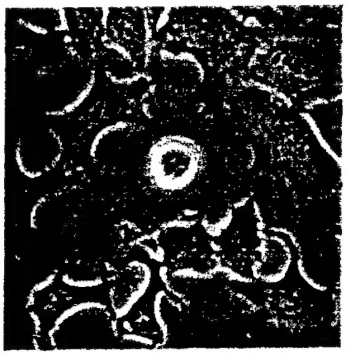

neo OM3D

neo OM5D

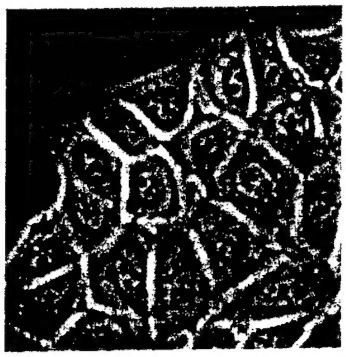

dnStat1 control

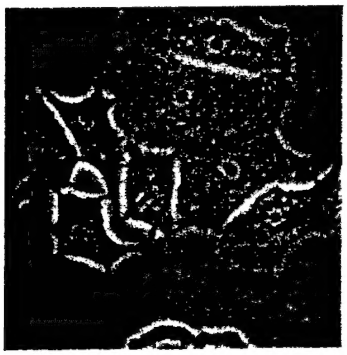

dnStat1 OM3D

dnStat1 OM5D

dnStat3 control

dnStat3 OM3D

dnStat3 OM5D

Figure 7

Figure 8

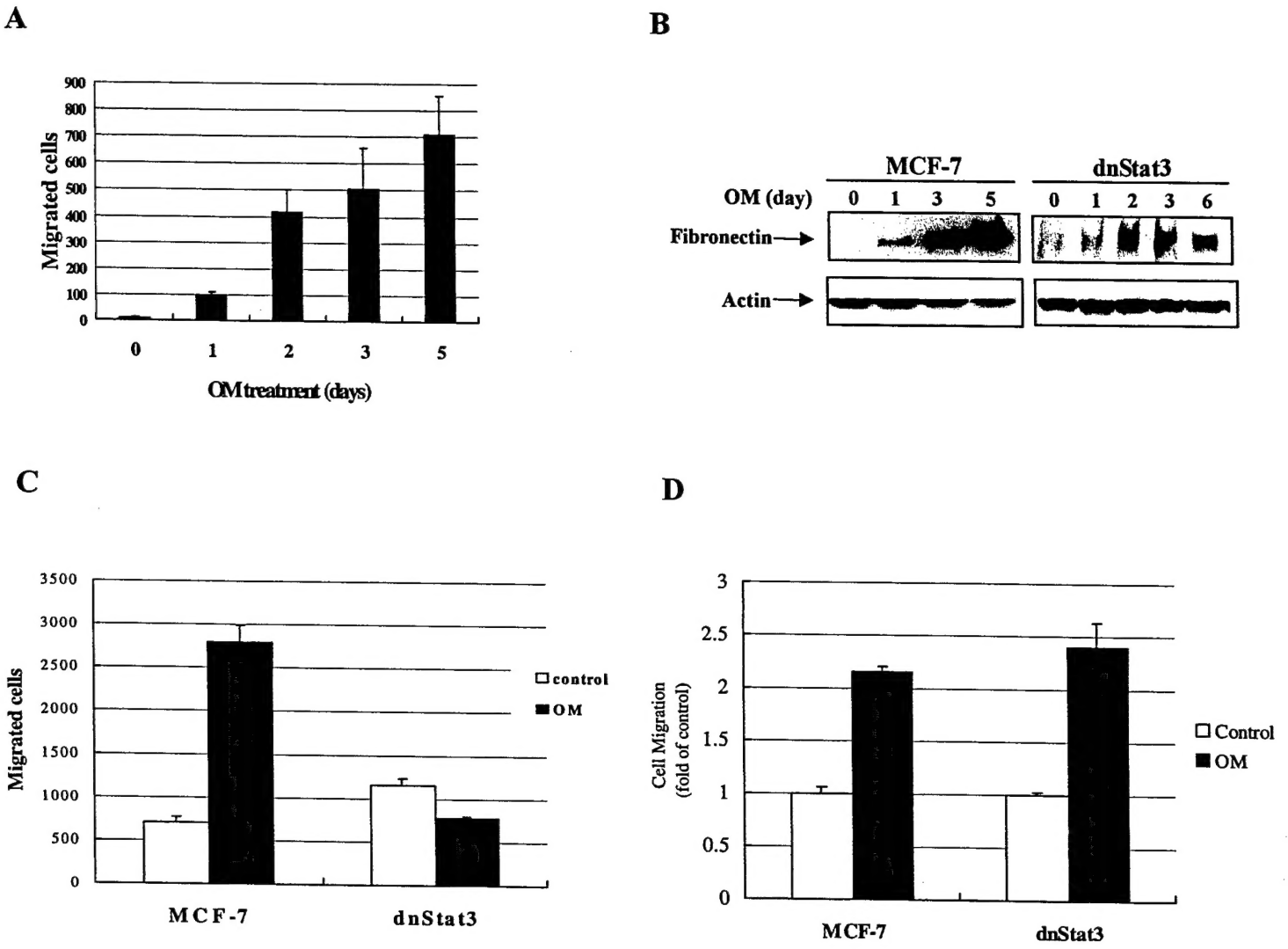
A
Migrated cells
900
800
700
600
500
400
300
200
100
0
0
1
2
3
5
OM treatment (days)
B
MCF-7
dnStat3
OM (day)
0 1 3 5
0 1 2 3 6
Fibronectin
Actin
C
Migrated cells
3500
3000
2500
2000
1500
1000
500
0
control
OM
MCF-7
dnStat3
D
Cell Migration
(fold of control)
3
2.5
2
1.5
1
0.5
0
Control
OM
MCF-7
dnStat3